

Old Dominion University

ODU Digital Commons

Theses and Dissertations in Biomedical
Sciences

College of Sciences

Winter 2009

Analysis of N-Linked Oligosaccharides of Prostate-Specific Antigen and Prostatic Acid Phosphatase in Prostatic Fluids

Krista Yaudes White
Old Dominion University

Follow this and additional works at: https://digitalcommons.odu.edu/biomedicalsciences_etds



Part of the [Biochemistry Commons](#), and the [Molecular Biology Commons](#)

Recommended Citation

White, Krista Y.. "Analysis of N-Linked Oligosaccharides of Prostate-Specific Antigen and Prostatic Acid Phosphatase in Prostatic Fluids" (2009). Doctor of Philosophy (PhD), Dissertation, , Old Dominion University, DOI: 10.25777/44gs-cd38
https://digitalcommons.odu.edu/biomedicalsciences_etds/97

This Dissertation is brought to you for free and open access by the College of Sciences at ODU Digital Commons. It has been accepted for inclusion in Theses and Dissertations in Biomedical Sciences by an authorized administrator of ODU Digital Commons. For more information, please contact digitalcommons@odu.edu.

**ANALYSIS OF N-LINKED OLIGOSACCHARIDES OF PROSTATE-
SPECIFIC ANTIGEN AND PROSTATIC ACID PHOSPHATASE IN
PROSTATIC FLUIDS**

by

Krista Yaudes White
B.S., 2001, University of North Carolina at Wilmington

A Dissertation Submitted to the Faculty of
Eastern Virginia Medical School and Old Dominion University
in Partial Fulfillment of the
Requirement for the Degree of

DOCTOR OF PHILOSOPHY

BIOMEDICAL SCIENCES

EASTERN VIRGINIA MEDICAL SCHOOL
OLD DOMINION UNIVERSITY
December 2009

Approved by:

Richard Drake (Director)

Neel Krishna (Member)

Julius Nvalwidhe (Member)

O. John Semmes (Member)

ABSTRACT

ANALYSIS OF N-LINKED OLIGOSACCHARIDES OF PROSTATE-SPECIFIC ANTIGEN AND PROSTATIC ACID PHOSPHATASE IN PROSTATIC FLUIDS

Krista Yaudes White
Eastern Virginia Medical School and Old Dominion University, 2009
Director: Dr. Richard R. Drake

Presently, prostate cancer is the most common cancer afflicting men in the United States, with serum PSA being the “gold standard” protein biomarker used in the clinic for detecting and diagnosing prostate cancer. Nonetheless, serum PSA levels can also be elevated in non-cancerous conditions as well, such as benign prostatic hyperplasia (BPH). Due to this overlap, many unnecessary biopsies and radical prostatectomies occur, leading to patient distress. Despite recent advances to clinical assays which consider other clinical parameters, there is still a great need for improved clinical detection methodologies for prostate cancer, including improved biomarkers. Therefore, this research project aims to examine the N-glycosylation patterns of prostate-specific antigen (PSA) and prostatic acid phosphatase (PAP) in prostate proximal fluids, as well as to examine the total glycan profile for prostate proximal fluids with the intent of discovering carbohydrate-based biomarkers for the detection of early prostate carcinomas. To this end, preliminary glycomic and proteomic studies were completed using seminal plasma samples, based on the disease cohorts normal, BPH, and prostate cancer. These samples resulted in sufficient protein levels of both PSA and PAP for glycopeptide and glycomic analyses. Furthermore, these studies led to additional knowledge of PSA and PAP glycosylation. In addition to this sample set, pools of disease-defined expressed prostatic

secretions (EPS) were generated and subsequently analyzed for detection of both protein levels and carbohydrate structures of PSA and PAP, as well as examined for their total glycomic profile. We succeeded in characterizing EPS fluids for both protein and carbohydrate content, as well as identified potential carbohydrate targets for the generation of new clinical assays for the detection of early prostate carcinomas. These targets are fucosylated, complex sub-type glycans which we found to be under-expressed in prostate carcinoma samples as compared to their non-cancerous counterparts. We believe EPS fluids have utility not only for discovery of cancer biomarkers, but also for use in future clinical assays.

This dissertation is dedicated to my husband Jeremy and my son Gabriel. I dedicate it to Jeremy for his continued support and patience throughout the past five years and to Gabriel for making my life more complete in a way I did not know was possible. I also dedicate this dissertation to my immediate family: my parents Ron and Wanda Yaudes, my sisters Cindy Yaudes, Debby Yaudes-Brown, and Michele Yaudes, my brother-in-law Tim Brown, my nephew Quinn, and my nieces Raven and Kierra. Without the love and support from my family I could not have survived the journey!

ACKNOWLEDGMENTS

I would like to first and foremost acknowledge my research advisor Richard Drake. Dr. Drake has been a strong and positive influence throughout my years as a doctoral student in his laboratory. Without his guidance I would not have found my passion for glycans, which ultimately allowed me to truly enjoy my project and made the difficulty of it an exciting challenge. I must also acknowledge the other three members of my dissertation committee: O. John Semmes, Neel Krishna, and Julius Nyalwidhe. They have provided me with a great deal of support and constructive criticism, allowing me to have a comprehensive project with well-defined goals and objectives. They are all brilliant scientists and researchers, and I feel fortunate for having their knowledge and expertise available to aid me throughout this process.

TABLE OF CONTENTS

	Page
LIST OF TABLES.....	viii
LIST OF FIGURES.....	ix
 Chapter	
I. INTRODUCTION.....	1
PROSTATE CANCER.....	1
PROTEIN GLYCOSYLATION.....	10
PROXIMAL FLUIDS OF THE PROSTATE FOR BIOMARKER DISCOVERY.....	20
PROTEOMICS, GLYCOMICS, AND THE HISTORY OF MASS SPECTROMETRY.....	21
 II. DISSERTATION RATIONALE AND SUMMARY OF AIMS.....	 37
 III. AIM I: DEVELOP METHODOLOGIES FOR THE CHARACTERIZATION OF N-LINKED GLYCANS OF PROSTATE-SPECIFIC ANTIGEN AND PROSTATIC ACID PHOSPHATASE IN SEMINAL FLUIDS.....	 42
INTRODUCTION.....	42
EXPERIMENTAL.....	45
RESULTS.....	49
DISCUSSION.....	65
 IV. AIM II: ESTABLISH EXPRESSED PROSTATIC SECRETIONS AS A SOURCE OF PROSTATE-SPECIFIC ANTIGEN AND PROSTATIC ACID PHOSPHATASE.....	 71
INTRODUCTION.....	71
EXPERIMENTAL.....	72
RESULTS.....	78
DISCUSSION.....	91
 V. AIM III: APPLICATION OF NEW METHODOLOGIES TO EXPRESSED PROSTATIC SECRETIONS FOR PROSTATE CANCER GLYCOPROTEIN BIOMARKER DISCOVERY.....	 95
INTRODUCTION.....	95
EXPERIMENTAL.....	96
RESULTS.....	102
DISCUSSION.....	121

VI. CONCLUSIONS AND FUTURE DIRECTIONS	126
AIM I.....	126
AIM II.....	128
AIM III	130
CONCLUDING REMARKS AND FUTURE DIRECTIONS OF AIMS I, II, AND III....	132
REFERENCES	139
APPENDIX	
A. COPYRIGHT INFORMATION FOR REPRINT OF PUBLICATION IN DISSERTATION.....	160
VITA.....	164

LIST OF TABLES

Table		Page
1.	Risk stratification schemes for prostate cancer prognosis	4
2.	Permethylated MALDI-TOF m/z and corresponding N-glycan structures for PAP	60
3.	Permethylated MALDI-TOF m/z and corresponding N-glycan structures for PSA	61
4.	PAP glycopeptides with corresponding N-glycan structures identified by QTRAP	67
5.	Proteins identified in pre-DRE urine	81
6.	Proteins identified in post-DRE "EPS" urine.....	83
7.	Proteins identified in direct EPS fluids.....	87
8.	Permethylated PAP glycans from normal, BPH, and PCa EPS urine pools analyzed by MALDI-TOF.....	105
9.	Permethylated PSA glycans from normal, BPH, and PCa EPS urine pools analyzed by MALDI-TOF.....	107
10.	EPS urine PAP glycopeptides and their corresponding N-glycan structures identified by triple quadrupole MS/MS analysis.....	112
11.	Permethylated glycans from EPS urine pools.....	116
12.	Permethylated glycans from low and intermediate direct EPS pools.....	117
13.	Shared PAP glycans between seminal plasma and EPS urine pools.....	123

LIST OF FIGURES

Figure	Page
1. The prostate gland.....	2
2. Example oligosaccharide structures of O- and N-linked protein glycosylation ...	12
3. N-linked oligosaccharide subtypes	13
4. Components of a mass spectrometer.....	26
5. Seminal plasma fractionation by thiophilic adsorption chromatography	51
6. Normal phase HPLC separation of 2-AB derivatized N-linked glycans from PAP.....	52
7. Normal phase HPLC separation of 2-AB derivatized N-linked glycans from PAP treated with sialidase.....	54
8. Normal phase HPLC separation of 2-AB derivatized N-linked glycans from PSA.....	55
9. Normal phase HPLC separation of 2-AB derivatized N-linked glycans from PSA treated with sialidase.....	56
10. Thiophilic adsorption chromatography of redefined seminal plasma pools.....	58
11. Normal phase HPLC separation of 2-AB derivatized N-linked glycans from PAP from the refined second sample pool.....	59
12. MALDI-TOF analysis of permethylated PAP glycans from prostate cancer seminal plasma.....	62
13. Precursor ion scan for 163 m/z hexose of tryptic PAP peptides.....	64
14. Precursor ion scan for 292 m/z hexose of tryptic PAP peptides.....	66
15. Comparison of pre-DRE urine to post-DRE urine.....	79
16. ID-PAGE analysis of TAC fractionated EPS urine samples	88
17. 2D-PAGE western blot analysis of PSA and PAP in EPS urine samples	90

18.	Concentration of PSA and PAP in EPS urines	92
19.	Triple quadrupole ion trap configuration for precursor ion scanning.....	101
20.	Thiophilic adsorption chromatography of EPS urine pools.....	103
21.	MALDI-TOF spectra of permethylated PAP glycans derived from EPS urine samples.....	106
22.	MALDI-TOF spectra of permethylated PSA glycans derived from EPS urine samples.....	108
23.	Precursor ion scan for 163 m/z hexose of chymotryptic EPS urine PAP peptides.....	110
24.	Precursor ion scan for 366 m/z hexose of tryptic EPS urine PAP peptides.....	111
25.	MALDI-TOF spectra of EPS urine N-glycans.....	114
26.	MALDI-TOF spectra for permethylated direct EPS N-glycans.....	115
27.	MALDI-TOF/TOF LIFT spectra of a permethylated glycan structure from EPS urine.....	118
28.	Heat map overview of MALDI-TOF spectra for peak 2793.....	119
29.	Heat map overview of MALDI-TOF spectra for peak 2967.....	120

CHAPTER I

INTRODUCTION

1.1 Prostate Cancer

Prostate cancer is the most common and second most fatal cancer afflicting men in the United States, excluding non-melanoma skin carcinomas. It is estimated that in 2009 there were 192,280 new cases of prostate cancer and 27,360 deaths attributable to prostate cancer¹. Studies show that prostate cancer prevalence is proportional to age², and can lead to osteosclerotic metastases³. Additionally, African-American men and men with a family history of prostate cancer are at increased risk for developing prostate cancer and death due to their cancer¹. The human prostate is a small walnut-sized glandular male reproductive organ that is located below the urinary bladder and in front of the rectum (Figure 1). There are three zones of the prostate (central, peripheral, and transition), with each zone being responsible for the three main disorders of the prostate in humans, namely prostatitis (infections), benign prostatic hyperplasia (BPH, organ enlargement), and carcinoma (malignant tumors)⁴. The central zone makes up approximately 25% of the prostatic glandular tissue, and is responsible for only 1-5% of carcinomas. The peripheral zone is the largest zone, is where most cases of prostatitis arise from, and up to 70% of carcinomas are located. Finally, the transitional zone is responsible for BPH and roughly 20% of carcinomas⁴ (Figure 1). The American

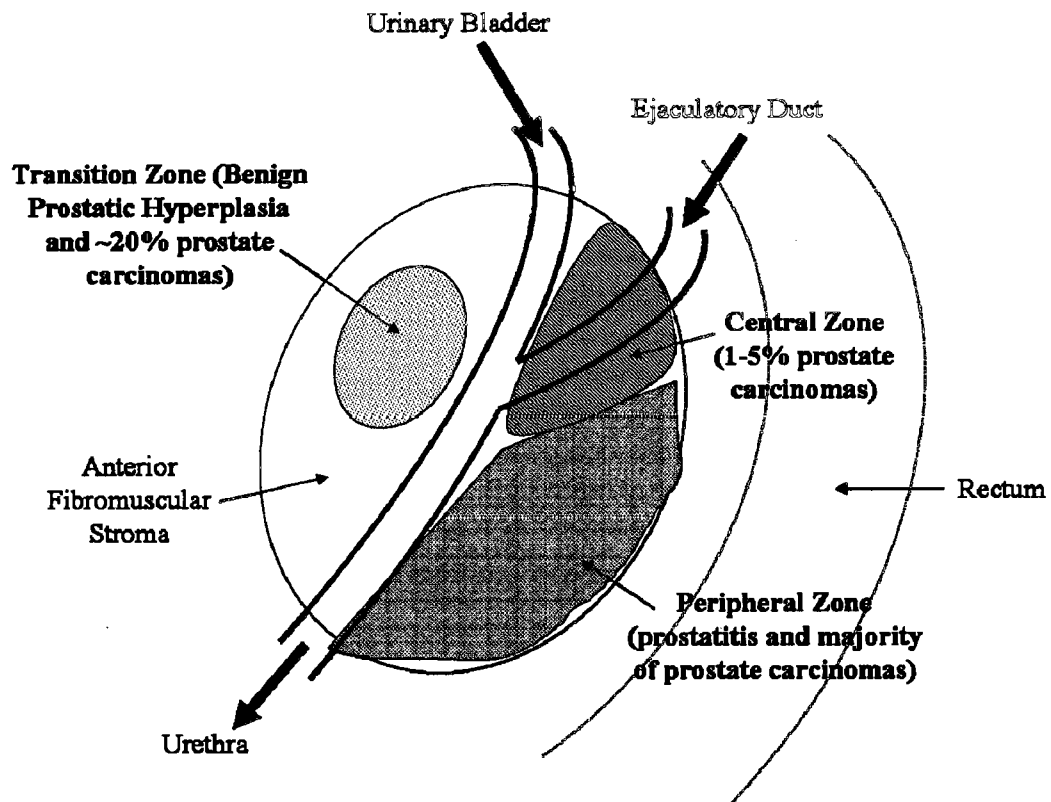


Figure 1. The prostate gland. There are three main zones of the prostate. The central zone is responsible for 1-5% of carcinomas, and makes up approximately 25% of the prostatic glandular tissue. The peripheral zone is the largest zone, is where most cases of prostatitis arise from, and up to 70% of carcinomas are located. Finally, the transitional zone is responsible for approximately 20% of carcinomas, and is the location for benign prostatic hyperplasia.

Urological Association (AUA) recommends for healthy men to start prostate cancer screening at age 50 (or as early as 40 for high-risk populations), with screening tests inclusive of a serum PSA test and a digital rectal exam (DRE). A PSA value above the age-specific median (i.e. 0.7 ng/ml for 40 year old men), or an abnormal DRE (size, contour, consistency) may prompt the clinician to recommend a prostatic biopsy. The next course of action will be determined based on the biopsy results, which can include watchful waiting/active surveillance, radical prostatectomy, radiation therapy, or brachytherapy if the presence of localized tumors are detected⁵. The Gleason score is a grading system which aids in determining the severity of a given prostate carcinoma. This system is named after Dr. Donald F. Gleason, who developed the technique along with other members of the Veterans Administration Cooperative Urological Research Group (VACURG)⁶. The Gleason grading system relies solely on the cellular growth patterns of prostate carcinomas, with a higher score indicating increasing cellular differentiation. There are nine growth patterns, all of which the Gleason grading system organizes into five histological grades⁶. From these five grades, a score between two and ten is assigned to the tumor based on the sum of the primary and secondary grade patterns (i.e. grade 3 + grade 4= Gleason score of 7). The primary grade represents the predominant pattern present, while the secondary grade represents the second most prevalent pattern⁶. It is imperative to know the two grades comprising the Gleason score, as 4+3 is a more severe score of seven than 3+4. The Gleason score, along with a serum PSA value and clinical staging of the tumor, allow for a clinician to assess a patient's cancer as low, intermediate, or high risk (Table 1). With the abundant advances in prostate cancer early detection, it has become evident that many cases involve clinically

Table 1. Risk stratification schemes for prostate cancer prognosis

Prostate Cancer Risk	serum PSA value	Gleason Score	Clinical Stage	Natural History
Low Risk	≤ 10 ng/ml	≤ 6	T1c or T2a	Often indolent disease, progression uncommon
Intermediate Risk	10 to 20 ng/ml	7	T2b, but not qualifying for high risk	Meaningful risk of progression that is of concern to most patients
High Risk	> 20 ng/ml	8 to 10	T2c	Significant risk of progression

Current clinical practices use a combination of factors to determine the risk of prostate cancer progression in men presenting with cancer-positive biopsies. A low risk classification indicates that the cancer is not likely to progress to a more severe state; with patients typically presenting with serum PSA values less than 10 ng/ml, a Gleason score of less than 6, and a clinical staging of T1c or T2a. Classification of intermediate risk is based on the patient presenting with a serum PSA value between 10 and 20 ng/ml, a Gleason score of 7, or a clinical staging of T2b. These tumors have a moderate potential of progressing to more aggressive disease, and treatment options should be evaluated. Finally, prostate tumors classified as high risk will most likely progress to aggressive disease, with patients presenting with a serum PSA value over 20 ng/ml, a tumor Gleason score of 8 to 10, or a clinical staging of T2c. Table adapted from D'amico et al., 1998 and Thompson et al., 2007.

insignificant prostate carcinomas. This has led to overdiagnosis of prostate cancer in men, and comes along with various other complications that these men may not have otherwise suffered from. The U.S. Preventative Services Task Force (USPSTF) determined that treatment of prostate cancer due to screening protocols may lead to erectile dysfunction, urinary incontinence, bowel dysfunction, and death⁷. In addition, the USPSTF determined that the risks and benefits of prostate cancer screening in men under 75 years of age cannot be assessed at this time, and that it is not recommended to screen for prostate cancer in men over 75 years old⁷.

Prostate Specific Antigen as a Biomarker

Prostate specific antigen (PSA) is a 28.4 kDa glycoprotein that is secreted by the prostatic epithelium. It is synthesized by both healthy and diseased prostate tissue^{8,9}, and its transcription is androgen-regulated¹⁰. It has a physiological role of liquefying seminal fluid^{11,12}, and is thought to do so by proteolytically digesting seminal fluid proteins such as semenogelin-1 and -2¹³. This kallikrein serine protease (hK3) was first described in 1966, further characterized in 1971 by Hara et al¹⁴, and first detected using a serum-based test in 1980 by Pasidero et al¹⁵. PSA levels in seminal fluid are typically within the range of 100-400 ug/ml, however they have been reported to be as high as 3 mg/ml¹⁶. With tight regulation, it is common for only small amounts of PSA to leak into the blood stream, leading to serum PSA concentrations to be normally 10-fold lower than PSA levels in seminal fluid¹⁷. Previously, and as early as 1960, other groups had performed various immunological studies and found multiple antigens specific to prostatic tissue¹⁸⁻²⁶, some of which were later found to be similar to PSA²⁷⁻²⁹. Initial studies on “prostate-

specific antigens” were focused on finding markers for chronic prostatitis, infertility, forensic purposes, contraception, and cancer²⁹. An immunoassay for the detection of PSA for prostate cancer diagnoses was developed and refined by Chu et al. in the early 1980s³⁰⁻³². Stamey et al. followed up these initial studies with a large study using a significantly higher number of serum samples in 1987, finding that PSA serum levels correlated with stages of prostate cancer as well as tumor volume, that PSA was a better biomarker than the current clinical biomarker prostatic acid phosphatase (PAP), and that PSA could also be used as a marker to monitor tumor response to radiation therapy³³. Clinically, serum PSA levels have been used as a diagnostic marker for prostate cancer, with Myrtle et al.³⁴ setting the threshold for serum PSA levels at 4.0 ng/ml in 1986, and the U.S. FDA approving PSA as a marker to monitor patients being treated for prostate cancer in the same year. PSA was not approved as a diagnostic prostate cancer biomarker by the U.S. FDA until 1994. To date, PSA is the clinical biomarker routinely measured in serum for detection of early prostate carcinomas^{33,35,36}. However, it has more recently been determined that the levels of PSA in serum do not efficiently distinguish between non-cancerous prostatic pathologies, such as benign prostatic hyperplasia (BPH) and prostatitis, and prostate cancer³⁷⁻³⁹. Outside of disease, other factors such as age, body mass index (BMI), and race also affect serum PSA concentrations⁴⁰. Therefore, the PSA index, which is defined as free PSA (fPSA) expressed as a percentage of total PSA (tPSA), has been used to improve PSA specificity⁴¹. However, this value does not facilitate diagnosing prostate cancer in patients with a serum PSA score of less than 10 ng/ml⁴², and additional studies report that there is a 20.5% mean prostate cancer incidence where serum PSA levels were between

2.5 and 4.0 ng/ml⁴³. These discrepancies lead to many unnecessary tissue biopsies, which in turn decrease patient quality of life, and therefore there is a pressing need to improve the specificity of PSA as a biomarker, and continue to evaluate additional biomarkers.

Prostatic Acid Phosphatase as a Biomarker

Prostatic acid phosphatase (PAP) is a 50 kDa dimeric glycoprotein which is found in several human tissues such as platelets, lungs, osteoclasts, erythrocytes, liver and kidney^{44, 45}, however it is present in 100-fold higher concentrations in human prostatic tissue as compared to other organs⁴⁶. As one of five functions by hydrolyzing organic monophosphate esters⁴⁷. A definitive physiological role of PAP within the reproductive tract of men has yet to be established. PAP was the earliest biomarker for prostate cancer, and is still used today in the clinic as a marker for metastatic prostate disease^{48, 49}. PAP was first linked to prostatic tissue in 1935³⁴, and subsequently deemed a prostate cancer biomarker for the next 50 years^{34, 50}. However, with the discovery of PSA and its apparent organ specificity, PAP was quickly replaced in part due to the wide-spread distribution of acid phosphatase isoenzymes throughout the human body³³. The original clinical assay for PAP assessed the levels of enzymatic activity in serum, yet early assays were unable to determine if the activity detected was from prostate-derived PAP. Various techniques were used to try to improve such assays, including the addition of L-tartrate to inhibit PAP derived directly from human prostatic tissues⁵¹, as well as the use of thymolphthalein phosphate substrates⁵². However, these additions still could not compete with the serum-based PSA test. Serum PAP's sensitivity was also criticized,

and it was found that for early screening, PAP had a sensitivity of 45%, which paled in comparison to a value of 96% sensitivity for PSA³³. In addition to early screening, serum PSA was also found to be a more sensitive marker than serum PAP for prostate cancer staging⁵³. In 1997, O'Dowd et al. declared that PAP was no longer useful in the clinical staging of early prostate carcinomas⁵⁴, which truly ended PAP's era as a prostate cancer biomarker.

Additional Prostate Cancer Biomarker Candidates

In addition to PSA and PAP, other candidate molecules have also been examined for their potential at diagnosing and staging prostate cancer. For example, prostate stem cell antigen (PSCA) is a glycosylphosphatidylinositol-anchored cell surface antigen located primarily in prostatic tissue and is thought to contribute to cellular proliferation and signal transduction⁵⁵. Elevated PSCA levels positively correlate with higher Gleason grades in advanced prostate carcinomas, and is also potentially associated with androgen-independent prostate cancer^{56, 57}. However, most of these studies utilize prostate tissue, with only one study which detected PSCA in peripheral blood samples⁵⁸. Additionally, it has yet to be determined if PSCA is a better diagnostic marker than PSA³⁴. Prostate-specific membrane antigen (PSMA) is a type II integral membrane protein which is found in the cytosol in normal prostate tissue and in the plasma membrane in prostate cancer tissue^{59, 60}. PSMA has been studied extensively with results showing that protein serum levels increase with prostate cancer and metastatic prostate cancer, and PSMA is detectable in both serum and prostate tissue⁶¹⁻⁶⁵. In addition, another study indicated that PSMA levels are much higher in prostate cancer patients as compared to healthy patients

and patients with BPH⁶⁶. However, more studies are needed to confirm the clinical utility of PSMA in early diagnosis of prostate carcinomas³⁴. Transmembrane protease serine 2 (TMPRSS2) is a transmembrane serine protease which is expressed primarily in prostate tissue⁶⁷. In situ hybridization and microarray studies have shown that *TMPRSS2* expression is androgen regulated, and that TMPRSS2 is expressed in normal and cancerous prostate basal cells, unlike other serine proteases, like PSA, which are found in the prostate secretory cells⁶⁷. This indicates the role TMPRSS2 may play in a smaller subset of prostate carcinomas, allowing for an additional and alternative route of prostate cancer diagnosis. Prostasin is another membrane-bound serine protease, which while it is expressed in most human tissues; its expression is highest in prostate tissue⁶⁸. The soluble form of prostasin is easily purified from seminal fluid⁶⁸, and is N-linked glycosylated⁶⁹, indicating its utility as a prostate cancer biomarker target. These candidate biomarkers are all localized to the cell surface and some are found in a secreted form as well, demonstrating their potential role in prostate carcinoma, as well as making them easier targets than intercellular molecules. Two additional candidate markers for prostate cancer, 73-kDa type II Golgi membrane antigen (GP73; GOLPH2) and α -methyl-Co-racemase (AMACR) are not localized to the cell surface; however they have been shown to be tissue-specific, and have proven to still be reliable markers. GP73 is a Golgi phosphoprotein which has previously been shown to be a useful serum marker for hepatocellular carcinoma⁷⁰⁻⁷³. More recently, GP73 mRNA transcripts found in human sedimented urine samples have shown effectiveness in diagnosing early prostate carcinomas⁷⁴. Additionally, it has been shown to be upregulated in prostate cancer tissues as compared to normal, healthy prostate tissues⁷⁵, showing its value as a prostate

cancer biomarker. Finally, *AMACR* is primarily localized to the peroxisomes and mitochondria within prostatic tissues, and has been found to be overexpressed in prostate carcinoma tissues⁷⁶⁻⁷⁸. Its clinical utility has been shown by the relatively high sensitivity and specificity *AMACR* has for diagnosing prostate cancer⁷⁹. Furthermore, genomic and single nucleotide polymorphism (SNP) studies of *AMACR* have indicated a role this gene plays in both early prostate carcinomas and familial prostate cancer⁸⁰⁻⁸². Overall, there are many candidate markers for the early diagnosis and prognosis of prostate cancer; however, none of these markers, like PSA and PAP, have yet to aid in decreasing the number of unnecessary biopsies and radical prostatectomies that still afflict many men today.

1.2 Protein Glycosylation

Subcellular molecules located both inside and outside the cell and containing carbohydrate components are called glycoconjugates, namely glycoproteins, glycolipids, proteoglycans, and glycosaminoglycans. Protein glycosylation is a common post-translational modification which has proven to be a useful disease marker^{83, 84}, with many studies outlining altered glycosylation patterns in cancerous samples as compared to normal healthy samples^{85, 86}. Protein glycosylation has long been shown to be altered in cancerous tissues as compared to normal tissues, suggesting that characterization of this type of post-translational modification could lead to more specific biomarkers in the clinic. Proteins become glycosylated in both the endoplasmic reticulum (ER) and the Golgi apparatus (Golgi), where post-translational processing occurs prior to transport. Fully processed glycoproteins are most commonly found in lysosomes, attached to the

outside of the cell surface, and in the extracellular matrix; however there have been several examples of both nuclear and cytoplasmic glycosylation⁸⁷⁻⁹¹, all of which seem to be an addition of a single monosaccharide, unlike the complex oligosaccharide structures seen on other glycoproteins⁹¹. There are two main types of glycosylation of proteins as they are processed in the ER and Golgi: O-linked and N-linked (Figure 2).

O-linked Glycosylation

O-linked glycosylation occurs in the Golgi apparatus and involves the attachment of monosaccharide residues to the hydroxyl group of either serine or threonine in a sequential manner. This is achieved by glycosyltransferases present in the Golgi. These carbohydrate chains are typically 1-4 units long, and most commonly begin with the addition of N-acetylgalactosamine to the protein (Figure 2). Therefore most often O-glycans refer to the O-GalNAc linkage, although O-GlcNAc and O-mannose are alternative linkages. The most common examples of an O-linked glycoprotein are mucins, which are a class of secreted and plasma membrane glycoproteins having several clusters of O-linked glycans. These proteins contain regions rich in serine, threonine and proline residues.

N-linked glycosylation

N-linked glycosylation is achieved through a more complex process than O-linked modifications and results in three main classes of N-linked oligosaccharides: 1) high-mannose-type, 2) complex-type, and 3) hybrid-type (Figure 3). A preformed 14-carbohydrate oligosaccharide which is attached to a dolichol donor is a structure common

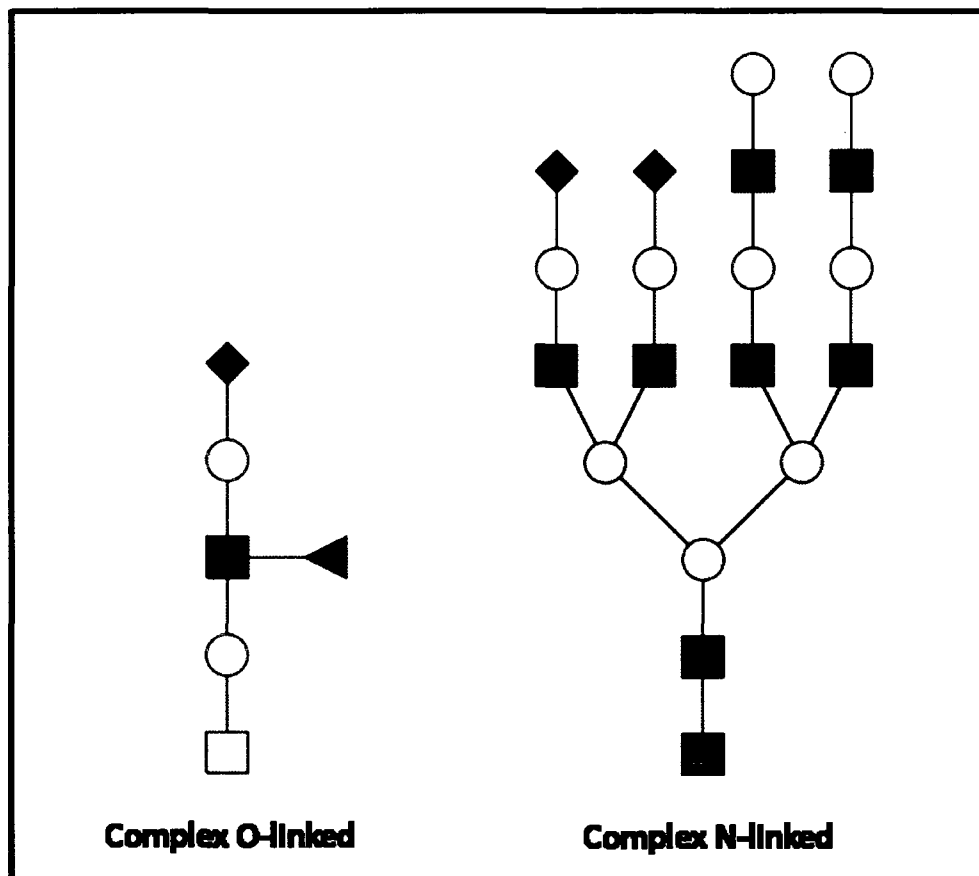


Figure 2. Example oligosaccharide structures of O- and N-linked protein glycosylation. O-GalNAc is the most commonly observed O-linkage to serine or threonine residues on proteins. This representative complex O-GalNAc glycoform can be found attached to human respiratory mucins. The most basic O-GalNAc core structure is observed linked to a single galactose residue, however it can be extended, branched, and terminated by fucose in various linkages, sialic acid in α 2-3 linkage, or sialic acid α 2-6-linked to the core GalNAc. N-linked oligosaccharides are typically more complex structures as compared to O-linked oligosaccharides, with extensive branching and extension off of the universal pentasaccharide core. Adapted from Varki et al, 2009. Cartoon representations are as follows: ■ =GlcNAc, ○ =Mannose, ○ =Galactose, ▲ =Fucose, ◆=NeuAc, □=GalNAc

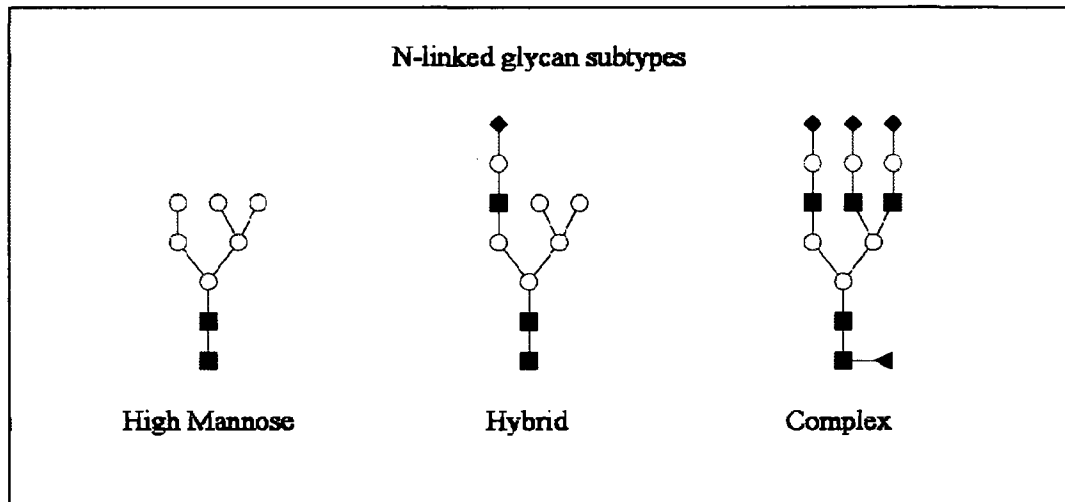


Figure 3. N-linked oligosaccharide subtypes. There are 3 distinct subtypes of N-linked glycans, each based on the type of monosaccharides present in the oligosaccharide branching chains. High-mannose structures consist of the core structure plus any number of mannose monosaccharides decorating the terminal branches. Complex subtypes consist of the core pentasaccharide with any number of monosaccharides and various branching patterns. These structures are usually decorated with a combination of N-acetylglucosamine, N-acetylgalactosamine, galactose, sialic acid and fucose monosaccharides. It is also common to see the core N-acetylglucosamine bound by a “core” fucose. Finally, the hybrid subtypes are classified by having one main arm resembling a high-mannose structure, while the other arm resembles a complex structure, therefore being termed a “hybrid” of these two different subtypes. Cartoon representations are as follows: ■ =GlcNAc, ○ =Mannose, ○ =Galactose, ▲=Fucose, ◆=NeuAc, □=GalNAc

to most eukaryotic cells. This compound consists of three glucose, nine mannose, and two N-acetylglucosamine molecules and is attached to dolichol by a pyrophosphoryl residue. Dolichol is a long-chained polyisoprenoid lipid embedded in the ER membrane. The carbohydrate residues are added in a concerted manner by specific enzymes. This process begins on the cytosolic face of the ER with the addition of the two GlcNAc and five mannose residues in a sequential manner. At this point, the structure “flips” so that it is now on the luminal face of the ER. The next seven carbohydrates (four mannoses and three glucoses) are added one at a time from a nucleotide-sugar donor (UDP) to a dolichol molecule embedded on the cytosolic face of the ER. The dolichol-sugar moiety then flips to the lumen face and each monosaccharide is transferred to the growing sugar chain. As a protein is being elongated co-translationally into the ER lumen, an N-linked glycosylation site will be recognized and the 14-mer oligosaccharide is transferred to the nascent protein chain by an enzyme called oligosaccharyl transferase. The oligosaccharide is covalently attached to the amide nitrogen of asparagine residues that are followed by any amino acid except proline, followed by either a serine or threonine (N-X-S/T). This tripeptide sequence is recognized and triggers the transfer of the oligosaccharide from dolichol to the protein en bloc. However, only about thirty percent of these sites end up being occupied, with the remaining sites believed to be blocked by the protein folding process which is occurring at the same time⁹². Immediately, the three glucose residues and one mannose residue are removed, each by a different glycosidase. It is thought that the glucose residues serve as a signal to indicate that the oligosaccharide is ready for transfer to the protein as well as to indicate that the protein has achieved proper folding and is ready for transport to the cis Golgi⁹². The glycoprotein will be

further processed in the ER and Golgi apparatus; however the pentasaccharide “core” of two GlcNAc and 3 mannose residues is common to all N-linked glycans. The glycopeptide will then be transported to the cis Golgi where it will be further modified. For example, secretory or plasma membrane proteins will lose an additional three mannose residues. Typically while in the medial Golgi, two more mannoses are removed, followed by the addition of two GlcNAc and one fucose residues. Finally, the glycoprotein will receive one GlcNAc, one galactose, and one sialic acid while in the trans Golgi⁹². The complexity and structure of N-linked carbohydrates is determined both by the sequence and conformation of the protein itself as well as the type of glycosyltransferases present in the Golgi during the glycosylation process. N-linked glycans are typically branched and can be highly decorated. By the time the protein reaches the trans Golgi, it will be completely modified and ready for transport. In disease states, it is believed that the great biodiversity of both glycosyltransferases and glycosidases present in the vertebrate Golgi are responsible for alteration of “normal” glycosylation patterns⁹².

The Carbohydrate-Cancer Connection

Cancer progression has several stages including proliferation, invasion, angiogenesis, metastasis, and immunity; all of which may be affected by a number of glycoconjugates as indicated by innumerable published studies^{83, 93-95}. The first stage, tumor proliferation, begins with the deregulation of the cell cycle by a disruption in the balance of tumor suppressors and oncogenes. Correlations between tumor proliferation and carbohydrates have been difficult to determine, however it seems that glycoproteins

and glycolipids most commonly play a role in this stage of cancer progression. For example, N-linked glycosylation of the insulin-like growth factor 1 receptor (IGF1R) has been shown to necessitate the phosphorylation and translocation of IGF1R, therefore leading to growth and survival of melanoma and sarcoma cells⁹⁶. In addition, extensive studies have shown the role of mucins and other O-linked glycans in the role of tumor proliferation⁹⁷⁻⁹⁹. The mucin MUC4 gene has been shown to be over-expressed on the surface of mammary tumor cells as compared to normal mammary epithelium¹⁰⁰. MUC4 is responsible for the up-regulation of the epidermal growth factor (EGF) receptor ERBB2, which then aids in the inhibition of apoptosis, a common occurrence in tumor proliferation⁹⁷.

After tumor cells begin to proliferate and the tumor continues to grow, the peripheral cells then begin to detach from each other and from the extracellular matrix, where they then invade and migrate through adjacent tissue. This invasion process requires many factors, including the alteration of cell-surface receptors and their ligands, as well as proteases and glycosidases to degrade the extracellular matrix. These changes require the aid of glycoconjugates such as N-linked and O-linked glycoproteins, and proteoglycans. For example, increased sialylation has been shown to play a vital role in tumor invasion, likely due to the highly negative nature of sialylated glycoforms which may aid in the cellular detachment stage^{93, 101}. Once tumor cells begin to rapidly grow and spread, they need additional nutrients and therefore must create their own vasculature to supply such nutrients, a process known as tumor angiogenesis. Heparan sulfate proteoglycans are the most commonly seen glycoconjugates involved in tumor angiogenesis. Certain pro-angiogenic factors, such as vascular epithelial growth factor

(VEGF), interleukin-8 (IL-8), and platelet-derived growth factor (PDGF) to name a few, bind heparan sulfate¹⁰², indicating a correlation between these proteoglycans and tumor angiogenesis.

The next stage in cancer progression involves the movement of tumor aggregates to distant organs, also known as metastasis. Selectins are cell-surface receptors responsible for cell-cell adhesions which are involved in tumor metastasis. Their ligands often carry O-linked oligosaccharides decorated with sialic acid, fucose, and sulfate^{92, 93}. Examples of these ligands are the Lewis type blood group antigens, specifically sialyl Lewis X (SLe^X) and sialyl Lewis A (SLe^A), which are shown to be over-expressed on tumor cells as compared to their normal cellular counterparts for lung, colon, gastric, and pancreatic cancers^{93, 103-105}. CA19-9 is a sialyl Lewis A serum tumor biomarker which is used to detect many gastrointestinal cancers. However, there are many false positives using this serum test, as CA19-9 will sometimes also recognize certain inflammatory states of the aforementioned tissues¹⁰⁶. Specific to prostate cancer, cancerous cells have a tendency to metastasize to bone, and it is thought that E-selectin with the aid of sialyl Lewis X is responsible for the binding of circulating prostate tumor cells to the bone marrow endothelial cells¹⁰⁷. The final stages of cancer progression involve the alteration of host immunity, which allows the tumor to continue to grow and spread throughout the host organism. While little is known about the role of glycosylation in this final stage, some studies have shown that certain glycosphingolipids and O-linked glycoproteins may be involved in immune silencing, allowing the tumor to evade the cytotoxic effects of the host immune system^{93, 108}.

Due to the widely-seen involvement of glycosylation in various cancer systems, it is likely that altered glycosylation states are involved in prostate cancer progression as well, and that these changes can be detected by mass spectrometry-based strategies. A few reports have shown that the overexpression of O-glycosylated mucins are involved in prostate cancer progression¹⁰⁹⁻¹¹¹, while others have associated altered N-glycosylation patterns with prostate cancer, either globally¹¹², or protein-specifically^{113, 114}. In particular, the glycosylation of PSMA was studied in prostate cancer tissues, serum, and metastatic cell lines (LNCaP), indicating the presence of complex N-linked glycans on in vivo sources of PSMA, and high mannose N-glycans on PSMA from immortalized cell lines¹¹³.

PSA glycosylation

Previous studies on PSA glycosylation have compared seminal plasma from healthy donors to prostate tumor metastatic cell line LNCaP¹¹⁵⁻¹¹⁷, as well as normal seminal plasma to prostate cancer and BPH sera¹¹⁸. PSA contains 8% carbohydrates by mass¹¹⁹, and has one glycosylation site at asparagine (Asn)-45¹²⁰. The structure of this glycan has been previously reported to be of either high-mannose subtype¹²¹ or a complex sub-type with frequent sialylation, core fucosylation, and a number of terminal N-acetylgalactosamines (GalNAc) when purified from healthy seminal plasma samples¹¹⁷. PSA glycans isolated from LNCaP cell lines have also been characterized as having some triantennary structures¹¹⁶, as well as decreased sialic acid content and the presence of increased fucose and GalNAc content¹¹⁵. Because of advances in the PSA serum test which include the comparison of different forms of PSA, a recent study was

completed that monitored the presence of sialic acid monosaccharides on free and proPSA in serum, seminal plasma and tissues from both healthy and prostate cancer patients¹²². This study did not detect any significant differences in sialylation among the different groups or sample sets¹²². A second study compared free and complexed PSA glycans derived from serum, concluding that the glycans from both forms of PSA were primarily sialylated and fucosylated biantennary structures¹²³. Although less prevalent, the presence of a few multiantennary complex structures were detected as well¹²³. However, for the aforementioned studies, the specific composition and anomeric structural configurations for each oligosaccharide isolated were not determined, and these studies involved analysis of samples obtained from very few clinical samples.

PAP glycosylation

PAP has three glycosylation sites at Asn-62, Asn-188, and Asn-301^{124, 125}, making it a more difficult target for site specific structural characterization, yet one that may be a suitable complement to PSA. Earlier X-ray crystallography of PAP from normal seminal plasma has found the Asn-62 and Asn-301 glycan modifications consisted of primarily high mannose oligosaccharides, while glycans at Asn-188 had more complex structures containing sialic acid and fucose¹²⁴. In relation to cancer, one study involving lectin analysis of PAP derived from tissue in BPH and prostate cancer patients found evidence of a decrease in the high mannose chains of Asn-62 and Asn-301, as well as an increase of non-fucosylated hybrid structures in prostate cancer as compared to BPH¹²⁵. Similar to the studies on PSA glycosylation, these studies on PAP oligosaccharide content lack in

detailed structural information, and include low numbers of clinical samples used for each study.

1.3 Proximal Fluids of the Prostate for Biomarker Discovery

Proximal fluids are defined as any fluid found adjacent to a given tissue. It is currently understood that proximal fluids are a great source for biomarker discovery¹²⁶, with seminal plasma and expressed-prostatic secretion (EPS) fluids both being proximal to the prostate. In addition, PSA and PAP protein concentrations are much higher in both seminal plasma and EPS fluids relative to blood¹²⁷, allowing for enhanced purification, detection, and analysis of these biomarkers. Seminal plasma consists of fluids originating not only from the prostate, but also from several other male accessory glands such as the seminal vesicles, epididymis, and Cowper's gland¹²⁸. Seminal fluid has been used in research and the clinic for many purposes outside of the cancer realm, and has also been analyzed in several studies for biomarker purposes related to both prostate and testicular cancers¹²⁸⁻¹³⁰. Clinically, the term "expressed" is used to describe the process of manually squeezing a gland, which results in fluid being expelled and subsequently collected. EPS represents the fluid being secreted by the prostate following a prostate massage, which in turn is excreted via the urethra alone or with urine. This fluid is commonly collected in the clinic to examine chronic prostatitis and inflammatory chronic pelvic pain syndrome¹³¹. In addition, the cellular sediment obtained from EPS fluids is currently being used for prostate cell-associated PCA3 mRNA testing (Gen-Probe Inc, San Diego, CA). These studies aim to develop a genetic based clinical assay by using the mRNA levels of PCA3 as a marker for prostate cancer^{74, 132-134}. Using these EPS fluids

for protein-based biomarker discovery or in the clinic for biomarker screening has yet to gain popularity. Because these fluids should be enriched for prostatic proteins that may be difficult to detect in serum, it seems likely that they have high utility in the clinic for the screening and potential staging of prostate cancer.

1.4 Proteomics, Glycomics and the Advances of Mass Spectrometry

With the completion of the Human Genome Project in 2001¹³⁵, researchers began focusing on the next level of discovery, that of the human proteome as well as proteomes of many other species. The term “proteome” was first coined in 1994¹³⁶ and was initially defined as the protein complement to the genome, with “proteomics” being defined as the study of protein structure and function in a specific sample (i.e. tissue, cell, or bodily fluid) at a specific time. While the human genome is complex, the complementing proteome contains even more information, due to the fact that individual genes can give rise to many different proteins and isoforms of a protein. These protein profiles may be altered due to the physiological and pathological states at a given time in a given subject, and commonly, post-translational modifications are responsible for differing disease phenotypes¹³⁷. Due to these factors, it is possible to detect a protein-based biomarker that can differentiate between healthy and diseased states for many conditions, including cancer.

Two-Dimensional Electrophoresis

Two-dimensional electrophoresis (2DE) was and is still used today for initial sample separation for proteomics analyses. This separation methodology as applied to

proteins relies on two independent parameters that are functional properties of all proteins: 1) their molecular mass and 2) their isoelectric point (pI), the pH at which the net charge of each protein is zero. The pI of a protein is a property unique to each protein dependent on the total number of positively and negatively charged constituent amino acids. At a pH above the pI, a protein carries a net negative charge, and at a pH below the pI, a protein carries a net positive charge. These same properties also allow 2DE to separate proteins based on their post-translational modifications (i.e. glycosylation), particularly if these modifications are charged or have substantial mass. For most applications, the first dimension for 2DE is an isoelectrofocusing (IEF) step, followed by a conventional sodium dodecyl sulfate (SDS)-polyacrylamide gel separation based on molecular mass in the second dimension. The fundamental aspects of the most commonly used approaches of 2DE for protein separations were reported independently by Klose¹³⁸ and O'Farrell¹³⁹ in 1975. Original innovations in isoelectric focusing relied on the inclusion of multi-charged chemicals termed ampholytes, that when placed in an electric field would generate and align the ampholyte molecules into a pH gradient. Originally, this was accomplished by combining the ampholytes with acrylamide, and then polymerizing these solutions in glass tubes (referred to commonly as "tube gels"). While this was an effective way to perform IEF separations of proteins, the method required specialized equipment and was difficult to reproduce gel to gel. A major improvement in IEF was originally reported in 1982 by Bjellqvist et al.¹⁴⁰, who reported the creation of immobilized pH gradient (IPG) strips. Ampholyte molecules were replaced by acidic and basic acrylamido derivatives that are co-formed with acrylamide gel polymerization on plastic backed strips; hence, the tube gels have been replaced by

these IPG plastic strips. These improvements in the IEF component of 2DE have driven increased use of this approach in proteomics. It is necessary to keep in consideration how the samples will be analyzed post-2DE. Protease inhibitors play an important role in maintaining the integrity of a sample's proteome; however some, such as phenylmethylsulfonyl fluoride (PMSF), can interfere with downstream analysis, such as tryptic digestion. Depending on the complexity of the sample(s) being analyzed, there may be too many spots to effectively compare and analyze with the human eye. Thus, there are various analysis programs available that can compare spots between gels. These programs are based on manually selecting a certain number of consistent landmarks between the gels to be analyzed, from which the software can then align the gels and determine any differential spots. Consequently, the most critical step of these analyses is spot detection and quantification. Alternatively, 2D gels can be transferred to a membrane such as PVDF for immunoblotting. At this point, proteins of interest can be detected by following a standard western blotting protocol, making this method useful when wanting to quickly visualize the possible multiple isoforms of one protein.

Development of Protein Sequencing Methods

After a decade of study, insulin was the first protein to be completely structurally characterized in 1954. This mammoth task was achieved by Frederick Sanger and his colleagues using a method termed the dinitrophenyl group-labeling (DNP) method, which covalently modifies the terminal amino acid in a peptide¹⁴¹. This DNP group gives the peptide a distinctive yellow color which allows for visualization using two-dimensional paper chromatography. In addition, the DNP group makes the derivatized amino acid

resistant to acid hydrolysis. In order to get a contiguous sequence, the sample was first fully hydrolyzed, and then sequential partial hydrolysis reactions were performed, allowing for larger and larger peptide fragments with overlapping sequence information. In concert with the DNP labeling method, partition (filter paper) chromatography, developed by A.J.P. Martin and R.L.M. Syngé in 1952, allows for the separation of the amino acids and peptides and was the basis for modern chromatography separation techniques¹⁴².

The year 1930 saw the first successful stepwise degradation of peptides performed by Abderhalden and Brockmann using phenylisocyanate (PIC)¹⁴³. However, it wasn't until Pehr Victor Edman altered the method and begun using phenylisothiocyanate (PITC) as a coupling reagent that the method gained popularity. The change in the reagent allowed for a more easily cleaved labeled amino acid, therefore allowing for more successful analysis. Today's amino-terminal sequencing methods are all based on the Edman degradation procedure¹⁴⁴. Edman degradation comprises of three steps. The first step is the coupling reaction where the free amino-terminal amino acid is labeled with PITC which forms a phenylthiocarbonyl (PTC) polypeptide. It is noteworthy that polypeptides that are modified at the amino terminal cannot be coupled with the PITC. The second step involves cleavage of the PTC-amino acid by acid hydrolysis creating an anilinothiazolinone (ATZ) amino acid. This step also results in a shortened polypeptide which can then be used for subsequent coupling and cleavage in repetitive cycles. The third and final step of Edman degradation involves conversion of the unstable ATZ amino acid into a more stable phenylthiohydantoin (PTH) derivative. Finally the derivatized amino acids are sequentially identified using HPLC. Automation of this

procedure was first performed in 1967 which automated the coupling and cleavage steps and allowed researchers to routinely identify the sequence of the first 30-40 amino acids in a given protein^{145, 146}.

History of Mass Spectrometry

While the Edman degradation method has been revamped and utilized for many years, the advances in mass spectrometry have almost but all replaced this protein sequencing method. Mass spectrometry based techniques are much more sensitive, can handle complex protein mixtures, and can be used in a more high-throughput manner. The idea of mass spectrometry dates back to 1897 when J.J. Thomson discovered electrons using cathode rays. He observed that the ions in the gaseous phase moved through the cathode ray tubes in a trajectory that were proportional to their “mass-to-charge” (m/z) ratios¹⁴². Based on his discovery, the first mass spectrometer called a parabola spectrograph was conceived. Over the decades more sophisticated instruments were developed. The first time-of-flight (TOF) analyzer was developed in 1946 by W.F. Stephens, with Wolfgang Paul creating the first quadrupole mass analyzer in the mid 1950's. Paul also created the first quadrupole ion trap, and the ion trap first became available commercially in 1983¹⁴⁷. Currently, TOF, quadrupole, and quadrupole ion trap technologies are the most widely used mass analyzers in mass spectrometry laboratories¹⁴⁷. All mass spectrometers have four basic components: an ionization source, a mass analyzer, a mass detector, and a data processor (Figure 4). The ionization source is responsible for converting the analytes from either their solid or liquid states into gaseous-phase ions. These ions are then transferred to the mass analyzer where they will be separated by either electric or

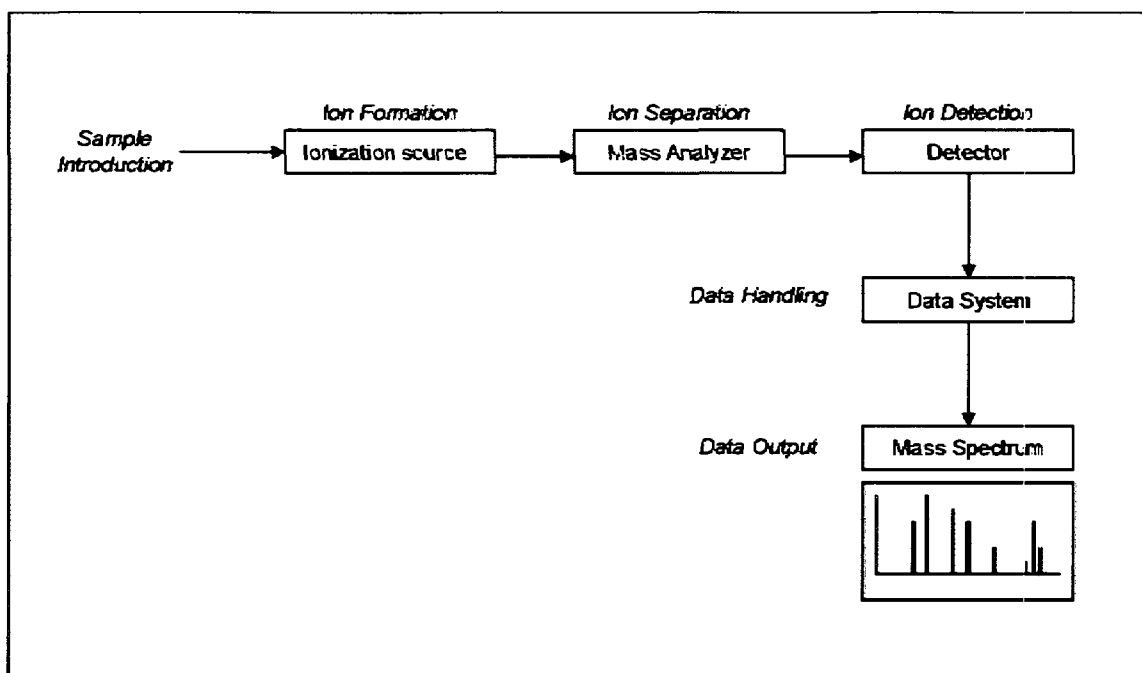


Figure 4. Components of a mass spectrometer. After the sample is introduced to the ionization source, the analytes are converted from either their solid or liquid states into gaseous-phase ions by the ionization source. The mass analyzer will then separate the ions by either electric or magnetic fields. The ions will then strike the detector individually based on their m/z value as they leave the mass analyzer. Finally, the data processor supplies the visual output of analyte information, showing both the m/z value and the relative abundance of each ion measured by the detector. Adapted from Simpson, 2003.

magnetic fields, which are commonly observed as a function of time. After traveling through the mass analyzer, the ions will strike the detector one at a time, based on their m/z value. The data processor is responsible for the visual output of analyte information, indicating both the m/z value and the relative abundance of each ion measured by the detector¹⁴².

Soft Ionization Mass Spectrometry

Fast atom bombardment ionization (FAB) was developed in the early 1980s^{148, 149} and was the first soft-ionization mass spectrometry technique available for use with proteins and peptides¹⁴². This technology works by dissolving the analyte (i.e. protein or peptide) in a nonvolatile liquid matrix (i.e. glycerol), which is then placed under vacuum in the instrument. Next, the sample-matrix mixture will be bombarded with a flow of fast-moving neutral atoms. These atoms usually derive from ionization of argon, and are used to change the analyte ions into a gaseous phase. This method allows for the analysis of ions that are 10,000 daltons or greater. Thus, this method is not optimal for small peptide fragments, or other small biochemical molecules.

For some instruments, a matrix is needed to help the analyte (sample) ionize and travel to the mass detector. Matrix-assisted laser desorption/ionization (MALDI) begins with the mixture of matrix and analyte. MALDI was first developed in 1988 by Karas and Hillenkamp¹⁵⁰. Matrices are acidic compounds which can be absorbed at different laser wavelengths, usually UV_{337nm}. The matrix is typically applied to the analyte in 1000-fold concentration¹⁴². For glycopeptide and glycan analyses, typically 2,5-dihydroxybenzoic acid (2,5-DHB) is used, as it is best at stabilizing the sialic acids on

acidic glycans. The analyte-matrix mixture is then applied as a few microliters to a target plate, where the plate itself can have different chemistries. The sample and matrix are allowed to co-crystallize prior to entering the instrument. Energy in the form of a pulsed UV laser is applied to the spot with the crystallized sample-matrix. The ions will excite and be desorbed from the solid matrix mixture and the matrix helps stabilize the singly-charged ions as they travel through a strong electric field, then through the TOF, and finally to the mass detector. The TOF mass analyzer will measure the m/z values of the analytes, which is calculated based on the time it takes for a specific ion to travel a set distance and strike the detector¹⁴².

Another soft-ionization technology termed electrospray ionization (ESI) was first developed in 1989 by Fenn et al¹⁵¹. Samples in a liquid phase (typically organic) are hit with a high-voltage potential as they are passed through a small capillary tube. The ions are then desorbed into the gaseous phase and rapidly evaporate into charged droplets. This process occurs due to both high heat and a strong electric field present at the tip of the capillary tube. From here, the samples will enter the mass analyzer, which is typically either an ion trap or a quadrupole. Unique to ESI, singly and multiply charged ions can arise from a single precursor ion as they travel out of the capillary and to the mass analyzer. This feature allows larger molecules (> 10,000 daltons) to be accurately evaluated by a mass analyzer such as the quadrupole or ion trap which typically have a limit of detection of 10,000 daltons. The number of charges an ion may carry as it evaporates off of the capillary is dependent on factors such as the voltage potential, the solvent pH and composition, and the analyte itself¹⁴². Fortunately, a high-resolving

instrument is capable of determining the charge state in addition to the mass of a given ion, providing the user with even more valuable data.

Tandem Mass Spectrometry and Liquid Chromatography Coupled to Tandem Mass Spectrometry

As a mass spectrometer first scans and detects the ions coming from the analyte, these initial spectra are full MS scans, representing parent ions. These intact parent ions can provide information all on their own, however even more information can be obtained by fragmentation of the parent ions. This secondary analysis is referred to as tandem MS, MS/MS, or MSⁿ. Fragmentation studies will offer structural information of the compound being analyzed. Most commercially available mass spectrometers using soft ionization are capable of tandem MS. A precursor (parent) ion is selected from the initial stage of analysis, an intermediate reaction event occurs, the resulting “product ions” are analyzed¹⁴². In the case of MSⁿ, these secondary stages are repeated consecutively on individual ion peaks until all information desired has been obtained. The intermediate reaction events are where the precursor ions are fragmented into product ions. These events require a source of high energy which varies based on the type of instrument being used, as well as the type of analyte being fragmented. The most common form of energy used is collision-induced dissociation (CID), which involves the use of an inert gas (i.e. helium or argon) to excite the ions and cause them to break apart.

There are two categories of tandem mass spectrometers. The first involves a tandem-in-space instrument which has multiple mass analyzers in tandem, each responsible for a specific set of analyses¹⁴². Examples of such instruments include

MALDI-TOF/TOF, triple quadrupole instruments, and hybrid mass spectrometers. The second category includes a tandem-in-time instrument that has only one mass analyzer, allowing for the tandem analyses to take place in the same analyzer; however the events are separated in time¹⁴². Examples of these types of tandem instruments include quadrupole ion trap analyzers coupled with either MALDI or ESI, and Fourier transform-ion cyclotron resonance (FT-ICR).

Numerous mass spectrometer instruments today work in conjunction with liquid chromatography (LC) systems, and these types of systems are commonly referred to as LC-MS/MS. These on-line systems allow for analyte separation prior to entry into the mass spectrometer, thus allowing for more in-depth analyses of a given sample. They also allow for gel-independent separation of highly complex peptide mixtures, which was first demonstrated by Hunt et al. in 1992^{136,152}. Most of these separations are achieved using reversed-phase high-performance liquid chromatography (RP-HPLC) coupled to ESI. This separation allows for complex mixtures to be applied to a mass spectrometer (i.e. seminal plasma or EPS fluids) without losing any protein or peptide information. To further improve the sensitivity of the MS/MS analysis, capillary columns can be utilized with this type of LC being referred to as nano-LC. These differ from traditional HPLC columns by being narrower, therefore slowing down the flow rate and also by functioning as the ionization source (i.e. nanospray ionization or NSI). This will also further concentrate the sample before it is sprayed into the mass spectrometer¹⁴².

Protein Identification by Mass Spectrometry

The emergence of protein databases began in the late 1970's and early 1980's as a result of the effectiveness of 2-DE protein profiles¹⁵³. Computer software programs capable of subtractive pattern analysis, clustering algorithms, and multivariate statistics were developed to complement these databases, allowing for further characterization of proteins isolated by 2-DE^{136, 154-157}. These early databases and software programs were never fully implemented due to the complexity of 2-DE analysis, as well as the growing popularity of soft ionization techniques in the late 1980's, causing for a surge of protein identification methods based on mass spectrometer analysis in the early 1990's^{136, 158}. Two main methods came from this decade: peptide mass finger printing (PMF) and tandem mass spectrometry. The first, PMF, is also known as peptide mapping or peptide mass mapping, and relies on a list of experimental peptide masses matching up to the calculated list of all peptide masses of a each protein entry in a given database, thus resulting in protein identification¹³⁶. Five groups separately, yet nearly concurrently, developed computer software capable of protein identification by PMF¹⁵⁹⁻¹⁶³. The PMF method is regularly used to identify gel-separated proteins, and almost universally used in conjunction with MALDI-TOF mass spectrometers¹³⁶. The second protein identification method utilizes tandem mass spectrometry by analyzing the fragmentation spectra and comparing it against a given database search engine using a mathematical algorithm, such as SEQUEST¹⁶⁴ or MASCOT, which can also be used for PMF searches¹⁶⁵. These two protein identification methods are still the most widely used today in proteomic studies today. The abovementioned search engines are used in conjunction with publically available sequence databases. Both protein sequence databases^{164, 166}, as well as the human genome library^{135, 167} have been established, with new protein sequences

constantly being added, thus allowing for on-going improvement to the accuracy of peptide searches.

Carbohydrate Structural Analysis by Mass Spectrometry

In 1988, Rademacher, Parekh, and Dwek first coined the term “glycobiology”, with the intention for the term to highlight the marriage of traditional carbohydrate chemistry and biochemistry disciplines to the modern cellular and molecular biology disciplines of glycans⁹². Today, the study of oligosaccharide, or glycan, structure and function can also be identified as glycomics. The term glycan is used to describe a chain of sugars, whether they be linear or branched.

Historically, structural N-glycan analysis is performed with the use of exoglycosidases and gel filtration chromatography, HPLC, or MALDI-MS¹⁶⁸. Full characterization of a given glycan molecule entails analysis of monosaccharide composition, sequence, branching, linkage, and anomericity of said glycan¹⁶⁹. However, obtaining all of the above information is difficult and tedious. The use of exoglycosidases and tandem MS are what allow for the elucidation of glycan structure and linkage. Exoglycosidases are enzymes with specificity for certain monosaccharides and in some cases, certain glycosidic bonds. For example, neuraminidase will only remove terminal sialic acids. The loss of the monosaccharide from the entire moiety is then monitored by the abovementioned methods. This stepwise process may be tedious and requires the availability of a wide range of exoglycosidases; however the end result is a complete structural determination of the glycan of interest. While this protocol was traditionally only applied to N-glycan analysis, it is commonly used for O-glycan

analysis as well¹⁷⁰. Most recently, the advances in mass spectrometers have allowed researchers to bypass the exoglycosidase steps and rely solely on MS/MS fragmentation data to analyze N-glycan structural information. Fast atom bombardment (FAB) mass spectrometry was the forefather in this type of analysis, but has been replaced by more sensitive technologies like ESI or MALDI ionization¹⁶⁸.

A second aspect of glycan analysis requires the cleavage of the intact oligosaccharide from the protein or peptide, which can be achieved by either chemical or enzymatic reactions. The chemical method typically relies on hydrazine, which will destroy any protein or peptide information, however it quickly and easily results in a cleaved glycan prepared for further analysis. Endoglycosidases are enzymes which will cleave N-linked oligosaccharides from proteins and peptides, and include two different types of cleavage. Enzymes such as Endo F and Endo H (both favor cleavage of high-mannose types)¹⁷¹, and Endo D (cleavage of complex glycans)¹⁷² cleave between the two core GlcNAc residues, therefore leaving the first GlcNAc residue attached to the protein⁹². Alternatively, PNGase A (purified from almonds, cleaves both high-mannose and complex glycans)¹⁷² and PNGase F remove the entire oligosaccharide cleaving between the first GlcNAc and the asparagine residues, and as a result, these enzymes are termed peptide *N*-glycosidases. The most popular enzyme today for removing an entire N-linked glycan from the protein is PNGase F (Peptide-N4-(acetyl- β -glucosaminyl)-asparagine amidase)¹⁷³. PNGase F gained its popularity because it is capable of hydrolyzing all types of N-glycans, including high-mannose, hybrid, and bi-, tri-, and tetraantennary structures in a rapid manner¹⁷³. PNGase F is purified from *Flavobacterium meningosepticum*, and recognizes the tripeptide N-glycosylation signal,

cleaving the covalent linkage between the asparagine residue and the first GlcNAc; as long as there is not a core α -(1-3)-linked fucose present. This modification doesn't seem to present a problem with mammalian-derived samples whose N-linked glycopeptides carry core fucoses with an α -(1-6) linkage. In addition to the removal of the intact N-glycan by PNGase F, the enzymatic cleavage reaction results in conversion of the asparagine residue to an aspartic acid residue. This alteration allows for additional analysis of the peptide portion of the glycopeptide. N-linked glycosylation sites that are truly occupied can be identified by first incubating a peptide mixture with PNGase F followed by capture of the deglycosylated peptides and mass spectrometry analysis of the peptides by either MALDI or ESI and a protein database search specific for the deamidation modification (one dalton mass difference) to the peptide¹⁷⁴. The resultant intact N-glycans from PNGase F digestions can be analyzed directly by mass spectrometry, or they can first be derivatized by either the addition of a fluorescent label (i.e. 2-Aminobenzoic acid, 2-AA; 2-Aminobenzamide, 2-AB) or by chemical modification (i.e. permethylation). Underivatized glycans are less stable and therefore more likely to fragment in full MS scans, thus complicating the subsequent structural analysis.

Glycopeptide analysis is widely used today in glycomic studies; however the properties of glycosylated peptides pose problems in mass spectrometry analyses. The two main issues are due to the fact that protein glycosylation is very heterogeneous, and that glycopeptides typically do not ionize as well as their nonglycosylated counterparts, and therefore these peaks are often suppressed. Despite these complications, both MALDI and ESI soft ionization techniques are capable of analyzing the carbohydrate

structures attached to the peptides, especially when used in a tandem mass spectrometry mode. MALDI is more commonly used for glycan identification and structural determination, while ESI is better at obtaining more detailed structural and linkage information¹⁷⁵. For some analyses, determining the peptide sequence is as important as identifying the glycan sequence. With traditional high energy MS/MS like collision induced dissociation (CID), the glycan structure will fragment primary to the peptide backbone, thus not providing much peptide information¹⁷⁶. Fourier transform ion cyclotron resonance mass spectrometry (FT-ICR-MS) allows for MS/MS analysis providing very high mass accuracy and mass resolution and ultimately definite protein identification¹⁷⁷. One soft fragmentation method unique to FT-ICR-MS/MS is electron-capture dissociation (ECD). This method will cleave the peptide backbone without disrupting the post-translational modifications (PTM), therefore allowing for significant sequence coverage, including the localization of the PTM, such as N- and O-linked glycosylation^{175, 178, 179}. In addition, this technique is gentle enough to analyze highly sialylated structures without premature loss of terminal sialic acids¹⁸⁰, which allows for more accurate N-linked oligosaccharide structural identification. Additionally, electron transfer dissociation (ETD) is a soft fragmentation method similar to ECD, and is performed in quadrupole ion trap mass spectrometers¹⁸¹. This method also cleaves the peptide backbone in such a manner to provide sequence and PTM linkage site information, indicating the utility of this fragmentation platform in glycoproteomic approaches¹⁸². Whether studying intact glycopeptides or cleaved glycans, it is commonly necessary to desalt the sample and remove organic contaminants prior to mass

spectrometry analyses, which can be achieved by using column chromatography with resins such as AG-3, AG-50, C18, and graphitized carbon^{183, 184}.

Finally, when analyzing either glycans or glycopeptides one can either isolate a single, purified protein as a target, or alternatively, global analysis of glycans from a given cell type, tissue, or fluid can be performed. Global glycomic analysis can provide an abundance of information, once its limitations have been addressed. As with proteomic analyses, the dynamic range of a given biological sample can make mass spectrometry analyses very difficult. One way to overcome this challenge is to utilize enrichment techniques such as affinity chromatography, with the most common being lectin affinity chromatography. Lectins are proteins which specifically bind monosaccharides, therefore separating out glycoconjugates in a particular sample from other non-glycosylated molecules. Additionally, if the starting sample material contains highly abundant proteins that are not of interest (i.e. albumin), then commercially available kits can be used to remove these contaminating proteins from the given sample, thus decreasing the dynamic range of the fluid, and increasing the concentration of the lower abundant targets. Further fractionation of the sample by an online-LC system will allow for more complete mass spectrometry analysis of global glycosylation patterns of a particular sample.

CHAPTER II

DISSERTATION RATIONALE AND SUMMARY OF AIMS

The goal of this research project is to examine the N-glycosylation patterns of prostate specific antigen (PSA) and prostatic acid phosphatase (PAP) in prostate proximal fluids, as well as to examine the total glycan profile for prostate proximal fluids with the intent of discovering carbohydrate-based biomarkers for the detection of early prostate carcinomas.

Currently, serum PSA is the “gold standard” protein biomarker used in the clinic for detecting and diagnosing prostate cancer. However, serum PSA levels can be elevated in non-cancerous conditions as well, such as benign prostatic hyperplasia. This overlap causes many unnecessary biopsies, radical prostatectomies, and patient anguish. While other clinical measures are taken into consideration for a more accurate diagnosis, there is still a great need for better clinical detection methodologies for prostate cancer, including improved biomarkers. **Therefore, the specific hypothesis of this dissertation is that characterization of the N-linked carbohydrates attached to known prostate-derived proteins as well as the N-linked carbohydrates present in prostate-derived fluids will allow for the discovery of new clinically-relevant biomarkers for the detection and diagnosis of prostate carcinomas.** The specific hypothesis will be tested by creating disease-defined pools of prostate-derived samples, which will be used in proteomic and glycomic-based assays utilizing mass spectrometry for the detection of both glycopeptides and cleaved carbohydrates.

Initial glycomic and proteomic studies will be completed using seminal plasma samples, pools of which were created based on their disease status: normal, BPH, or prostate cancer. These samples will provide ample protein levels of both PSA and PAP for glycopeptide and glycomic analyses which will add to current knowledge of PSA and PAP glycosylation. In addition to this sample set, pools of disease-defined expressed prostatic secretions (EPS) will be generated and subsequently analyzed for detection of both protein levels and carbohydrate structures of PSA and PAP, as well as examined for their total glycomic profile. Because EPS fluids are more readily collected in the clinic, we believe these samples can be used not only for discovery of cancer biomarkers, but also for their validation and applications in future clinical assays.

The hypothesis of this dissertation was evaluated by addressing the following specific aims:

Aim I. Develop methodologies for the characterization of N-linked glycans of prostate-specific antigen and prostatic acid phosphatase in seminal fluids. This aim entails:

A. Generating sample sets and fractionation of pools in order to obtain purified forms of prostate specific antigen and prostatic acid phosphatase. Protein content and quality will be examined by immunoblotting and MALDI-TOF mass spectrometry.

B. Analysis of PAP glycopeptides by hybrid triple quadrupole/linear ion trap mass spectrometry in order to better understand which subtypes of carbohydrates are attached at each N-linked glycosylation site for PAP in seminal plasma samples.

C. Permethylation of cleaved N-linked carbohydrates attached to both PSA and PAP and analysis of the derivatized structures by MALDI-TOF mass spectrometry.

Aim II. Establish expressed prostatic secretions as a source of prostate specific antigen and prostatic acid phosphatase. This aim entails:

A. Collection and preparation of EPS samples for protein-based assays. Both individual and pooled sample sets will be utilized for the detection of both PSA and PAP.

B. Detection of PSA and PAP in individual samples by LC-ESI mass spectrometry in order to compare a common urine collection to an EPS urine collection for the presence of prostate-derived proteins. Additionally, an individual direct EPS sample will also be analyzed by LC-ESI mass spectrometry for the presence of PSA and PAP and other prostate-derived proteins.

C. Two-dimensional PAGE analysis and comparison of a urine sample to an EPS urine sample in order to visualize the different protein patterns between these two types of fluid collections.

D. Two-dimensional PAGE and immunoblotting analysis of pooled EPS urine samples for the detection of both PSA and PAP. The ability to visualize the various isoforms of PSA and PAP in these fluids will allow for further proteomic and glycomic analyses.

E. Enzyme-linked immunosorbent assay analysis of PSA and PAP concentrations in individual EPS urine and direct EPS samples. Determining PSA and PAP levels in these proximal fluids will aid in determining the value of expressed prostatic secretions as a source of protein-based biomarkers for evaluating prostatic diseases.

Aim III. Application of new methodologies to expressed prostatic secretions for prostate cancer glycoprotein biomarker discovery. This aim entails:

A. Generation of EPS urine and direct EPS pools based on disease stratification.

These pools will be concentrated by centrifugal filtration, allowing for enrichment of targeted glycoproteins. The protein pools will be used for the purification of PSA and PAP for N-linked glycosylation analysis, as well as for total N-linked glycan analysis by mass spectrometry.

B. Permethylation of cleaved N-linked carbohydrates attached to both PSA and PAP and analysis of the resulting derivatized structures by MALDI-TOF mass spectrometry. Parent masses will be assigned a biologically relevant carbohydrate structure determined by database searches, and the total structures identified will be catalogued.

C. Analysis of PAP glycopeptides by hybrid triple quadrupole/linear ion trap mass spectrometry in order to better understand which subtypes of carbohydrates are attached at each N-linked glycosylation site for PAP in EPS urine fluids. Both tryptic and chymotryptic digestions will be utilized in order to obtain more complete coverage of the N-linked glycopeptides and their corresponding N-glycan structures.

D. Total glycan analysis of permethylated cleaved N-glycans for both EPS urine and direct EPS fluids by MALDI-TOF/TOF. Disease-defined pools will be compared for their N-glycan profile, with the intention of determining any differences among disease states which can be used in future carbohydrate-targeted assays.

E. Computational data analysis of MALDI-TOF spectra using Clinprot software. Peak intensities of disease-defined pools will be compared to determine if there are any glycan differences among the sample cohorts.

In summary, the above Specific Aims will aid in the discovery of carbohydrate targets for new clinical markers of prostate carcinoma diagnosis and prognosis. Due to the close link between altered glycosylation and cancer, it is likely that a number of changes occur to the N-linked glycans of prostate-derived proteins, all of which should be detectable with the above glycoproteomic and glycomic platforms. Following discovery of any N-linked glycosylation alterations present, the target carbohydrates can then be used in validation assays and subsequently in high-throughput clinical assays. These tests would utilize the clinically relevant EPS fluids and a multi-well plate platform in order to allow for rapid results.

CHAPTER III

AIM I: DEVELOP METHODOLOGIES FOR THE CHARACTERIZATION OF N-LINKED GLYCANS OF PROSTATE-SPECIFIC ANTIGEN AND PROSTATIC ACID PHOSPHATASE IN SEMINAL FLUIDS

4.1 Introduction

The clinical measurement of the concentration and activities of two prostate derived glycoproteins, prostate specific antigen (PSA) and prostatic acid phosphatase (PAP), in serum has been assessed for decades in attempts to detect prostate cancers. Concentrations of PSA in serum above 10 ng/ml reliably indicate the presence of cancers, yet PSA testing is limited in its ability to differentiate prostate cancer from benign prostate hyperplasia (BPH), and specificity of the test diminishes significantly at lower PSA values below 10 ng/ml³⁷⁻³⁹. Digital rectal exams (DRE) and determination of serum prostatic acid phosphatase (PAP) were the principal method for prostate cancer detection and staging before the advent of PSA testing, and they too have many limitations^{185, 186}. Serum PAP levels can still be used as an indicator of metastatic disease and possibly recurrence prediction^{48, 49}, but it has proven to have low specificities and sensitivities as a detection biomarker as compared to PSA³³. While X-ray crystal structures have been reported for both human PSA and PAP^{124, 187}, there was little resolution of the glycan constituents of these proteins. Because of the known associations of changes in glycosylation associated with cancer progression⁸³⁻⁸⁶, characterization of the glycan constituents of PSA and PAP derived from clinical samples representing healthy and

different prostatic disease states could identify new biomarker candidates for prostate cancer detection.

PSA contains 8% carbohydrate by mass¹¹⁹, and has one glycosylation site at asparagine (Asn)-45¹²⁰. Previous studies on PSA glycosylation have compared seminal plasma from healthy donors to prostate tumor metastatic cell line LNCaP¹¹⁵⁻¹¹⁷. PSA purified from the seminal fluid of healthy subjects have been characterized as having sialylated complex biantennary glycans, frequent core fucose modifications, high mannose glycans, and some terminal N-acetylgalactosamines^{117, 121}. PSA glycans isolated from LNCaP cell lines have also been characterized as having some triantennary structures¹¹⁶, as well as decreased sialic acid content and the presence of increased fucose and GalNAc content¹¹⁵. A recent comparison of the sialic acid content of free PSA and proPSA isolated from serum, seminal plasma and tissues from non-cancer control subjects and prostate cancer subjects was reported¹²². Essentially no differences in sialylation content for the different forms of PSA were detected for any condition or sample¹²². A separate study of serum PSA derived glycans compared structural differences between free and complexed PSA¹²³. Both forms of PSA were found to have mostly sialylated and fucosylated biantennary structures, while a few multiantennary complex structures were also identified¹²³. These previous studies did not evaluate the specific structural configurations for each oligosaccharide isolated, and very few numbers of clinical samples were used. PAP has three glycosylation sites at Asn-62, Asn-188, and Asn-301^{124, 125}, making it a more difficult target for site specific structural characterization, yet one that may be a suitable complement to PSA. An X-ray crystal structure of PAP from normal seminal plasma had reported that Asn-301 had glycan

modifications consisting of primarily high mannose oligosaccharides, while glycans at Asn-188 were less resolved, but consistent with complex structures containing sialic acid and fucose¹²⁴. In relation to prostate cancer, a previous serial lectin analysis of PAP isolated from tissue in BPH and cancer subjects reported a decrease in high-mannose and hybrid glycans with core fucoses in cancer relative to BPH, and an increase of non-fucosylated hybrids in PCa as compared to BPH¹²⁵.

The objective of our study described herein was to obtain purified forms of both PSA and PAP from a clinical cohort of seminal plasma from healthy, BPH and prostate cancer subjects for further glycan structural analyses. We hypothesized that characterization of these PSA and PAP glycoforms across specified clinical sample sets would identify a subset of glycan constituents as biomarker candidates for the detection of prostate cancers. Following a purification step using thiophilic chromatography, the released glycans from PSA and PAP were characterized using HPLC separation of aminobenzoate derivatives, permethylation and MALDI-TOF/TOF profiling, and glycopeptide analysis on a hybrid triple quadrupole/linear ion trap mass spectrometer. The cumulative structures obtained for both PSA and PAP are reported and potential disease specific classes of glycoforms are identified. Specific assignments of glycan structural subtypes have also been determined for each of the three glycosylation sites on PAP. The glycan structures reported for PAP represent the first description of its glycan constituents using mass spectrometry based methods.

4.2 Experimental

Seminal plasma samples

Seminal fluid was obtained from men seen at the EVMS Department of Urology/Divine Tidewater Urology clinic for prostate cancer screening from 1989-2003. A semen collection kit was provided for each donor. Following semen collection, an instant freeze pack was applied to each tube for storage, and brought with the donor to the urology clinic. Following transport to the Virginia Prostate Center biorepository at EVMS, each sample was thawed, centrifuged to remove sperm, and stored in 0.5 ml aliquots. Initially, Normal (n=65), BPH (n=59), and PCa (n=92) pools (8-10 mls total/pool) were compiled from samples previously aliquoted for expression profiling studies (0.05 to 0.2 ml per sample), and matched for age. Each aliquot went through less than 2 freeze/thaw cycles, and average serum PSA values were 10.4 ng/ml (range 0.01 - 225.8) for PCa, 3.6 ng/ml (range 0.15 - 13.9) for BPH, and 1.5 ng/ml (range 0.3 - 4.8) for normal. The pooled samples were then subjected to a low-speed spin (4°C, 12k RPM, 20 minutes) to remove any cellular contaminants, followed by ultracentrifugation (4°C, 37K RPM, 1 hour) to pellet out the prostasomes (membrane-bound storage vesicles secreted by prostate epithelial cells¹⁸⁸). The supernatant was collected and 400ul aliquots were stored at -80° C. A more defined subset of seminal plasma pools were created for each clinical group, with each cohort having defined serum PSA values in the 2-7 ng/ml range. Nine samples, 500ul per sample, were used to make each seminal plasma pool, and the samples used were collected between 1997 and 2003. The mean serum PSA values were 3.58 ng/ml for normal, 2.64 ng/ml for BPH, and 5.83 ng/ml for prostate cancer. BPH cases were defined as being biopsy negative, and the cancer samples were predominantly

Gleason grade 6 (3+3). These pools were processed as previously mentioned. The final supernatant of approximately 4.5 ml was aliquoted and stored at -80°C until needed.

Protein concentrations were determined for all seminal plasma pools.

Thiophilic adsorption chromatography (TAC)

PSA and PAP were purified from seminal plasma pools using thiophilic adsorption chromatography (TAC) following the methods outlined by Kawiniski et al.¹⁸⁹. Thiophilic adsorption chromatography uses a resin that consists of sulfone and thioether groups bound to agarose beads, which in turn binds proteins primarily via tryptophan and phenylalanine residues¹⁸⁹⁻¹⁹¹. Briefly, seminal plasma pools were applied to Fractogel® EMD TA “T-gel” (Merck KGaG, Darmstadt, Germany) columns (2 cm x 0.5 cm) equilibrated in 1M sodium sulfate, and eluted in decreasing salt fractions. Protein content of each pool was normalized to 3.0 mg, with the samples in a final volume of 1ml in 25mM HEPES/1M sodium sulfate. Next, the sample was applied to the column, followed by 2ml of column buffer, and allowed to flow through by gravity; this three milliliter fraction collected is named “unbound”. The column was washed with 8 bed volumes of column buffer. Batch elution with decreasing sodium sulfate molarities (0.8M, 0.6M, 0.4M, 0.2M, and 0.0M) was performed using a low-pressure peristaltic pump. For each concentration, approximately 3ml fractions were collected, aliquoted, and stored at -80°C. The presence of PSA and PAP were confirmed by Western blot, and MALDI peptide mass fingerprinting of the corresponding excised gel bands was done to assess relative purity. MASCOT scores of greater than 100 and sequence coverage of greater than 45% were routinely observed for both PAP and PSA bands.

Normal Phase HPLC

Rapid glycan sequencing of both PSA and PAP was performed by using previously optimized procedures¹⁹². Briefly, PSA and PAP gel slices were digested with PNGase F, then the released free glycans were labeled with 2-aminobenzamide (2-AB) for subsequent normal phase HPLC analysis¹⁹³. A subset of samples were treated with *Arthrobacter ureafaciens* sialidase as previously described by Guile *et al.*¹⁹⁴. The resulting peaks, separated by time of appearance, correspond to specific glycan structures on the basis of glucose unit values (data not shown)¹⁹⁴. All HPLC analyses were performed using a Waters Alliance HPLC System and quantified using the Millennium Chromatography Manager (Waters Corporation, Milford, MA).

N-glycan permethylation

TAC-purified PSA and PAP gel bands derived from seminal plasma pools were permethylated¹⁹⁵ following trypsin digestion. Gel bands were first reduced and alkylated, and then dried *in vacuo* prior to proteolytic digestion. Trypsin digestions were performed at 37°C for 18 hours, followed by peptide extraction with 50% acetonitrile/0.1% TFA and dried *in vacuo*. Next, trypsin was denatured by heating the sample at 100°C for 5 minutes, and 1500 units of PNGase F (New England Biolabs, Ipswich, MA) was added to the peptide mixture and incubated at 37°C for 18 hours. The final digested product was purified using Resprep™ C18 cartridges (Restek Corporation, Bellefonte, PA). The N-glycan fraction was collected in 5% acetic acid, and subsequently dried under reduced

pressure. Dried N-glycans were permethylated following the protocol described by Ciucanu and Kerek¹⁹⁵. The permethylated N-glycans were purified using C18 columns, eluted in 85% acetonitrile, and then dried under a nitrogen stream.

MALDI-TOF/TOF

The dried permethylated N-glycans were reconstituted in 20 microliters of 100% methanol. Sample was mixed 1:1 with 2,5-Dihydroxybenzoic acid (DHB) matrix (20mg/ml in 50% methanol) and spotted on a polished steel MALDI-TOF target plate and allowed to crystallize at room temperature in the dark. Each sample was analyzed in positive ion mode using an UltraFlex III MALDI-TOF/TOF instrument (Bruker Daltonics, Germany). FlexControl and FlexAnalysis software (Bruker Daltonics, Germany) were used for spectra processing. Additionally, the glycan database offered by the Consortium for Functional Glycomics (<http://www.functionalglycomics.org>) was used to search permethylated glycan masses correlating to peaks of interest in MALDI-TOF spectra. Glycan “cartoons” representing mass peaks were built using GlycanBuilder ver 1.2 build 3353¹⁹⁶.

Hybrid triple quadrupole/linear ion trap mass spectrometry

A hybrid triple quadrupole/linear ion trap mass spectrometer 4000 (QTRAP[®] LC/MS/MS system, Applied Biosystems, Foster City, CA) coupled to a Tempo NanoLC system (Eksigent Technologies, Dublin, CA) was used to determine the structures of the glycans attached to each of the three PAP linkage sites: Asn-62, Asn-188, and Asn-301. The methods described by Sandra et al.¹⁹⁷ were used with minor modifications to

optimize for our samples and instrumentation. Briefly, TAC-purified PAP gel slices derived from seminal plasma were reduced, alkylated, and digested with a saturated solution (in 50mM ammonium bicarbonate) of either 750 ng of trypsin or 950 ng of chymotrypsin. After an overnight digestion, the resultant peptides were extracted from the gel slice using 50% acetonitrile/0.1% TFA in water and dried *in vacuo*. The digested product was reconstituted in 20 microliters of Buffer A (5% acetonitrile/0.1% formic acid/0.005% heptafluorobutyric acid in water) and 8 microliters was injected into the nanoLC system for fractionation and analysis. Both the linear ion trap and the triple quadrupole capabilities of the QTRAP were utilized in these analyses. Glycopeptides were identified in the digestion mixtures by monitoring for unique marker oxonium ions such as m/z 163 (Hex^+), 204 (HexNAc^+), 292/274/256 (NeuAc^{+1}), and 366 (HexHexNAc^+) that originate from fragmented glycopeptides^{197, 198}. In this approach the peptides are scanned in quadrupole 1 (Q1) to determine their masses and retention times. The peptides are then transmitted to quadrupole 2 (Q2) which acts as a collision cell where fragmentation occurs. Quadrupole 3 (Q3) is set to transmit only the mass of the diagnostic oxonium ions. Upon their detection, an enhanced product ion scan (EPI) of the precursor ion is triggered where fragmentation occurs in Q2, the fragmented ions are captured in the ion trap and then scanned out generating an MS/MS spectrum containing the ions from the both the peptide and the linked carbohydrate structures.

4.3 Results

Purification of PSA and PAP from seminal plasma pools

A large repository of seminal plasma fluids collected over the last 18 years were used to create pooled sample cohorts representative of normal control, benign prostatic hyperplasia (BPH) and prostate cancer conditions. A thiophilic adsorption chromatography (TAC) approach adapted from Kawiniski et al.¹⁸⁹ was used to purify PSA and PAP from the prostatesome depleted, pooled seminal plasma fluids. Following sequential batch elution, the resulting protein fractions were separated by SDS-PAGE, as shown in Figure 5. Under the conditions used, PAP did not bind to the TAC resin, and PSA eluted in both the 0.6M and 0.4M sodium sulfate fractions. Both PSA and PAP were readily detected by Coomassie staining, and their identities were confirmed in their respective fractions by western blotting and peptide mass fingerprinting. For both PSA and PAP isolated from gel slices, MASCOT scores of over 100 and sequence coverage of at least 45% were obtained. Lastly, there was no indication of other protein sequences present with significant scores.

Rapid glycan sequencing analysis of PAP and PSA glycans

The TAC fractions containing PSA and PAP were used for preparative SDS-PAGE separations, stained with Coomassie blue, and gel slices corresponding to PSA or PAP excised. Each gel band was digested with trypsin, followed by PNGaseF digestion and 2-aminobenzamide derivatization of the released glycans as previously described¹⁹³. Glycans from PSA and PAP for each of the three clinical groups were then separated by normal phase HPLC and their elution positions used to define structural classes¹⁹⁴. The elution profile of PAP derived 2AB modified glycans from each pool is shown in Figure 6. It is clear that there are major differences in glycosylation patterns detected for PAP,

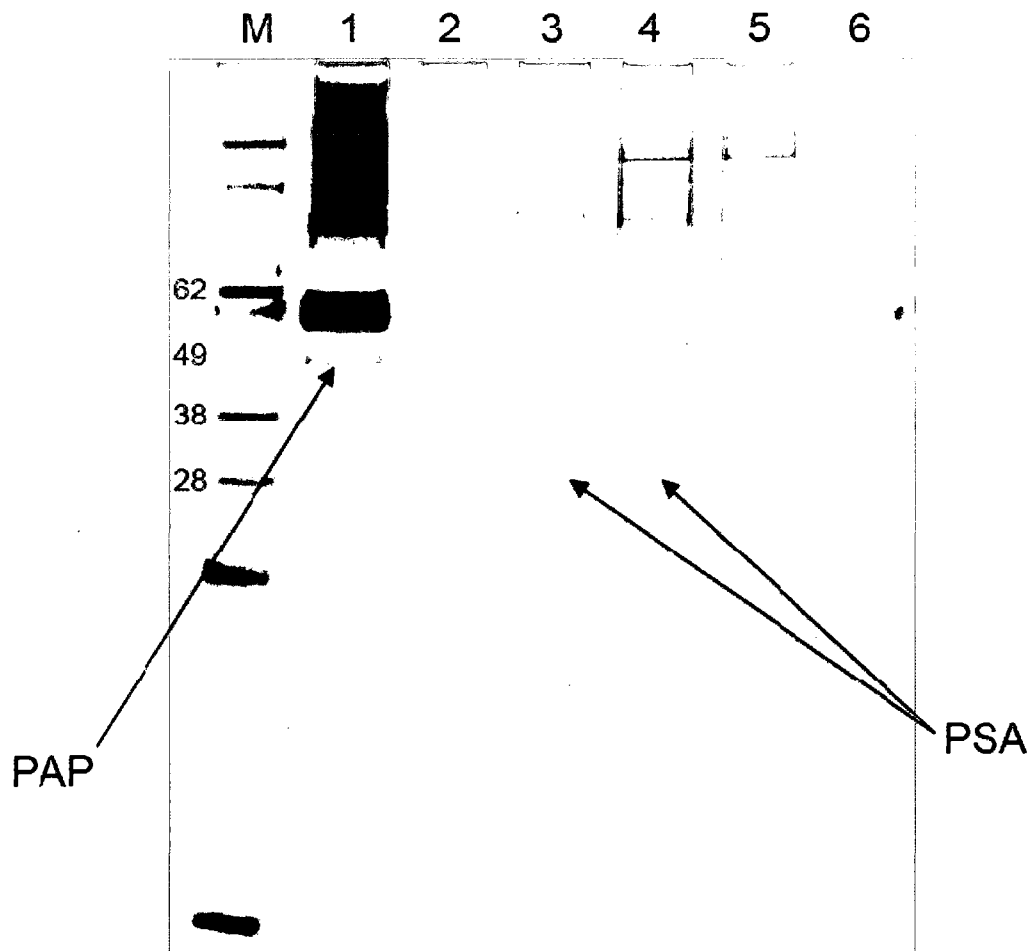


Figure 5. Seminal plasma fractionation by thiophilic adsorption chromatography. Seminal plasma protein fractions purified by thiophilic adsorption chromatography (TAC) were separated on a 12% Bis-Tris NuPAGE SDS-gel (Invitrogen) and stained with Coomassie blue. Unbound proteins are shown in Lane 1, with protein from the 0.8M NaSO₄ elution in Lane 2, 0.6M (Lane 3), 0.4M (Lane 4), 0.2M (Lane 5) and 0 M/25mM HEPES (Lane 6). This gel shows the proteins from normal seminal plasma, and is representative of the purifications of the benign and cancer samples. PAP and PSA identities were confirmed in the above fractions by staining, western blots and MALDI-TOF analysis.

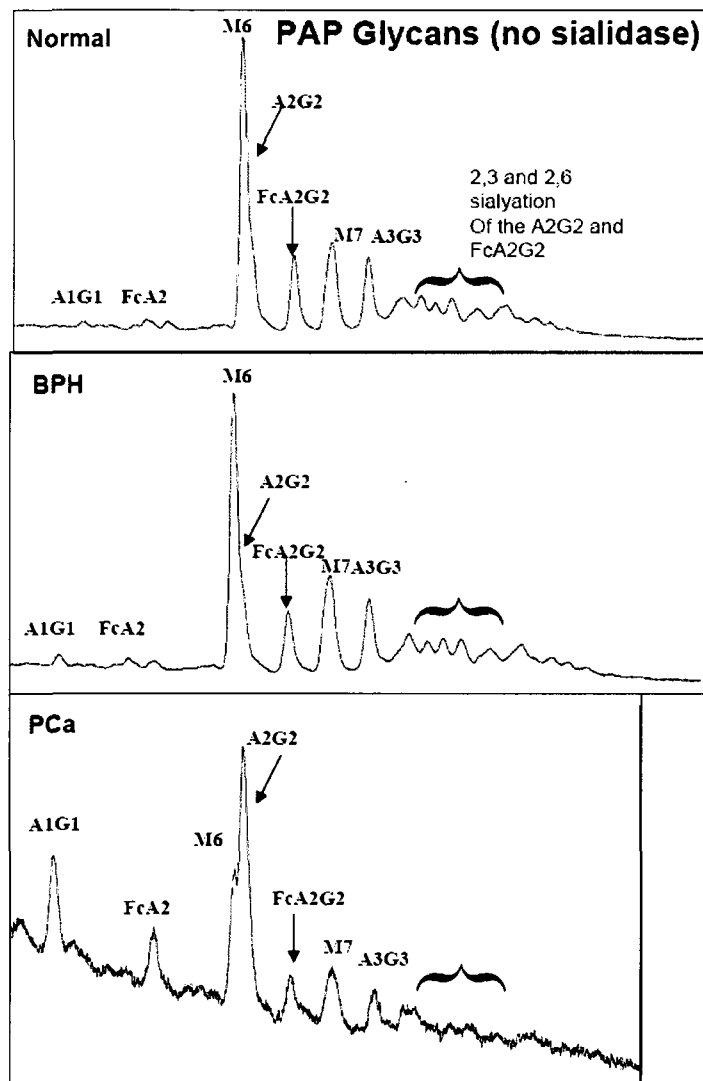


Figure 6. Normal phase HPLC separation of 2-AB derivatized N-linked glycans from PAP. The relative levels of N-linked glycans from PAP isolated from normal control, benign (BPH) and prostate cancer (PCa) conditions separated by normal phase HPLC. Structural designation are as follows: A1G1, hybrid glycan with a single galactose residue on the 1,6 arm; FcA2, core fucosylated (1,6) agalactosylated biantennary glycan; Man6, High mannose glycan with 6 mannose residues, A2G2, biantennary N-glycan; Man7, High mannose glycan with 7 mannose residues; A3G3, triantennary N-linked glycan; FcA3G3, core fucosylated (1,6) triantennary N-linked glycan; A4G3, tetraantennary N-linked glycan with 3 galactose residues; A4G4, tetraantennary N-linked glycan; FcA4G4, core fucosylated (1,6) tetraantennary N-linked glycan. B indicates bisecting GlcNAc residues.

particularly in the comparison of healthy and benign relative to the cancer samples. Because of the known instabilities of terminal sialic acid residues during processing and HPLC analysis²⁶, digestion with *Arthrobacter ureafaciens* sialidase was also done prior to normal phase HPLC separation to compare the non-sialylated structures. As summarized in Figure 7, there were still significant decreases in the fucosylated bi- and tetraantennary classes, FcA2G2 and FcA4G4, in the cancer samples. Either with or without sialidase treatment, there was also an apparent decrease in high mannose (Man6) structures in the cancer samples, and dramatic increases in cancer for truncated A1G1 structures. A similar analysis for 2-AB labeled PSA glycans was done, as summarized in Figure 8 (no sialidase) and Figure 9 (with sialidase). Cumulatively, the types of glycan structures detected in these HPLC separations are consistent with previously reported structures for PSA¹¹⁵⁻¹¹⁷. There were no dramatic differences in expression of sub-types across the three clinical conditions, with the exception of the A2G2 structures in BPH in the non-sialidase treated preparation. Because this difference was not detected in the sialidase treated samples, this could reflect differential stabilities or sample processing differences. This will need to be further investigated in follow up studies.

The seminal plasma pools used for these initial analyses represent a broad range of clinical samples reflecting the disease severity spectrum of prostate cancers and benign conditions collected from 1990 to 2003, a time frame that spans the pre-PSA testing era to current clinical practice. Using the PSA levels for each individual in the pool of these samples, a refined pooled subset of 9 samples per condition was generated based on dates of collection after 1997 and serum PSA levels between 2-7 ng/ml. This PSA range better

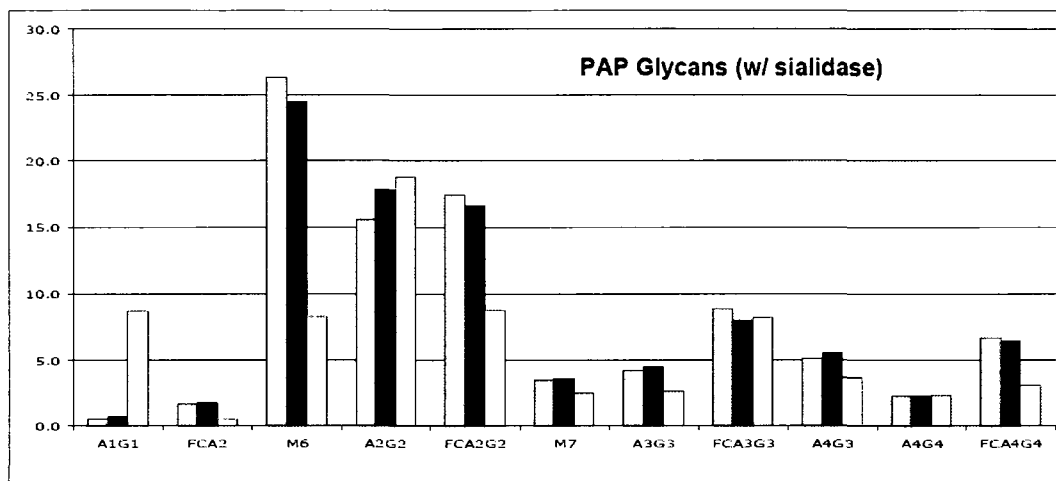


Figure 7. Normal phase HPLC separation of 2-AB derivatized N-linked glycans from PAP treated with sialidase. N-linked glycans from PAP isolated from normal control, benign (BPH), and prostate cancer (PCa) were treated with sialidase prior to normal phase HPLC separation. Shown are the relative intensities of each indicated structure per condition, normal (Gray bars); BPH (Black bars); PCa (White bars). Structural abbreviations are described in the legend for Figure 6.

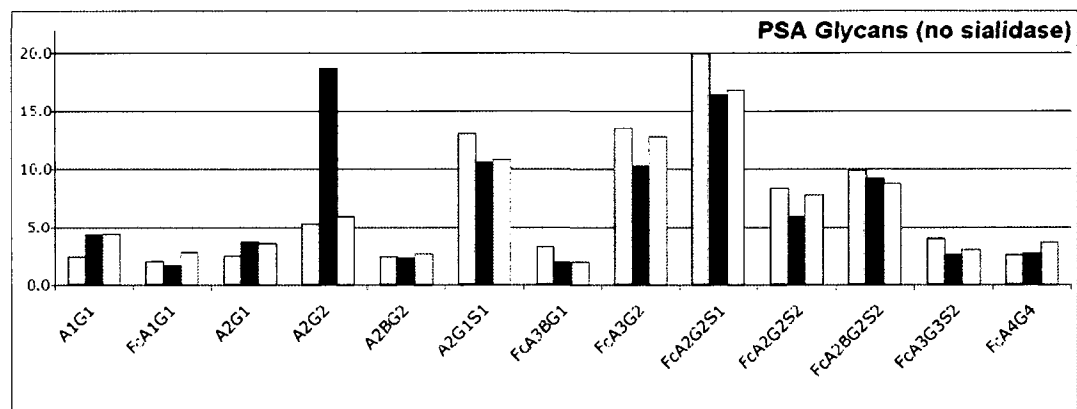


Figure 8. Normal phase HPLC separation of 2-AB derivatized N-linked glycans from PSA. N-linked glycans from PSA isolated from normal control, benign (BPH) and prostate cancer (PCa) were separated by normal phase HPLC. Shown are the relative intensities of each indicated structure per condition, normal (Gray bars); BPH (Black bars); PCa (White bars). Structural abbreviations are described in the legend for Figure 6.

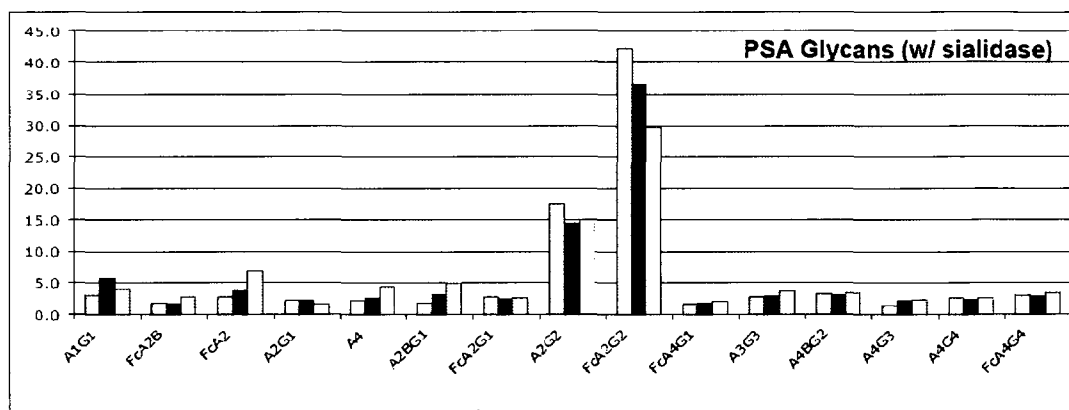


Figure 9. Normal phase HPLC separation of 2-AB derivatized N-linked glycans from PSA treated with sialidase.

N-linked glycans from PSA isolated from normal control, benign (BPH), and prostate cancer (PCa) were treated with sialidase prior to normal phase HPLC separation. Shown are the relative intensities of each indicated structure per condition, normal (Gray bars); BPH (Black bars); PCa (White bars). Structural abbreviations are described in the legend for Figure 6.

reflects the majority of benign and prostate cancer subjects detected in the PSA screening/testing era, and hence results from these samples should be more reflective of current urological practice. The same sample preparation and TAC purification was done for each new pool. PAP and PSA eluted in their respective fractions as described in Figure 5 (Figure 10). As shown in Figure 11 for PAP, similar results to the larger pool data were obtained. There continued to be a larger proportion of fragmented glycans (A1G1, FcA2, A2G1, FcA2) in the prostate cancer samples relative to the healthy and BPH cohorts. PSA and PAP purified from this new cohort was used for all subsequent analyses.

MALDI-TOF analysis of permethylated PSA and PAP glycans

In order to further define the structural repertoire of PSA and PAP glycans, permethylation¹⁹⁵ of the PNGase F released glycans was done for each clinical cohort, followed by MALDI-TOF/TOF analysis. Because of the broad diversity of the indicated structural classes from the HPLC analyses, the goal was not to identify disease specific changes, but to better define all of the possible glycan structures detected on seminal plasma PSA and PAP. Permethylation of glycans aids in the stability of the terminal sialylated residues for detection by MALDI-TOF/TOF, and simplifies the spectra to primarily Na⁺ adducts, allowing for less complex annotation of mass peaks. From the permethylation experiments, we were able to detect multiple glycoforms for both PAP and PSA (Table 2 and Table 3). A representative MALDI-TOF spectra of PAP derived permethylated glycans from prostate cancer samples are shown in Figure 12. Cumulatively, 21 structural classes of PAP glycans were detected representing primarily

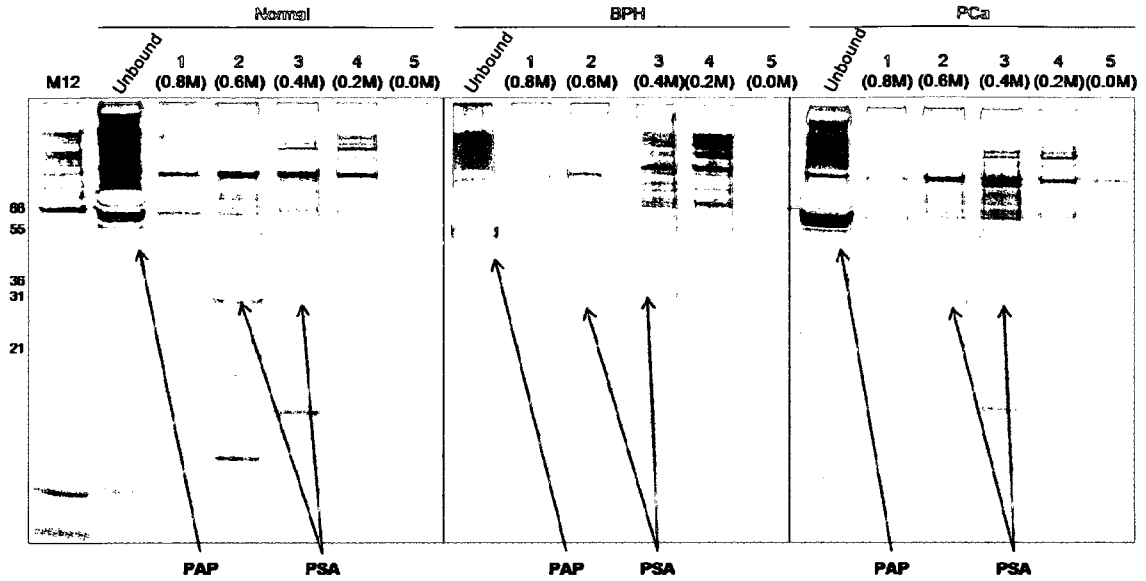


Figure 10. Thiophilic adsorption chromatography of redefined seminal plasma pools. Seminal plasma protein fractions from normal, BPH, and PCa defined pools purified by thiophilic adsorption chromatography (TAC) were separated on a 12% Bis-Tris NuPAGE SDS-gel (Invitrogen) and silver stained. Proteins that did not bind the TAC resin are shown in the lane marked Unbound, with protein from the 0.8M NaSO₄ elution in Lane 1, 0.6M (Lane 2), 0.4M (Lane 3), 0.2M (Lane 4) and 0 M/25mM HEPES (Lane 5). PAP and PSA identities were confirmed in the above fractions by staining, western blots and MALDI-TOF analysis.

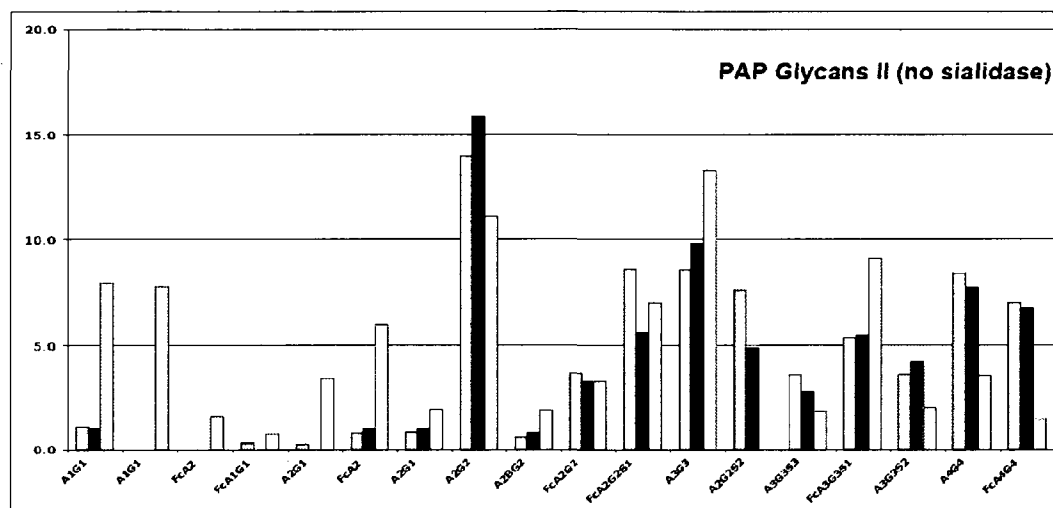



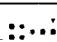
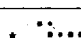
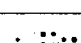
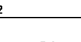
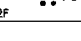
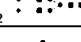



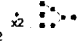
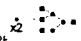

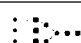
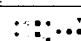
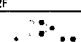


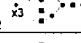


Figure 11. Normal phase HPLC separation of 2-AB derivatized N-linked glycans from PAP from the refined second sample pool.

N-linked glycans from PAP isolated from the second pool of normal control, benign (BPH) and prostate cancer (PCa) seminal fluids stratified to PSA levels and other clinical parameters. Shown are the relative intensities of each indicated structure per condition following normal phase HPLC separation: normal (Gray bars); BPH (Black bars); PCa (White bars). Structural abbreviations are described in the legend for Figure 6.

Table 2. Permethylated MALDI-TOF m/z and corresponding N-glycan structures for PAP

Number	m/z	Proposed Glycan Structure	Sub-Type
1	1784.016	M6N2 	High Mannose
2	1987.958	M7N2 	High Mannose
3	2070.189	Gal2N2M3N2 	Complex
4	2244.268	Gal2N2M3N2F 	Complex
5	2314.091	Hex5HexNAc5 	Complex
6	2432.339	NeuAc1Gal2N2M3N2 	Complex
7	2606.425	NeuAc1Gal2N2M3N2F 	Complex
8	2793.503	NeuAc2Gal2N2M3N2 	Complex
9	2881.559	NeuAc1Gal3M3N2 	Complex
10	2967.587	NeuAc2Gal2N2M3N2F 	Complex
11	3055.647	NeuAc1Gal3M3N2F 	Complex
12	3242.719	NeuAc2Gal3M3N2 	Complex
13	3416.793	NeuAc2Gal3M3N2F 	Complex
14	3504.838	NeuAc1Gal4N4M3N2F 	Complex
15	3603.894	NeuAc3Gal3N3M3N2 	Complex
16	3777.971	NeuAc3Gal3N3M3N2F 	Complex
17	3867.027	NeuAc2Gal4N4M3N2f 	Complex
18	3963.779	Hex6HexNAc5NeuAc4 	Complex
19	4053.873	NeuAc3Gal4N4M3N2 	Complex
20	4227.294	NeuAc3Gal4N4M3N2f 	Complex
21	4588.57	NeuAc4Gal4N4M3N2F 	Complex

Permethylated PAP glycans from normal, BPH, and PCa seminal plasma pools were analyzed by MALDI-TOF. Identified m/z values were used for database searches, and corresponding masses that could be assigned to a biologically relevant N-glycan structure are listed. An asterisk denotes structures that are one representation of multiple possible glycoforms for a given mass. The shown structure in these cases was chosen based on its apparent prevalence in mammalian species. Cartoon representations are as follows: ■

=GlcNAc, ● =Mannose, ○ =Galactose, ▲ =Fucose, ◆ =NeuAc, □ =GalNAc

Table 3. Permethylated MALDI-TOF m/z and corresponding N-glycan structures for PSA

Number	m/z	Proposed Glycan Structure	Sub-Type	Number	m/z	Proposed Glycan Structure	Sub-Type
1	1344.917	M3N2F	Complex	21	2767.61	Hex5dHex4HexNAc4	Complex
2	1580.069	M5N2	High Mannose	22	2779.64	NeuAc1Gal2N2M3N2F2	Complex
3	1590.051	NM3N2F	Complex	23	2793.652	NeuAc2Gal2N2M3N2	Complex
4	1784.208	M6N2	High Mannose	24	2880.654	NeuAc1Gal3N3M3N2	Complex
5	1907.156	N3M3N2	Complex	25	2893.731	Hex4dHex1HexNAc6NeuAc1	Complex
6	2111.231	Hex4HexNAc5	Complex	26	2967.686	NeuAc2Gal2N2M3N2F	Complex
7	2244.425	Gal2N2M3N2F	Complex	27	3024.789	NeuAc1Gal2N3M3N2F2	N/A
8	2315.331	Hex5HexNAc5	Complex	28	3132.772	Gal6N3M3N2	Complex
9	2356.526	Hex4HexNAc6	Complex	29	3142.734	Gal4N4M3N2F	Complex
10	2377.534	Hex6dHex2HexNAc3	Hybrid	30	3211.806	NeuAc2Gal2N3M3N2F	Complex
11	2419.445	Hex5dHex2HexNAc4	Complex	31	3242.891	NeuAc2Gal3N3M3N2	Complex
12	2432.413	NeuAc1Gal2N2M3N2	Complex	32	3345.936	Hex8dHex1HexNAc5	Complex
13	2472.384	NeuAc1GalN3M3N2	Complex	33	3416.859	NeuAc2Gal3N3M3N2F	Complex
14	2518.443	Gal3N3M3N2	Complex	34	3593.05	Hex8dHex1HexNAc7	Complex
15	2549.473	Hex6dHex3HexNAc3	Hybrid	35	3605.045	NeuAc3Gal3N3M3N2	Complex
16	2561.577	Hex5HexNAc6	Complex	36	3777.062	NeuAc3Gal3N3M3N2F	Complex
17	2593.532	Hex5dHex3HexNAc4	Complex	37	3866.523	NeuAc2Gal4N4M3N2F	Complex
18	2606.502	NeuAc1Gal2N2M3N2F	Complex	38	3912.098	Hex9dHex1HexNAc6NeuAc1	Complex
19	2677.545	NeuAc1Gal2N3M3N2	Complex	39	3965.198	Hex6HexNAc5NeuAc4	Complex
20	2694.765	Gal3N3M3N2F	Complex	40	4416.599	NeuAc4Gal4N4M3N2	Complex

Permethylated PSA glycans from normal, BPH, and PCa seminal plasma pools were analyzed by MALDI-TOF. Identified m/z values were used for database searches, and corresponding masses that could be assigned to a biologically relevant N-glycan structure are listed. An asterisk denotes structures that are one representation of multiple possible glycoforms for a given mass. The shown structure in these cases was chosen based on its apparent prevalence in mammalian species. Cartoon representations are as follows: ■

=GlcNAc, ● =Mannose, ○ =Galactose, ▲ =Fucose, ◆ =NeuAc, □ =GalNAc

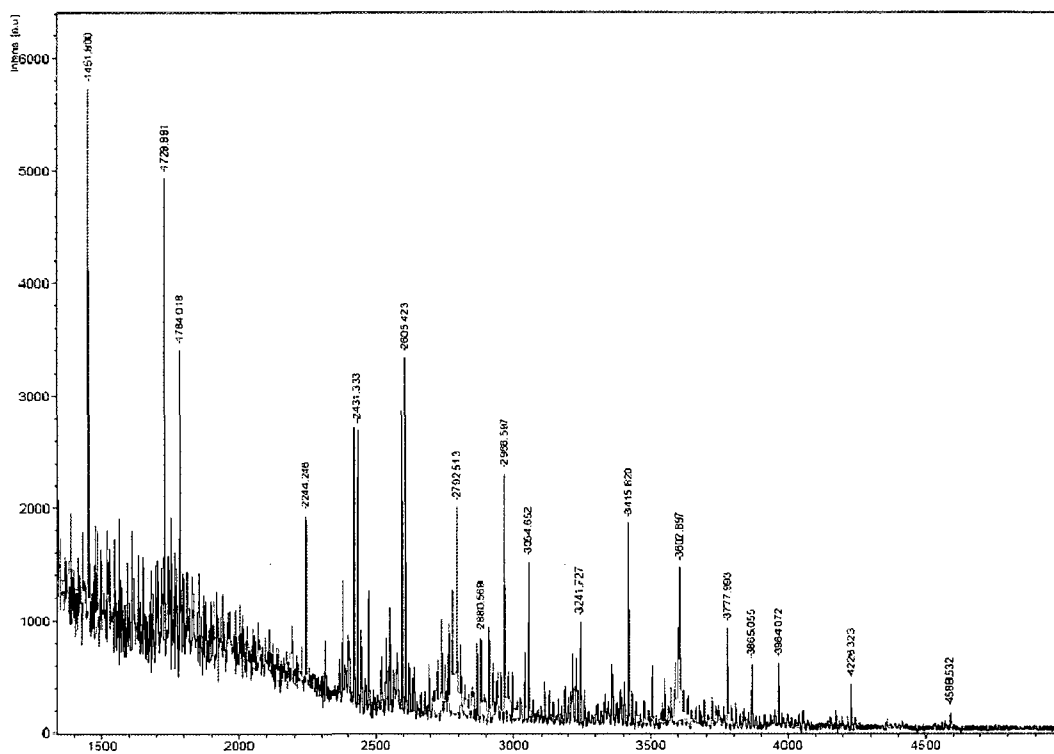


Figure 12. MALDI-TOF analysis of permethylated PAP glycans from prostate cancer seminal plasma. A representative MALDI spectrum for permethylated PAP is shown. Combined with the structures determined in the control and BPH permethylated PAP samples, glycan structures corresponding to detected m/z peaks are listed in Table 2.

high-mannose and complex sub-types, with a few potential hybrid sub-types represented as well (Table 2). Permethylated glycans cleaved from PSA seemed to be mostly bi- and tri-antennary structures of the complex sub-type, but represented 40 potential classes, including high mannose and hybrid sub-types detected as well (Table 3). These results are consistent with structures previously reported for PSA glycans from serum and seminal fluids^{115-117, 122}.

Triple-quadrupole mass spectrometry analysis of PAP glycopeptides

Because PAP has three distinct glycan sites, and the previously reported crystal structure was only able to definitively assign one high-mannose containing site, individual glycopeptide analysis of the three sites was initiated. SDS-PAGE separated PAP was proteolytically digested with trypsin or chymotrypsin, and peptides fractionated by nanoLC system in-line with triple quadrupole mass spectrometer. The instrument was operated in the precursor ion (PI) scan mode for individual sugar molecules at specific m/z values of either 163 for Hexose⁺¹ (Hex), 204 for N-acetylhexoseamine⁺¹ (HexNAc), 292/274/256 for N-acetylneuraminic acid⁺¹ (NeuAc), or 366 for Hex-HexNAc⁺¹. An enhanced product ion scan is triggered upon detection of the specified diagnostic ion, generating information on the sugar composition and the amino acid sequence of the glycopeptides in a single assay. An example is shown in Figure 13 for the tryptic peptide with one missed cleavage encompassing the high mannose site at Asn 301 (GEYFVEMYRNETQHEPYPLMLPGCSPSCPLER), as determined by the precursor ion scan for oxonium ion 163. Knowing the parent mass allows for annotation of the remaining triply charged ion peaks in the third quadrupole (Q3) for identification of sugar

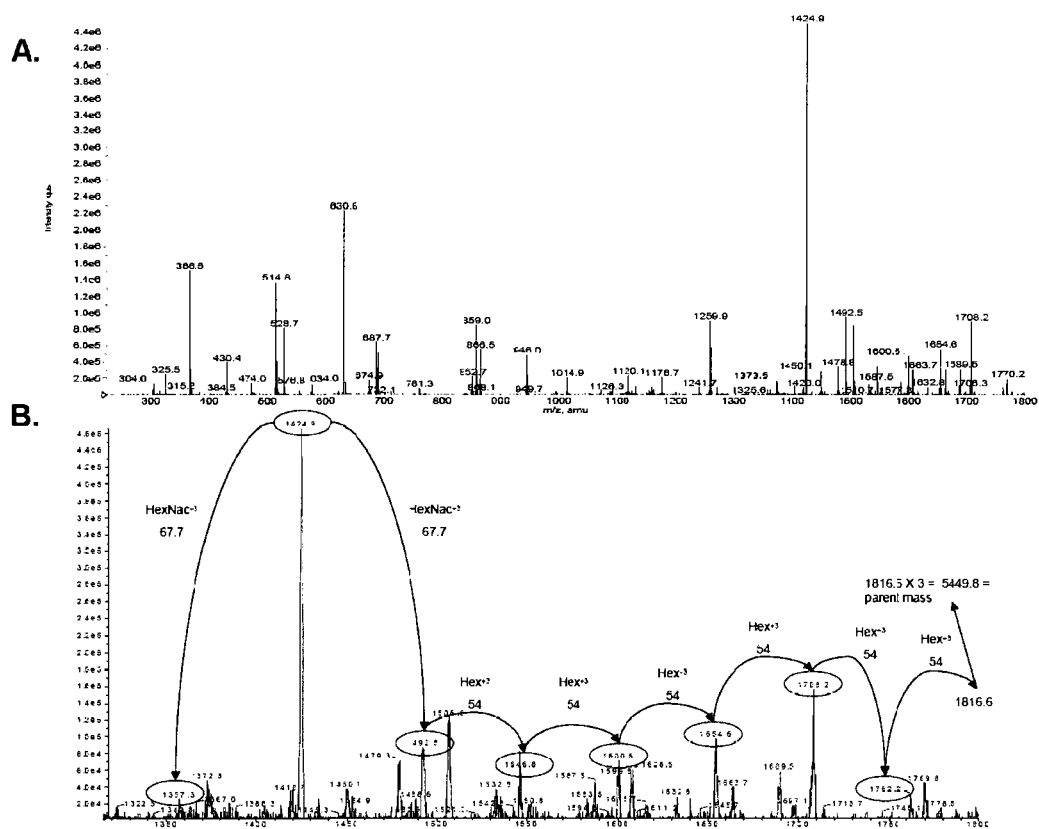


Figure 13. Precursor ion scan for 163 m/z hexose of tryptic PAP peptides.

A) Enhanced Product Ion (EPI) scan of a quadrupole-charged PAP glycopeptide with parent mass of 5449.0.

B) Expanded window of above EPI scan showing fragmentation of the parent ion that corresponds to the tryptic peptide GEYFVEMYRNETQHEPYPLMLPGCSPSCPLER containing the glycosylation site Asn-301 and a Man6 N-glycan.

constituents and fragments. The annotation of these glycans was greatly simplified as this site contains only high mannose structures, with Man6 being the major constituent, and Man7 a minor one, which is consistent with the PAP crystal structure¹²⁴. Additionally, Figure 14 illustrates an example of the tryptic peptide with one missed cleavage encompassing the high mannose site at Asn 62 (FLNESYKHEQVYIR), as determined by the precursor ion scan for oxonium ion 292. As listed in Table 4, this approach has been useful for identifying complex biantennary and triantennary glycans at Asn 62. This site had previously been poorly resolved in the PAP crystal structure, such that complex glycan structures were proposed to be unlikely constituents⁹. Like in the crystal structure, the site at Asn 188 has proven elusive to glycan analysis, particularly when trypsin was used for digestion, which we believe was due to a combination of mixed tryptic cleavages combined with large tetra-antennary glycans. However, use of chymotrypsin allowed detection of an Asn 188 containing glycopeptides, consistent with attached tetraantennary glycan structures (Table 4).

4.4 Discussion

The need for improved prostate cancer biomarkers beyond the serum PSA test is increasingly evident. Because this test is applied to population screening, there is a wealth of data that indicates its strength in increasing detection of prostate cancers, but its use has also led to increased over-treatment and unnecessary surgeries for indolent disease. Despite its widespread use, there is still much characterization of PSA to be done, particularly in regards to its structural glycosylation properties and physiological function. Proximal fluids of the prostate like seminal fluid that are enriched for prostate

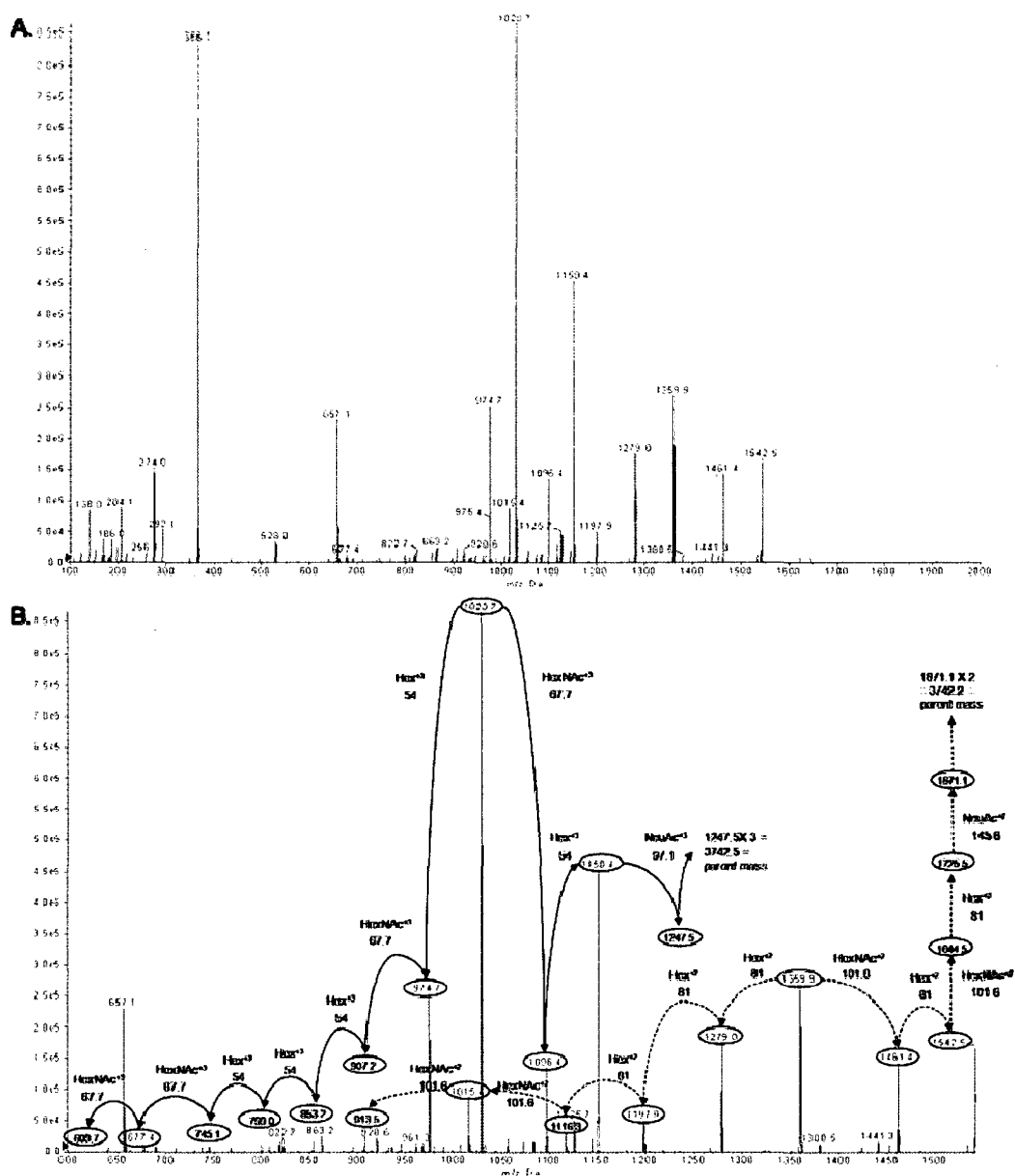








Figure 14. Precursor ion scan for 292 m/z hexose of tryptic PAP peptides.

A) Enhanced Product Ion (EPI) scan of a quadrupole-charged PAP glycopeptide with parent mass of 3744.0.

B) Expanded window of above EPI scan showing fragmentation of the parent ion that corresponds to the tryptic peptide FLN⁶²ESYKHEQVYIR containing the glycosylation site Asn-62 and a complex biantennary, singly sialylated N-glycan.

Table 4. PAP glycopeptides with corresponding N-glycan structures identified by QTRAP

N-linked Glycosylation site	Peptides generated by enzymatic digestion	Structures Identified
Asn-62	Trypsin Digestion FLNESYKHEQVYIR 1825.9 KFLNESYKHEQVYIR 1954.0	
	Chymotrypsin Digestion RKFLNESYKHEQVY 1840.9	
Asn-188	Trypsin Digestion N/A	
	Chymotrypsin Digestion CESVHNFTLPSW 1476.7 DPLYCESVHNFTLPSW 1964.9 YCESVHNFTLPSWATEDM 2304.0	
Asn-301	Trypsin Digestion NETQHEPYPLMLPGCSPSCPLER 2712.2 GEYFVEMYRNETQHEPYPLMLPGCSPSCPLER 4049.9	
	Chymotrypsin Digestion RNETQHEPYPLM 1530.7 RNETQHEPYPLMLPGCSPSCPLERF 2974.3	

Both tryptic and chymotryptic PAP digests were analyzed by the QTRAP as described in the experimental section. PI scans for oxonium ions 163, 366, and 292 are represented in the above table. Certain EPI scans revealed glycopeptide information that allowed for the assignment of both peptide and glycan.

derived secreted glycoproteins like PSA have long been a source of this enzyme, particularly as it is generally present at concentrations that range from 100-400 ug/ml in this fluid. Using a large cohort of archived seminal plasma samples reflective of healthy, benign and prostate cancer conditions allowed systematic characterization of PSA for similarities and differences in its disease specific glycosylation patterns. While PSA glycosylation has been previously studied by many other groups^{115-118, 122}, to our knowledge we are the first to examine PSA glycoforms across matched, disease-defined sample sets reflective of multiple samples. For a glycoprotein with one site of N-glycosylation, the number of different glycan structures identified across the conditions analyzed is highly variable, ranging from predominant complex bi- or tetraantennary structures, to hybrid and high mannose glycoforms. In this regards, use of pooled samples to identify disease specific variants of PSA will be highly limiting. While it is appropriate to define the repertoire of potential structures, there were no conclusions that could be reached regarding specific disease glycoform variants of PSA. Methods that facilitate characterization of individual samples like targeted lectin-ELISA assays¹⁹⁹ or specific selective reaction monitoring (SRM) approaches using instrumental configurations like the hybrid triple quadrupole MS assay for PAP will be necessary to better define disease specific glycoform changes for PSA. The diversity of glycan structures detected for PSA, and the well established role of PSA in clinical medicine and prostate disease, certainly warrant these types of approaches on larger sample cohorts.

The cumulative glycan results for PAP represent the first characterization of PAP structures using mass spectrometry approaches. Previous reports indicated that PAP glycosylation at Asn-301 was of the high-mannose type, while it was hypothesized that

the Asn-188 site contained complex-type glycans and the Asn-62 site contained non-complex structures¹²⁴. Our results confirm that high-mannose glycoforms are present at the Asn-301 site, with the presence of Man6 and Man7 glycans observed for this site. Based on the data summarized in Table 4, we have found that sialylated complex-type glycans occupy the site at Asn-62, with bi- and tri-antennary structures present. The glycans attached to Asn-188 are less defined, but the preliminary results indicate a larger glycan constituent, most likely the tetra-antennary complex sialylated and fucosylated structures observed in the characterization studies (Table 3). Clearly, application of alternative proteases besides trypsin could better clarify the glycopeptide constituents of the Asn-188 site. Emerging improvements in computer programs like SimGlycan (Applied Biosystems/PremierBiosoft) that allow annotation of large complex glycan constituents will also facilitate this characterization. Conversely, the HPLC and MALDI-TOF profiling indicated the presence of truncated glycan species predominantly in the prostate cancer samples. Their further characterization at the structural level, as well as their site of attachment, could lead to specific PAP glycan biomarker assays. Additionally, the described purification and analysis approaches for both PAP and PSA glycans are compatible with emerging quantitative isotope labeling strategies²⁰⁰. Missing for both PAP and PSA are any determinations of the anomeric linkages for the different glycan species, as linkage differences and positions of the sialic acid residues in particular could dictate biological and clinical differences. The permethylation strategies already utilized are equally valid for providing PSA and PAP glycans for more detailed MS/MSⁿ structural characterization approaches^{201, 202}, and these are currently ongoing in our laboratories.

The cumulative glycan structural information from PSA and PAP is being used in a prostate cancer biomarker “pipeline” to develop specific lectin-ELISA assays¹⁹⁹ targeting fucosylation and sialylation differences, as well as targeted SRM and/or multiple reaction monitoring (MRM) assays in proximal prostatic fluids. These approaches are particularly advantageous for the analysis of many individual seminal plasma samples, as well as other proximal prostatic fluids termed expressed prostatic secretions (EPS) being collected for molecular genetic biomarker assays^{74, 134}. Expressed prostatic secretions are collected in voided urine following a standard urological digital rectal exam combined with prostate massage, and analysis of their glycoprotein constituents could complement and extend results reported in seminal plasma. In conclusion, there are multiple glycan targets of potential clinical relevance that warrant continued structural analysis of PAP and PSA glycopeptide species. The use of seminal plasma derived proteins will continue to facilitate this characterization, and can also be readily adapted to other clinical relevant proximal fluids of the prostate.

CHAPTER IV

AIM II: ESTABLISH EXPRESSED PROSTATIC SECRETIONS AS A SOURCE OF PROSTATE-SPECIFIC ANTIGEN AND PROSTATIC ACID PHOSPHATASE

5.1 Introduction

Expressed prostatic secretions (EPS) are fluids derived directly from the prostate, which can be collected in different manners. EPS fluids have been routinely collected in the clinic since the late 1960's for the purpose of the diagnosis of chronic prostatitis and inflammatory chronic pelvic pain syndrome^{131, 203, 204}. Historically for the analysis of prostatitis, the prostate is forcefully massaged and the small amount of prostatic fluid is collected from the penis²⁰⁴, however this procedure can cause considerable pain for the patient. A second method involves squeezing the prostate ex vivo following a prostatectomy and collecting the fluid that drips from the gland²⁰⁵. A third method can be performed by the urological surgeon prior to surgery whereby the prostate is vigorously massaged while the patient is under anesthesia and prostatic fluid is pushed through the urethra and collected from the penis. It is this third method that is used to collect the direct EPS samples analyzed in this dissertation. A fourth method, and easiest to obtain clinically, is the collection of EPS in voided urine following a routine digital rectal exam (DRE) in the clinic. In this case, the prostate is gently massaged on both sides during the DRE exam, and is comparably less painful for the patient relative to the other collection methods. These fluids not only contain secreted proteins from within the prostatic infrastructure, but they also contain epithelial cells that are shed during the massaging process. EPS fluids are considered proximal fluids of the prostate and

Figures 17 and 18 are adapted from Drake, RR et al., J of Proteomics. 2009 Aug 20;72(6):907-917.

therefore have potential as a rich source of biomarkers for prostatic diseases, especially cancer. In recent years, EPS fluids have been used for the development of genetic-based assays for prostate cancer detection have gained increased popularity^{74, 132-134, 206-210}. A subset of these assays focus on the cellular sediment obtained from EPS fluids for the use in prostate cell-associated PCA3 mRNA testing (APTIMA PCA3, Gen-Probe Inc, San Diego, CA), without analyzing the supernatant^{132, 206-210}. Another epithelial-based target from the EPS urine sediment is the TMPRSS2-ERG fusion transcript which has been shown to positively correlate with prostate cancer^{74, 134, 211}.

EPS fluids have yet to gain popularity for the detection and discovery of current and new protein-based prostate cancer biomarkers. We hypothesize that EPS fluids are an enriched source of prostate derived proteins like PSA and PAP, and therefore can be useful for development of subsequent assays involving these two biomarkers. The objective of this aim is to determine how readily detectable PSA and PAP are in EPS fluids, and to determine if these fluids can be used in proteomic and glycomic based experiments. We found through fractionation, gel-separation, and mass spectrometry technologies that EPS fluids are indeed an enriched source of both PSA and PAP and have great potential for discovery, validation, and clinical collection for future early prostate carcinoma detection assays.

5.2 Experimental

Expressed prostatic secretions and urine samples

Urine samples, EPS urine samples, and direct EPS samples were acquired from the Virginia Prostate Center (VPC) Biorepository, with EPS sample collection beginning

in January 2007. Individuals providing the EPS urines are men who are scheduled for a prostate biopsy at the clinic and have consented to having additional samples collected for research purposes. When patients also provide a non-EPS urine sample, the voided urine is collected one hour prior to the DRE. EPS urines are collected following the DRE (10-20 ml), and are stored on ice for less than one hour at the clinic prior to transport to the biorepository. Once at the biorepository the samples are centrifuged to remove the cellular sediment, aliquoted, and all fractions and aliquots are stored at -80°C .

Two samples were collected from one individual on the same day. The first sample was collected prior to the DRE, and was noted as “pre-DRE urine.” The second sample was collected following a routine DRE, and was termed “post-DRE urine” or “EPS urine.” Approximately two milliliters were obtained of each sample, and protein concentrations were determined prior to any analysis. These samples were used for 2D-PAGE and LC-ESI-MS/MS analyses.

A single direct EPS sample was collected from a patient prior to a radical prostatectomy. The collection of this sample involves a vigorous massage of the prostate gland while the patient is under anesthesia during the pre-surgery exam, resulting in the collection of pure prostatic secretions via the urethra (0.5-1 ml). The sample is then stabilized in a sterile saline solution prior to centrifugation to obtain the cellular sediments and subsequently aliquoted and stored at -80°C .

In addition to individual sample analysis, pools of samples were generated, based on clinical diagnoses. An initial set of five pools were created based on the following disease risk stratification: normal, BPH, low PCa, intermediate PCa, and high PCa (Table 1). Each pool comprised of six individual EPS urines; four milliliters per individual, for

a total volume of 24 milliliters. The individual samples were first subjected to a low-speed centrifugation (RT, 5K RPM, five minutes) to remove any additional contaminants prior to pooling. The pools were concentrated using Amicon Ultra centrifugal filter devices with a 10 kDa cut-off (Millipore, Carrigtwohill, Co. Cork, Ireland) and low-speed centrifugation (4°C, 4.5K RPM, approximately 1 hour), resulting in a final volume of approximately two milliliters per pool. Protein concentrations were determined for each enriched pool. These pools were used for 1D-PAGE, 2D-PAGE, western blotting, and 2DE western blotting.

A second set of EPS urine pools were created based on the following stratifications BPH, low PCa risk, high PCa risk, and metastatic PCa (Table 1). Four milliliters each of six samples were combined to create each EPS urine pool. These pools were generated following the same protocol as for the above set of pools, with a final volume of approximately two milliliters, and protein concentrations were also obtained. This subset of pools was used for TAC, 1D-PAGE, and western blot analyses.

Two-dimensional PAGE

Two-dimensional PAGE was performed following the manufacturer's protocol (BioRad Laboratories Inc, Hercules, CA). Briefly, protein mixtures were combined with a rehydration buffer, applied to an IEF strip (11cm, pH 3-10), and passively rehydrated at room temperature overnight. The strips were then applied to the first dimension in a BioRad IEF focusing unit, followed by two equilibration steps and the second dimensional SDS-PAGE. For gels undergoing 2D-PAGE alone, the gels were either silver stained or Coomassie blue stained. For 2DE western blotting, the gels were then

transferred to PVDF membrane and processed following a standard western blotting protocol. Two hundred micrograms of each EPS urine pool (normal, BPH, low PCa, intermediate PCa, high PCa) was albumin and IgG depleted using commercially available spin columns (Sigma) following the manufacture's protocol and precipitated (10% TCA) prior to 2DE analysis and silver staining. Additionally, thirty micrograms per pool were combined together for a total protein concentration of 150 micrograms; in duplicate. These two pools were albumin and IgG depleted (ProteoPrep® Immunoaffinity albumin and IgG Depletion Kit, Sigma-Aldrich, St. Louis, MO) and 10% TCA precipitated prior to 2-DE analysis. One gel was silver stained while the mirror gel was transferred to PVDF for western blotting.

Western blotting

Western blotting for the detection of both PSA and PAP was performed following a standard western blot protocol. Briefly, gel-separated proteins were transferred to PVDF membrane using a semi-dry transfer element (BioRad Laboratories Inc, Hercules, CA). Blots were blocked with 5% milk in tris-buffered saline (TBS) for one hour followed by an overnight incubation in primary antibody. For PSA, a primary antibody was applied at a 1:3000 dilution in a 5% milk-TBS solution (goat anti-PSA affinity purified, Biodesign International, Saco, ME). For PAP, a primary antibody generated by our laboratory (mouse anti-PAP, protein A purified) was applied at a 1:1000 dilution in a 5% milk-TBS solution. After removal of the primary antibody, blots were washed before addition of secondary antibodies (for PSA used 1:50,000 dilution of anti-goat IgG-HRP;

for PAP used 1:5000 dilution of donkey anti-mouse IgG-HRP, Santa Cruz Biotechnology). After one hour incubation with secondary antibody, the blots were washed and a chemiluminescent buffer system was added to the blot for protein detection (Immun-Star HRP, BioRad Laboratories Inc, Hercules, CA).

Enzyme-linked immunosorbent assay (ELISA)

An ELISA assay was performed following a protocol previously reported by Alexander et al²¹². Briefly, 50 microliters of EPS urines were diluted 1:1 in coating buffer (10 mM NaCl/50 mM NaPO₄, pH 7.5) and incubated overnight at 4°C in 96-well plates. The plate wells were next blocked with the same coating buffer and 0.5% bovine serum albumin, followed by an overnight incubation at 4°C with rabbit polyclonal primary antibodies for PSA (1:500 dilution) or PAP (1:1000 dilution) (Abcam Inc, Cambridge, MA). Finally, enzyme activity was detected using a secondary antibody conjugated peroxidase assay (BioRad Laboratories Inc, Hercules, CA). Commercially available purified standards from seminal fluids (Fitzgerald Industries, Concord, MA) were used to generate linear standard curves for both PSA and PAP.

Thiophilic adsorption chromatography (TAC)

Thiophilic adsorption chromatography (TAC) was performed as previously described in Chapter IV with minor modifications to optimize the protocol for this physiologically different fluid. Briefly, 0.75 milligrams of total protein per pool (BPH, low PCa risk, high PCa risk, metastatic PCa) was loaded onto each column with a total

volume of three milliliters (sample and column buffer). Approximately four milliliters was collected for each unbound fraction, and two milliliters for each subsequent fraction.

LC-ESI-MS/MS

Three individual samples (“pre-DRE urine”, “post-DRE EPS urine”, and “direct EPS”) were trypsin digested and analyzed for protein content using an LTQ™ Linear Ion Trap (ThermoFinnigan, San Jose, CA). Ten micrograms of each sample was acetone precipitated and the pellets were reconstituted in ten microliters of 25 mM ammonium bicarbonate prior to digestion with paramagnetic immobilized trypsin beads (EnzyBeads™ Trypsine, Agro-Bio, La Ferte Saint Aubin, France) following a protocol developed by our laboratory. Briefly, samples were reduced by adding 100 mM of DTT to each sample and incubating them at 56°C for one hour. After samples cooled to room temperature, samples were alkylated in the dark for twenty minutes using 100 mM iodoacetamide. While samples alkylate, 25 μ l of trypsin beads were washed three times with 25 mM ammonium bicarbonate. The wash buffer was removed from the beads, and ten microliters of sample was added to the beads and mixed thoroughly. The bead and sample mixture was incubated at 37°C for thirty minutes. The reaction was quenched by removing the sample from the beads (using a magnetic separator) and placing the sample in a new vessel. Two microliters of each sample was then used for LTQ analysis. Digests were resuspended in 20 μ l Buffer A (5% acetonitrile, 0.1% formic acid, 0.005% heptafluorobutyric acid) and 10 μ l were loaded onto a 12-cm \times 0.075 mm fused silica capillary column packed with 5 μ m diameter C-18 beads (The Nest Group, Southborough, MA) using a N2 pressure vessel at 1100 psi. Peptides were eluted over

300 minutes, by applying a 0–80% linear gradient of Buffer B (95% Acetonitrile, 0.1% Formic Acid, 0.005% HFBA) at a flow rate of 150 $\mu\text{l}/\text{min}$ with a pre-column flow splitter resulting in a final flow rate of ~ 200 nl/min directly into the source. A LTQ™ Linear Ion Trap (ThermoFinnigan, San Jose, CA) was run in an automated collection mode with an instrument method composed of a single segment and 5 data-dependent scan events with a full MS scan followed by 4 MS/MS scans of the highest intensity ions. Normalized collision energy was set at 28%, activation Q was 0.250 with minimum full scan signal intensity at 1×10^5 with no minimum MS² intensity specified. Dynamic exclusion was turned on utilizing a three minute repeat count of 2 with the mass width set at 1.0 m/z. Protein searches were performed with MASCOT version 2.2.0 v (Matrix Sciences, London GB) using the SwissProt version 51.3 database. Parent ion mass tolerance was set at 1.5 and MS/MS tolerance 0.5 Da.

5.3 Results

2-D PAGE analysis of matched urine and EPS fluids

A matched set of urine samples were collected from one patient in the clinic, with one sample being collected prior to the DRE exam and the other sample being collected following the DRE exam. Seven hundred microliters of each sample was acetone precipitated, the proteins were separated by 2D-PAGE and the gels were silver stained. These gels were compared to one another to look for differences in protein patterns among the two samples, specifically in the mass ranges where we expect to find PSA (32 kDa) and PAP (50 kDa). There are clear differences in spot patterns all over the gel as well as in the mass ranges we expect to PSA and PAP (Figure 15).

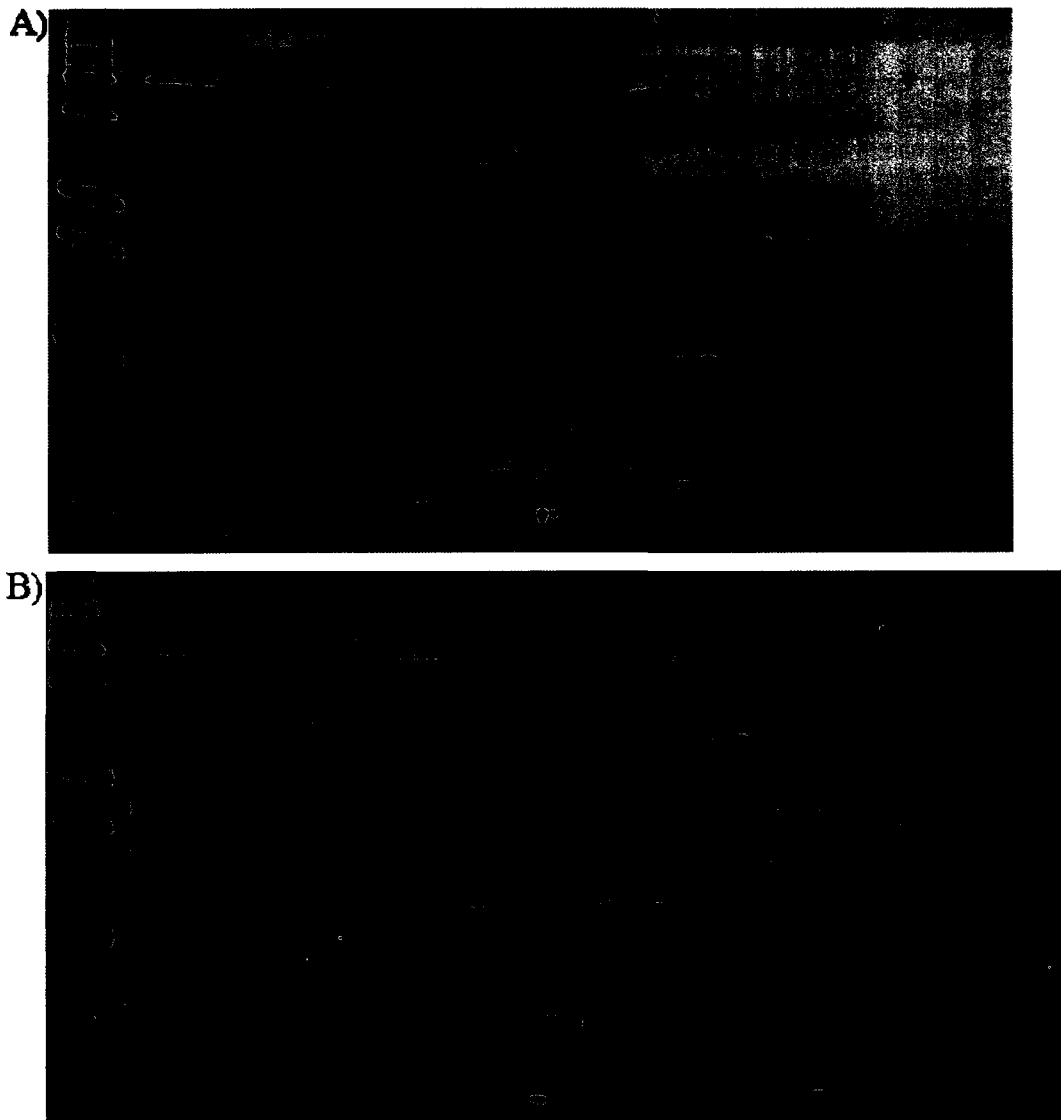


Figure 15. Comparison of pre-DRE urine to post-DRE urine. A matched set of urine samples were collected from one patient in the clinic, with one sample being collected prior to the DRE exam (panel A) and the other sample being collected following the DRE exam (panel B). Each sample was acetone precipitated, the proteins were separated by 2D-PAGE, and the gels were silver stained.

LC-ESI-MS/MS analysis of protein content of matched urine and EPS fluids

Ten micrograms of precipitated protein from the above matched samples was trypsin digested and run on the LTQ instrument in order to analyze the total protein content. The samples were first reduced and alkylated before being proteolytically digested using trypsin bound to magnetic beads. The tryptic peptides were run against the standard peptide identification gradient and the resultant spectrum were searched by MASCOT for identification of proteins. For the pre-DRE urine sample, PSA and PAP are not on the list of 45 significantly identified proteins, whereas for the post-DRE EPS urine sample, 65 proteins were significantly identified, with PSA and PAP being in the top 10 significant hits (Table 5 and Table 6). For the single direct EPS sample analyzed, 10 micrograms of protein was trypsin digested, and the digested peptides were also run on the LTQ instrument and analyzed for protein content. MASCOT searches identified 74 significant proteins, with PSA and PAP being among the top 20 significant hits (Table 7).

TAC fractionation of EPS fluids and detection of PSA and PAP by western blot

The subset of pools containing disease stratifications BPH, low PCa, high PCa, and metastatic PCa were TAC fractionated as described in the experimental section. A 100ul aliquot of each eluted fraction was 10% TCA precipitated in duplicate, the proteins were separated by 1D-PAGE, and the gels were subsequently either silver stained or transferred to PVDF for western blot analysis. Figure 16 shows the resulting 1D-PAGE gels for each disease condition. PAP was found to elute in the unbound fraction, therefore not binding to the TAC resin. PSA was found to elute across fractions 2, 3, and

Table 5. Proteins identified in pre-DRE urine

	Proteins significantly identified	emPAI score	peptide matches
1	Serum albumin	27.13	138
2	Uromodulin	2.66	82
3	Osteopontin	2.04	14
4	Prothrombin	0.44	14
5	Ig kappa chain C region	6.80	11
6	Kininogen-1	0.50	15
7	Vasorin	0.22	7
8	Protein AMBP	0.32	5
9	Serotransferrin	0.15	9
10	CD59 glycoprotein	2.38	7
11	Insulin-like growth factor-binding protein 7	0.63	8
12	Ig alpha-1 chain C region	0.33	11
13	Ribonuclease pancreatic	0.22	4
14	Clusterin	0.23	5
15	Ig lambda chain C regions	2.38	5
16	Pro-epidermal growth factor	0.18	11
17	Polymeric immunoglobulin receptor	0.04	7
18	Actin, alpha skeletal muscle	0.09	7
19	Actin, alpha cardiac muscle	0.09	5
20	Actin, cytoplasmic 1	0.09	4
21	ANKRD26-like family C member 1A	0.03	5
22	ANKRD26-like family C member 1B	0.03	5
23	Inter-alpha-trypsin inhibitor heavy chain H4	0.07	4
24	Ig gamma-2 chain C region	0.35	5
25	Cubilin	0.01	6
26	Alpha-2-HS-glycoprotein	0.31	6
27	L-lactate dehydrogenase B chain	0.10	2
28	Lysosomal alpha-glucosidase	0.07	3
29	Attractin	0.02	9
30	Urokinase-type plasminogen activator	0.08	1
31	Mannan-binding lectin serine protease 2	0.05	3
32	Golgi membrane protein 1	0.17	3
33	Immunoglobulin J chain	0.25	1
34	Vitamin D-binding protein	0.07	1
35	Ubiquitin conjugation factor E4 B	N/A	5
36	CD44 antigen	0.05	3
37	Ig gamma-1 chain C region	0.10	4

38	Sperm flagellar protein 2	N/A	7
39	Beta-2-microglobulin	0.29	1
40	Bone morphogenetic protein receptor type-1B	N/A	4
41	Vitronectin	0.07	2
42	GPN-loop GTPase 1	0.09	1
43	Ciliary neurotrophic factor receptor alpha	0.09	2
44	Mitochondrial GTPase 1	0.10	2
45	Transcription factor BTF3 homolog 3	0.16	2

Two micrograms of reduced, alkylated and trypsin digested peptides were applied to an LTQ™ Linear Ion Trap (ThermoFinnigan) mass spectrometer in the data-dependent acquisition mode for mass spectrometry analysis. Survey full scan MS spectra (m/z 300 to 1800) were acquired, with the four most intense ions in a scan sequentially isolated and fragmented in the linear ion trap by MS/MS. The peptide sequences were identified from their tandem mass spectra using Mascot in conjunction with the SwissProt database, and by using the following search criteria: carbamido-methylation of cysteine and oxidation of methionine residues as variable modifications, 1 missed enzyme cleavage site, and an error tolerance of 1.5 Da for MS and 0.5 Da for MS/MS.

Table 5, Continued.

Table 6. Proteins identified in post-DRE "EPS" urine

	Proteins significantly identified	emPAI score	peptide matches
1	Serum albumin	18.53	109
2	Lactotransferrin	3.21	50
3	Uromodulin	1.97	49
4	Prostatic acid phosphatase	2.36	41
5	Ig kappa chain C region	13.02	16
6	Ig alpha-1 chain C region	0.61	9
7	Prostate-specific antigen	2.05	12
8	Alpha-2-HS-glycoprotein	0.58	7
9	Polymeric immunoglobulin receptor	0.19	9
10	Prothrombin	0.23	8
11	Osteopontin	0.22	6
12	Transmembrane protease, serine 2	0.14	3
13	Collagen alpha-1(VI) chain	0.03	5
14	IgGfc-binding protein	0.01	8
15	Protein AMBP	0.44	7
16	Annexin A1	0.20	2
17	Brain acid soluble protein 1	0.17	3
18	Ig gamma-1 chain C region	0.49	4
19	Serotransferrin	0.05	6
20	Amyloid beta A4 protein	0.04	3
21	Ig gamma-2 chain C region	0.35	3
22	Vasorin	0.11	2
23	Carboxypeptidase E	0.15	4
24	Plasma protease C1 inhibitor	0.22	7
25	CD9 antigen	0.32	3
26	Myeloperoxidase	0.04	3
27	Kallikrein-2	0.28	4
28	Complement C3	0.04	7
29	Lysosomal alpha-glucosidase	0.04	4
30	CD59 glycoprotein	1.08	4
31	Vitamin D-binding protein	0.07	2
32	Haptoglobin-related protein	0.10	2
33	Leucine-rich repeat-containing protein 47	0.06	2
34	Heat shock protein HSP 90-alpha	0.04	4
35	Ribonuclease pancreatic	0.22	2
36	Ig heavy chain V-III region GA	0.30	1
37	Isocitrate dehydrogenase [NADP] cytoplasmic	0.08	3

38	Metallothionein-1G	0.70	4
39	Metallothionein-1M	0.70	3
40	Metallothionein-1E	0.71	4
41	Metallothionein-2	0.71	2
42	Receptor-type tyrosine-protein phosphatase eta	0.03	3
43	Aminopeptidase N	0.07	4
44	Ig heavy chain V-III region WEA	N/A	1
45	Non-secretory ribonuclease	0.21	2
46	Talin-1	0.01	7
47	Ras-related protein R-Ras2	0.16	3
48	L-xylulose reductase	0.15	3
49	Peptidyl-prolyl cis-trans isomerase A	0.21	2
50	Heat shock 70 kDa protein 1	0.11	2
51	Tetraspanin-6	0.14	2
52	Collagen alpha-1(XV) chain	0.03	2
53	14-3-3 protein theta	0.14	2
54	Heat shock 70 kDa protein 6	0.05	2
55	Heat shock 70 kDa protein 1L	0.05	3
56	Heat shock cognate 71 kDa protein	0.05	2
57	RNA-binding protein 28	0.04	2
58	Protein GRINL1A	N/A	2
59	Cofilin-1	0.21	1
60	Deoxyribonuclease-2-alpha	0.09	1
61	Alpha-enolase	0.08	1
62	Ryanodine receptor 2	0.01	10
63	Splicing factor 3B subunit 1	N/A	1
64	Syndecan-4	0.18	2
65	Serine/threonine-protein kinase SMG1	0.01	10

Two micrograms of reduced, alkylated and trypsin digested peptides were applied to an LTQ™ Linear Ion Trap (ThermoFinnigan) mass spectrometer in the data-dependent acquisition mode for mass spectrometry analysis. Survey full scan MS spectra (m/z 300 to 1800) were acquired, with the four most intense ions in a scan sequentially isolated and fragmented in the linear ion trap by MS/MS. The peptide sequences were identified from their tandem mass spectra using Mascot in conjunction with the SwissProt database, and by using the following search criteria: carbamido-methylation of cysteine and oxidation of methionine residues as variable modifications, 1 missed enzyme cleavage site, and an error tolerance of 1.5 Da for MS and 0.5 Da for MS/MS.

Table 6, Continued.

Table 7. Proteins identified in direct EPS fluids

	Proteins significantly identified	emPAI score	peptide matches
1	Protein-glutamine gamma-glutamyltransferase 4	1.94	33
2	Serum albumin	3.04	54
3	Brain acid soluble protein 1	2.32	11
4	Lactotransferrin	0.43	9
5	Ig kappa chain C region	0.46	2
6	Aminopeptidase N	0.29	9
7	Zinc-alpha-2-glycoprotein	1.57	13
8	Creatine kinase B-type	0.71	19
9	Actin, cytoplasmic 1	0.55	9
10	Prostate-specific antigen	1.21	13
11	Phosphatidylethanolamine-binding protein 1	0.24	2
12	Neprilysin	0.11	4
13	Prostatic acid phosphatase	0.86	10
14	Myristoylated alanine-rich C-kinase substrate	0.34	3
15	Ig alpha-1 chain C region	0.44	8
16	Cytochrome b561	0.39	2
17	Semenogelin-2	0.15	5
18	Actin, aortic smooth muscle	0.24	7
19	ANKRD26-like family C member 1A	0.08	11
20	Transmembrane BAX inhibitor motif-containing protein 1	0.14	2
21	Isocitrate dehydrogenase [NADP] cytoplasmic	0.34	5
22	Serotransferrin	0.13	5
23	Ig kappa chain V-III region SIE	0.46	2
24	Galectin-3-binding protein	0.07	3
25	Heat shock protein HSP 90-beta	0.12	3
26	Peptidyl-prolyl cis-trans isomerase A	0.28	2
27	Putative zinc-alpha-2-glycoprotein-like 1	0.48	3
28	Ig gamma-1 chain C region	0.66	6
29	Ig lambda chain C regions	0.48	3
30	Semenogelin-1	0.30	6
31	Ig gamma-4 chain C region	0.29	3
32	Macrophage migration inhibitory factor	1.04	2
33	Kappa-actin	0.12	7
34	Beta-actin-like protein 2	0.12	6
35	Putative heat shock protein HSP 90-beta 4	0.08	9
36	Heat shock protein HSP 90-alpha	0.06	3

37	Endoplasmin	0.05	5
38	Transthyretin	0.33	2
39	Ig gamma-2 chain C region	0.14	5
40	Receptor-type tyrosine-protein phosphatase S	0.02	9
41	Dipeptidyl peptidase 4	0.11	2
42	IgGFc-binding protein	0.01	11
43	Polymeric immunoglobulin receptor	0.06	4
44	Annexin A5	0.14	3
45	Ras-related protein Rab-4A	N/A	3
46	Ras-related protein Rab-8B	N/A	3
47	Ras-related protein Rab-39B	N/A	2
48	Ras-related protein Rab-30	N/A	2
49	Ras-related protein Rab-15	0.20	5
50	Ras-related protein Rab-35	N/A	2
51	Ras-related protein Rab-3B	N/A	2
52	Ras-related protein Rab-6A	N/A	3
53	Ras-related protein Rab-3C	N/A	4
54	Ras-related protein Rab-37	N/A	4
55	Ras-related protein Rab-3A	N/A	2
56	Ras-related protein Rab-1A	N/A	2
57	Ras-related protein Rab-33B	N/A	1
58	Calcineurin subunit B type 1	0.26	5
59	Glycogen phosphorylase, brain form	0.05	1
60	Ras-related protein Rab-27A	0.20	2
61	Annexin A3	0.13	2
62	Heat shock 70 kDa protein 1	0.07	4
63	Prostasin	0.29	4
64	Apoptosis-inducing factor 2	N/A	3
65	Structural maintenance of chromosomes protein 5	N/A	7
66	Protein S100-A8	0.50	2
67	Zinc finger protein ZXDC	N/A	3
68	Nephrocystin-3	0.03	9
69	Fatty acid synthase	0.02	3
70	Synaptotagmin-like protein 5	N/A	5
71	RalBP1-associated Eps domain-containing protein 2	N/A	3
72	BUD13 homolog	N/A	7
73	Myosin-Ixb	N/A	4
74	Paraneoplastic antigen Ma2	0.12	5

Table 7, Continued.

Two micrograms of reduced, alkylated and trypsin digested peptides were applied to an LTQ™ Linear Ion Trap (ThermoFinnigan) mass spectrometer in the data-dependent acquisition mode for mass spectrometry analysis. Survey full scan MS spectra (m/z 300 to 1800) were acquired, with the four most intense ions in a scan sequentially isolated and fragmented in the linear ion trap by MS/MS. The peptide sequences were identified from their tandem mass spectra using Mascot in conjunction with the SwissProt database, and by using the following search criteria: carbamido-methylation of cysteine and oxidation of methionine residues as variable modifications, 1 missed enzyme cleavage site, and an error tolerance of 1.5 Da for MS and 0.5 Da for MS/MS.

Table 7, Continued.

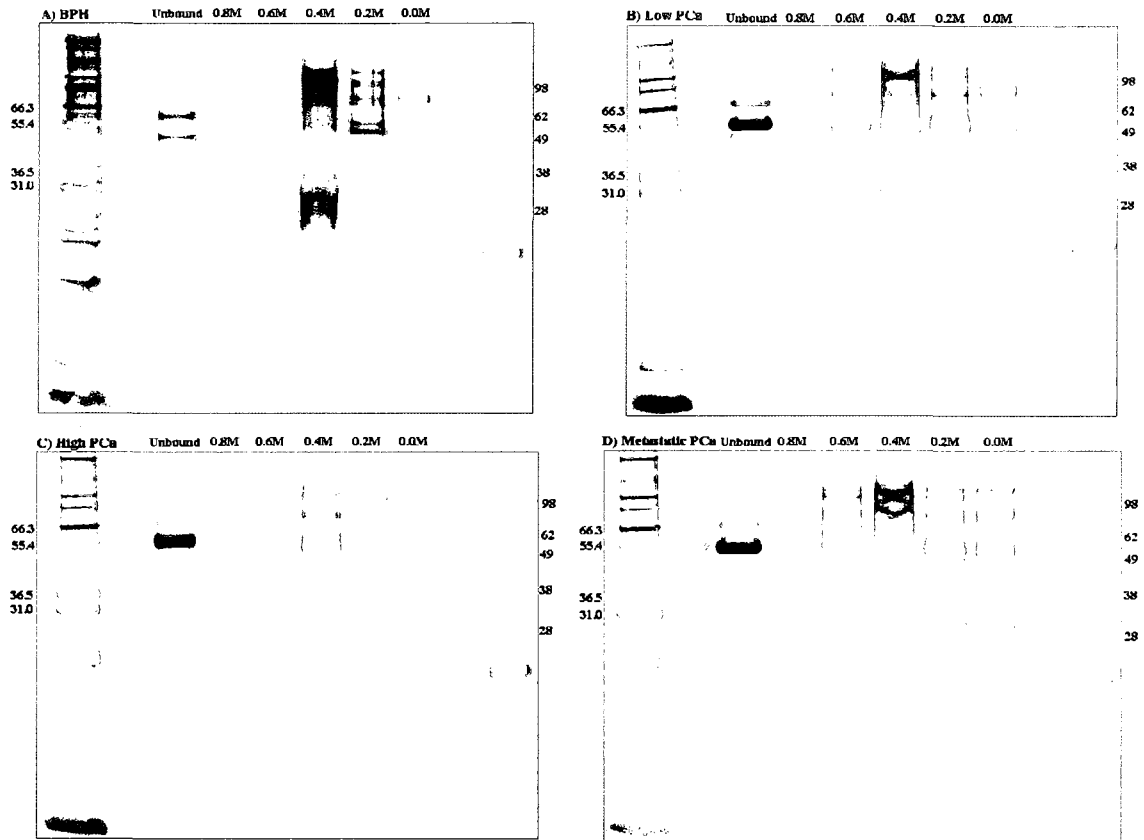


Figure 16. 1D-PAGE analysis of TAC fractionated EPS urine samples. Thiophilic adsorption chromatography (TAC) was used to fractionate pooled EPS urine fluids. The collected fractions were then run on 12% Bis-Tris gels, and silver stained. The disease-defined pools fractionated were BPH (Panel A), low risk PCa (Panel B), high risk PCa (Panel C), and metastatic PCa (Panel D). Lane 1 contains proteins that did not bind the TAC resin, with subsequent sodium sulfate elutions in Lane 2 (0.8M), Lane 3 (0.6M), Lane 4 (0.4M), Lane 5 (0.2M), and Lane 6 (0.0M). PSA and PAP were detected in respective fractions by gel staining and western blotting.

four which represent 0.6M, 0.4M, and 0.2M sodium sulfate elution fractions respectively, with the majority of PSA being detected in the 0.4M fraction (Figure 16).

2-DE western blot analysis for PSA and PAP from EPS fluids

A large pool of a subset of EPS urine pools (normal, BPH, low PCa risk, intermediate PCa risk, and high PCa risk) was created to examine the feasibility of detecting PSA and PAP in these fluids. In order to better examine the isoforms of both PSA and PAP, western blot analysis was performed on 2D-PAGE separated proteins. The total 150 ug of protein (in duplicate) was first albumin and IgG depleted using spin columns and then 10% TCA precipitated prior to 2D-PAGE analysis of mirror gels. One gel was silver stained for total protein content examination, while the second gel was transferred to PVDF membrane for western blotting. The blot was first probed and detected for PAP, then stripped of the primary and secondary antibodies as well as the ECL reagents (Restore western blot stripping buffer, Pierce-Thermo Fisher Scientific Inc, Rockford, IL), followed by probing for and detection of PSA. Figure 17 illustrates the 2D-PAGE map of all proteins detected by silver staining from EPS urines, as well as the 2D-PAGE pattern for both PSA and PAP isoforms and glycoforms in these EPS urine fluids²¹³.

ELISA analysis of PSA and PAP concentrations in EPS fluids

ELISA assays were performed in order to examine the levels of PSA and PAP present in the EPS samples used in the aforementioned experiments. We found that for the majority of EPS urines there is a detection range of 10-40 ug/ml for PSA and 3-10 ug/ml for PAP. Additionally, we observed a range of 80-120 ug/ml for PSA and 20-40

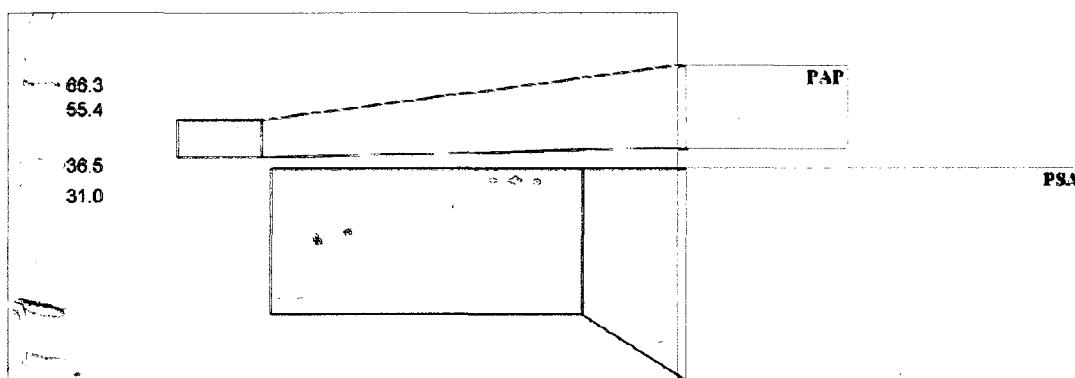


Figure 17. 2D-PAGE western blot analysis of PSA and PAP in EPS urine samples. Five disease-defined pools (normal, BPH, low risk PCA, intermediate risk PCa, high risk PCa) of EPS urines were combined together to make a general EPS urine pool unrelated to disease state and used for 2D-PAGE immunoblotting for the detection of both PSA and PAP. Two identical 8-16% Criterion Tris-HCl gels (BioRad) were run concurrently following the first dimension separation of EPS urine proteins. Following the gel electrophoresis, one gel was silver stained, while the second gel was transferred to PVDF membrane and western blot analysis was performed for both PSA and PAP. The silver stained gel and the PSA and PAP western blots are shown above with PAP and PSA spots highlighted on the silver stained gel. Adapted from Drake et al., 2009.

ug/ml for PAP in direct EPS fluids derived from cancer patients. Figure 18 illustrates the PSA and PAP levels across non-cancer (normal and BPH) and prostate cancer disease states (low risk, intermediate risk, high risk) in EPS urines. Lower levels of both PSA and PAP are observed in the prostate cancer EPS fluids as compared to the non-cancer samples.

5.4 Discussion

EPS fluids have routinely been collected in the clinic for the detection of prostatitis and chronic pelvic inflammatory disease, and the epithelial cell pellets resulting from these fluids are being used in a number of genetic-based assays for prostate cancer detection^{74, 132-134, 206-210}. Proteomic profiling of other bodily fluids such as seminal fluid and urine have been conducted^{127, 128}, however with no published studies to date, other than ours²¹³, involving protein analysis of the EPS fluids, our current analyses are novel and therefore are capable of providing the field with a wealth of new knowledge. With our present studies, we have determined that post-DRE “EPS” urines are an enriched source of prostate-derived proteins (Table 6), with PSA and PAP being the most important targets for this dissertation.

We have observed a clear difference in protein content between urine and EPS urines collected from the same patient within the same day, with a detectable presence of prostate-related proteins in the post-DRE urines as compared to the pre-DRE urines. This has been demonstrated by both 2D-PAGE analysis and LC-ESI mass spectrometry analysis of the pre-DRE and post-DRE urine collections (Figure 15, Table 5, and

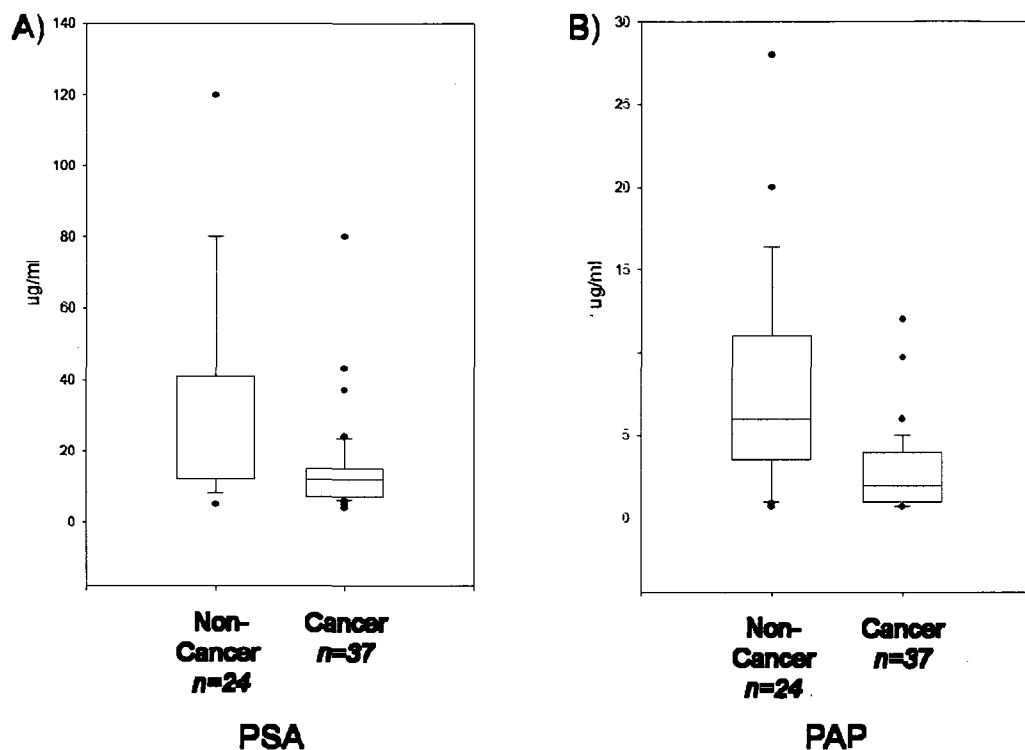


Figure 18. Concentration of PSA and PAP in EPS urines. ELISA assays were used to assess the concentrations of PSA (A) and PAP (B) in non-cancer (normal and BPH) and cancer (low risk, intermediate risk, and high risk) EPS urines, with the results displayed in the above box plots. The EPS urines were combined 1:1 with coating buffer (10 mM NaCl/50 mM NaPO₄, pH 7.5), and incubated overnight at 4°C in 96-well plates. On the next day, the wells were blocked with 0.5% bovine serum albumin in coating buffer; followed by an overnight incubation with primary antibody at 4°C. Finally, secondary antibodies conjugated to peroxidase allowed for detection of the enzyme activity on the next day. The above diagram plots the mean, 10th, 25th, 75th and 90th percentiles as vertical boxes with error bars, with outlier samples shown as dots outside of the box. Adapted from Drake et al., 2009.

Table 6). These analyses indicate a relative increase in protein abundance in the post-DRE urine as compared to the pre-DRE urine based on the spot patterns observed in the 2D-PAGE gels and the increase in numbers of proteins identified by mass spectrometry. In addition, we have found that both PSA and PAP are among the top most significant proteins identified in both EPS urine and direct EPS fluids (Table 5, Table 6, and Table 7) based on the LC-ESI mass spectrometry analysis. Additionally, we have successfully fractionated EPS urines by thiophilic adsorption chromatography, and have identified both PSA and PAP in their respective fractions (Figure 16). This fractionation scheme provides us with partially purified forms of PSA and PAP which can be further gel-purified and used in subsequent mass spectrometry-based assays for both protein and carbohydrate analyses. In addition, we have also effectively used 2D-PAGE western blot analysis to detect individual isoforms of both PSA and PAP derived from EPS urines (Figure 17). These isoforms likely indicate various glycoforms of PSA and PAP, therefore providing us with the ability to use these fluids to identify and target individual glycoforms for both proteins, which may be indicative of various prostate disease states, such as BPH and cancer. Finally, we used ELISA assays to examine the concentration of PSA and PAP in EPS fluids (Figure 18). We observed that there are decreased levels of both PSA and PAP in the cancer samples as compared to the non-cancer samples, which correlate with increased PSA and PAP levels seen in blood of some cancer patients. For the EPS urine samples used the non-cancer group had an average serum PSA level of 4.6 ng/ml (+/- 2.0; range 0.7– 7.9), and the cancer group had an average serum PSA level of 6.8 ng/ml (+/-5.0; range 0.1–24.5). It is likely that we are seeing lower protein levels

derived from the prostate as these proteins are leaked into the blood stream in some prostate cancer states.

All of these abovementioned characteristics will allow us to use these types of prostatic fluids in more targeted glycoproteomic and glycomic studies, with the intention of discovering superior biomarkers for the early diagnosis of prostate carcinomas. While direct EPS fluids are a great discovery fluid, they are not readily obtained in the clinic during a routine physical exam, as these fluids are collected under anesthesia prior to radical prostatectomy. However, EPS urines are useful as a discovery tool and are easily collected in the clinic during a routine physical exam, therefore making EPS urine fluids relevant for validation and use in clinical assays for the detection of early prostate carcinomas in the near future.

CHAPTER V

AIM III: APPLICATION OF NEW METHODOLOGIES TO EXPRESSED PROSTATIC SECRETIONS FOR PROSTATE CANCER GLYCOPROTEIN BIOMARKER DISCOVERY

6.1 Introduction

As previously stated, EPS fluids are proximal to the prostate and therefore are an enriched source of potential biomarkers for the detection of early prostate cancer. We have also demonstrated in aim II the enriched presence of prostate-derived proteins in post-DRE urines as compared to pre-DRE urines (Table 5 and Table 6). While genetic-based tests are already on the market^{74, 132-134, 206-210}, the use of EPS fluids for proteomic analyses and assays is not widely observed. In addition to potential protein biomarkers, the carbohydrate structures attached to glycoproteins may also provide the diagnostic information needed for better disease biomarkers. We hypothesize that by performing initial glycomic and glycoproteomic studies using EPS samples we will build the foundation for more targeted biomarker studies with the focus on the carbohydrate structures attached to secreted glycoproteins. As PSA and PAP are two prominent prostate-derived proteins, they make ideal targets for glycoproteomic and glycomic studies.

In addition to these two specific targets, total glycan approaches also have great utility in glycomic studies. First, the total glycan profile for a given fluid across differing disease states, such as cancer versus non-cancer, may provide a panel of altered glycoforms that can be used diagnostically for the detection of a given disease state, such

as prostate cancer. Secondly, once candidate glycoforms are identified, it may be possible to determine which proteins these glycoforms are attached to, allowing for the subsequent generation of protein-based biomarker clinical assays. The objective of this aim is to examine the glycosylation state of both PSA and PAP in EPS urine samples, as well as to examine the total glycan constituents in EPS urine and direct EPS samples. These goals will be achieved by first obtaining cleaved glycans from PSA and PAP derived from EPS urine samples, permethylating the free structures, and analyzing them by MALDI-TOF mass spectrometry. Next, we will use EPS urine-derived PAP in glycopeptide analyses using a triple quadrupole mass spectrometer in precursor ion scanning mode with the intent to identify individual glycoforms at each N-linked glycosylation site of PAP. And finally, we will obtain a fraction of cleaved glycans from EPS urine and direct EPS pools, permethylate these structures and analyze them by MALDI-TOF/TOF. We have determined that EPS urine-derived PAP glycans have a great potential in providing glycomic targets for better clinical assays. Additionally, total glycan profiles of EPS urine and direct EPS fluids may also provide valuable diagnostic glycan-based biomarkers for the detection of early prostate carcinomas.

6.2 Experimental

Expressed prostatic secretion samples

EPS urine and direct EPS samples were acquired from the Virginia Prostate Center (VPC) Biorepository, with EPS sample collection beginning in January 2007. Individuals providing the EPS urines are men who are scheduled for a prostate biopsy at the clinic and have consented to having additional samples collected for research

purposes. When patients also provide a non-EPS urine sample, the voided urine is collected one hour prior to the DRE. EPS urines are collected following the DRE (10-20 ml), and are stored on ice for less than one hour at the clinic prior to transport to the biorepository. Once at the biorepository the samples are centrifuged to remove the cellular sediment, aliquoted, and all fractions and aliquots are stored at -80°C .

Direct EPS samples were collected from patients prior to a radical prostatectomy. The collection of this sample involves a vigorous massage of the prostate gland while the patient is under anesthesia during the pre-surgery exam, resulting in the collection of pure prostatic secretions via the urethra (0.5-1 ml). The sample is then stabilized in a sterile saline solution prior to centrifugation to obtain the cellular sediments and subsequently aliquoted and stored at -80°C .

Pools of EPS urine and direct EPS samples were generated based on clinical diagnoses. The set of five pools that were previously described in chapter V and were created based on the following disease risk stratification: normal, BPH, low PCa, intermediate PCa, and high PCa, were used for total glycan analyses of EPS urine fluids (Table 1). Each pool comprised of six individual EPS urines; four milliliters per individual, for a total volume of 24 milliliters. The individual samples were first subjected to a low-speed centrifugation (RT, 5K RPM, five minutes) to remove any additional contaminants prior to pooling. The pools were concentrated using Amicon Ultra centrifugal filter devices with a 10 kDa cut-off (Millipore, Carrigtwohill, Co. Cork, Ireland) and low-speed centrifugation (4°C , 4.5K RPM, approximately 1 hour), resulting in a final volume of approximately two milliliters per pool.

A set of three EPS urine pools were created based on the following disease risk stratification: normal, BPH, and PCa. Each pool comprised of ten individual EPS urines; four milliliters per individual, for a total volume of 40 milliliters. The individual samples were first subjected to a low-speed centrifugation (RT, 5K RPM, five minutes) to remove any additional contaminants prior to pooling. The pools were concentrated using Amicon Ultra centrifugal filter devices with a 10 kDa cut-off (Millipore, Carrigtwohill, Co. Cork, Ireland) and low-speed centrifugation (4°C, 4.5K RPM, approximately 1 hour), resulting in a final volume of approximately two milliliters per pool. Protein concentrations were determined for each enriched pool. These pools were used for 1D-PAGE, western blotting, TAC, glycan analyses, and glycopeptide analyses.

A set of direct EPS pools were created based on the following stratifications: low risk PCa and intermediate risk PCa (Table 1). Four milliliters each of six samples were combined to create each EPS urine pool. These pools were generated following the same protocol as for the above sets of pools, with a final volume of approximately two milliliters, and protein concentrations were also obtained. This set of pools was used for total glycan analyses.

Thiophilic adsorption chromatography (TAC)

PSA and PAP were purified from a set EPS urine pools (normal, BPH, PCa) using thiophilic adsorption chromatography (TAC) as previously described in chapter III with a few adjustments based on the protein concentrations and volumes available for the new pools. Briefly, 1.0 milligram of total protein per pool was loaded onto each column with a total volume of four milliliters (sample and column buffer). Approximately four

milliliters was collected for each unbound fraction, and two milliliters for each subsequent fraction.

N-glycan permethylation

TAC-purified PSA and PAP gel bands derived from EPS urine pools were permethylated¹⁹⁵ following trypsin digestion as previously described in chapter III. Briefly, gel bands were reduced and alkylated, and then tryptically digested at 37°C for 18 hours. Next, trypsin was denatured at 100°C for 5 minutes, and PNGase F (New England Biolabs, Ipswich, MA) was added to the peptide mixture and incubated at 37°C for 18 hours. The resulting sample was purified by C18 columns and the N-glycans were collected in 5% acetic acid, and subsequently dried under reduced pressure. Dried N-glycans were permethylated following the protocol described by Ciucanu and Kerek¹⁹⁵. The permethylated N-glycans were purified using C18 columns, eluted in 85% acetonitrile, and then dried under a nitrogen stream.

In addition to gel bands, total glycan analysis was performed on tryptic peptides derived from EPS urine and direct EPS pools. Non-PCa and PCa sample sets were created from previously described EPS urine pools. For direct EPS samples, low PCa risk and intermediate PCa risk stratifications were used to generate the pooled sample sets. Each pool to be permethylated consisted of 180 micrograms of protein, which was subsequently precipitated prior to trypsin digestion, PNGase digestion, and permethylation.

MALDI-TOF/TOF

The dried permethylated N-glycans were prepared and analyzed by MALDI-TOF as previously described in chapter III. Briefly, the dried permethylated N-glycans were reconstituted in 100% methanol, and the sample was mixed 1:1 with 2,5-Dihydroxybenzoic acid (DHB) matrix (20mg/ml in 50% methanol), and then spotted on the MALDI-TOF target plate. Each sample was analyzed in positive ion mode and FlexControl and FlexAnalysis software (Bruker Daltonics, Germany) were used for spectra processing. The MALDI-TOF LIFT cell was utilized for MS/MS fragmentation analysis of permethylated glycans from total EPS pools. A glycan database offered by the Consortium for Functional Glycomics (<http://www.functionalglycomics.org>) was used to search permethylated glycan masses correlating to peaks of interest in MALDI-TOF spectra, and glycan “cartoons” representing mass peaks were built using GlycanBuilder ver 1.2 build 3353¹⁹⁶.

Hybrid triple quadrupole/linear ion trap mass spectrometry

A hybrid triple quadrupole/linear ion trap mass spectrometer 4000 (QTRAP[®] LC/MS/MS system, Applied Biosystems, Foster City, CA) coupled to a Tempo NanoLC system (Eksigent Technologies, Dublin, CA) was used to determine the structures of the glycans attached to each of the three PAP linkage sites: Asn-62, Asn-188, and Asn-301. The methods described by Sandra et al.¹⁹⁷ were used with minor modifications to optimize for our samples and instrumentation, and are detailed in chapter III. Figure 19 illustrates how the QTRAP was used in precursor ion scanning mode.

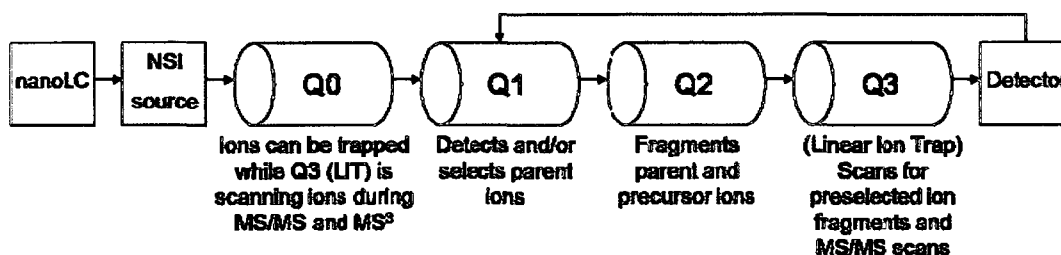


Figure 19. Triple quadrupole ion trap configuration for precursor ion scanning. Dried tryptic and chymotryptic peptides are reconstituted in 20 microliters of Buffer A (5% acetonitrile/0.1% formic acid/0.005% heptafluorobutyric acid in water) and 8 microliters per experiment is injected into the nanoLC system for fractionation prior to being applied to the nanospray ionization (NSI) source and trapped in quadrupole 0 (Q0). Next, the peptides are scanned in quadrupole 1 (Q1) to determine their masses and retention times. The peptides then travel to quadrupole 2 (Q2) which acts as a collision cell where fragmentation of the parent ions occurs. The ions then reach Quadrupole 3 (Q3) which is set to transmit only the mass of the diagnostic oxonium ions to the detector, such as m/z 163 (Hex^+), 204 (HexNAc^+), 292/274/256 (NeuAc^{+1}), and 366 (HexHexNAc^+). Upon their detection, an enhanced product ion scan (EPI) of the precursor ion is triggered causing fragmentation of the selected parent ions in Q2, then fragmented ions are captured in the ion trap and scanned out generating an MS/MS spectrum containing ions from the both the peptide and the attached carbohydrate structure. Additionally, the charge state of the parent ion will be reported, allowing for complete annotation of the spectrum, as illustrated in Figure 13.

ClinProt computational data analysis

ClinProt software version 2.0 (Bruker Daltonics, Germany) was used to baseline subtract, normalize spectra (using total ion current) and determine peak m/z values and intensities in the mass range of 1,000 to 6,000 daltons for the EPS PAP and EPS urine total glycan MALDI-TOF data. A mass window of 0.5% was used to align the spectra, and a k -nearest neighbor genetic algorithm was used to identify statistically significant differences in protein peaks in the three groups analyzed. Comparison of relative peak intensity levels between groups was also calculated within the software suite.

6.3 Results

Purification of PSA and PAP from EPS urine pools

Pooled sample sets representative of normal, benign prostatic hyperplasia (BPH) and prostate cancer conditions were generated using a biorepository of EPS urine samples. Thiophilic adsorption chromatography (TAC)¹⁸⁹ was used to purify PSA and PAP from the concentrated, pooled EPS urine fluids by batch elution. Approximately six milliliters was collected as flow-through and labeled as the unbound fraction, while approximately three milliliters was collected for each subsequent salt elution fraction. The consequential protein fractions were separated by SDS-PAGE, and it was observed that PAP did not bind to the TAC resin, while PSA eluted in the 0.6M, 0.4M, and 0.2M sodium sulfate fractions (Figure 20). We detected both PSA and PAP by Coomassie blue staining, and PSA and PAP identities were confirmed in their respective fractions by western blotting.

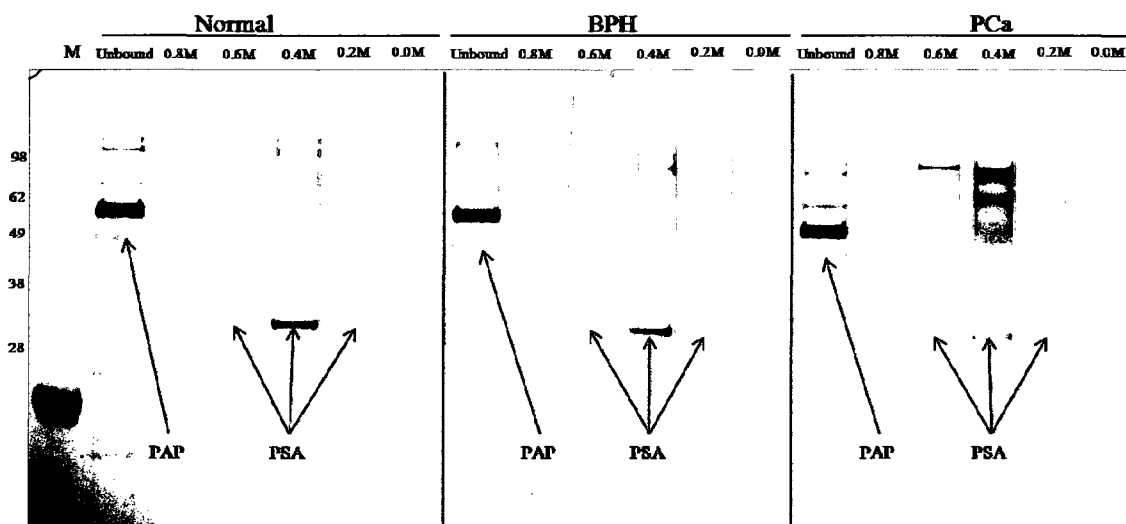


Figure 20. Thiophilic adsorption chromatography of EPS urine pools. EPS urine protein fractions from normal, BPH, and PCa defined pools purified by thiophilic adsorption chromatography (TAC) were separated on a 12% Bis-Tris NuPAGE SDS-gel (Invitrogen) and silver stained. Proteins that did not bind the TAC resin are shown in the lane marked Unbound, with protein from the 0.8M NaSO₄ elution, 0.6M, 0.4M, 0.2, and 0 M/25mM HEPES in the following lanes. PAP and PSA identities were confirmed in the above fractions by staining and western blots.

MALDI-TOF analysis of permethylated PSA and PAP glycans from EPS urines

Permethylation¹⁹⁵ of PNGase F cleaved glycans and MALDI-TOF analysis of the derivatized structures was performed for each of the EPS urine clinically-defined groups in order to further characterize PSA and PAP glycans. For PAP, 36 glycan structures were positively identified by MALDI-TOF, with the majority of these being complex sub-types, and a few representatives of the high-mannose sub-type were present as well (Table 8). For some structures, the sub-type was not able to be determined; however these structures would ultimately be classified as either a complex or hybrid subtype. Figure 21 represents the MALDI-TOF spectra collected for the permethylated PAP glycans from the normal, BPH, and PCa cohorts. Permethylated glycans cleaved from PSA in these EPS urine sample pools were not as readily detectable as structures from PAP, with only 23 structures being confidently identified (Table 9). The structures detected were mostly of the complex and high-mannose sub-types, with these results remaining consistent with glycan structures previously reported for PSA arising from serum and seminal fluids^{115-117, 122}, as well as seen from our seminal plasma studies (Table 3). MALDI-TOF spectra obtained for the PSA glycans for the EPS urine samples is shown in Figure 21.

Triple-quadrupole mass spectrometry analysis of PAP glycopeptides derived from EPS urines

As in aim I, glycopeptide analysis of the three N-linked glycosylation sites for PAP found in EPS urine fluids was performed using a triple-quadrupole mass spectrometer. PAP-containing EPS urine fractions were separated by SDS-PAGE and

Table 8. Permethylated PAP glycans from normal, BPH, and PCa EPS urine pools analyzed by MALDI-TOF

Number	m/z	Proposed Glycan Structure	Sub-Type	Number	m/z	Proposed Glycan Structure	Sub-Type
1	1784.08	Man6 *	High Mannose	19	3416.8	NeuAc2Gal3N3M3N2F x2	Complex
2	1988.05	Man7	High Mannose	20	3504.84	NeuAc1Gal4N4M3N2F	Complex
3	2040.08	GalN2M3N2F	Complex	21	3603.89	NeuAc3Gal3N3M3N2	Complex
4	2070.08	Gal2N2M3N2	Complex	22	3665.83	Hex7dHex4HexNac6 x3	Complex
5	2110.12	Hex4HexNac5 *	N/A	23	3691.9	NeuAc2Gal4N4M3N2 x2	Complex
6	2187.13	Hex5HexNac3NeuAc1 *	N/A	24	3777.98	NeuAc3Gal3N3M3N2F	Complex
7	2192.39	Man8 *	High Mannose	25	3866.05	NeuAc2Gal4N4M3N2F x2	Complex
8	2214.17	Hex4dHex2HexNac4 *	N/A	26	3949.06	Hex6dHex2HexNac5NeuAc3	Complex
9	2228.19	NeuAc1Gal1N2M3N2	Complex	27	4053.21	NeuAc3Gal4N4M3N2 x3	Complex
10	2244.19	Gal2N2M3N2F	Complex	28	4227.31	NeuAc3Gal4N4M3N2F x3	Complex
11	2315.18	Hex5HexNac5 *	N/A	29	4402.47	Hex9dHex1HexNac8NeuAc1	N/A
12	2432.3	NeuAc1Gal2N2M3N2	Complex	30	4414.47	NeuAc4Gal4N4M3N2	Complex
13	2606.39	NeuAc1Gal2N2M3N2F	Complex	31	4576.69	Hex9dHex2HexNac8NeuAc1 x2	N/A
14	2793.48	NeuAc2Gal2N2M3N2	Complex	32	4589.58	Hex9HexNac8NeuAc2	Complex
15	2880.51	NeuAc1Gal3N3M3N2	Complex	33	4676.63	Hex8dHex1HexNac7NeuAc3 x2	N/A
16	2967.57	NeuAc2Gal2N2M3N2F	Complex	34	4765.67	Hex11HexNac10	N/A
17	3055.62	NeuAc1Gal3N3M3N2F	Complex	35	4840.52	Hex10dHex3HexNac9 x3	N/A
18	3242.71	NeuAc2Gal3N3M3N2 x2	Complex	36	5035.76	Hex8dHex1HexNac7NeuAc4 x3	Complex

Identified m/z values were used for database searches, and corresponding masses that could be assigned to a biologically relevant N-glycan structure are listed. An asterisk denotes structures that are one representation of multiple possible glycoforms for a given mass. The shown structure in these cases was chosen based on its apparent prevalence in mammalian species. Cartoon representations are as follows: ■ =GlcNAc, ●

=Mannose, ○ =Galactose, ▲=Fucose, ◆=NeuAc, □=GalNAc

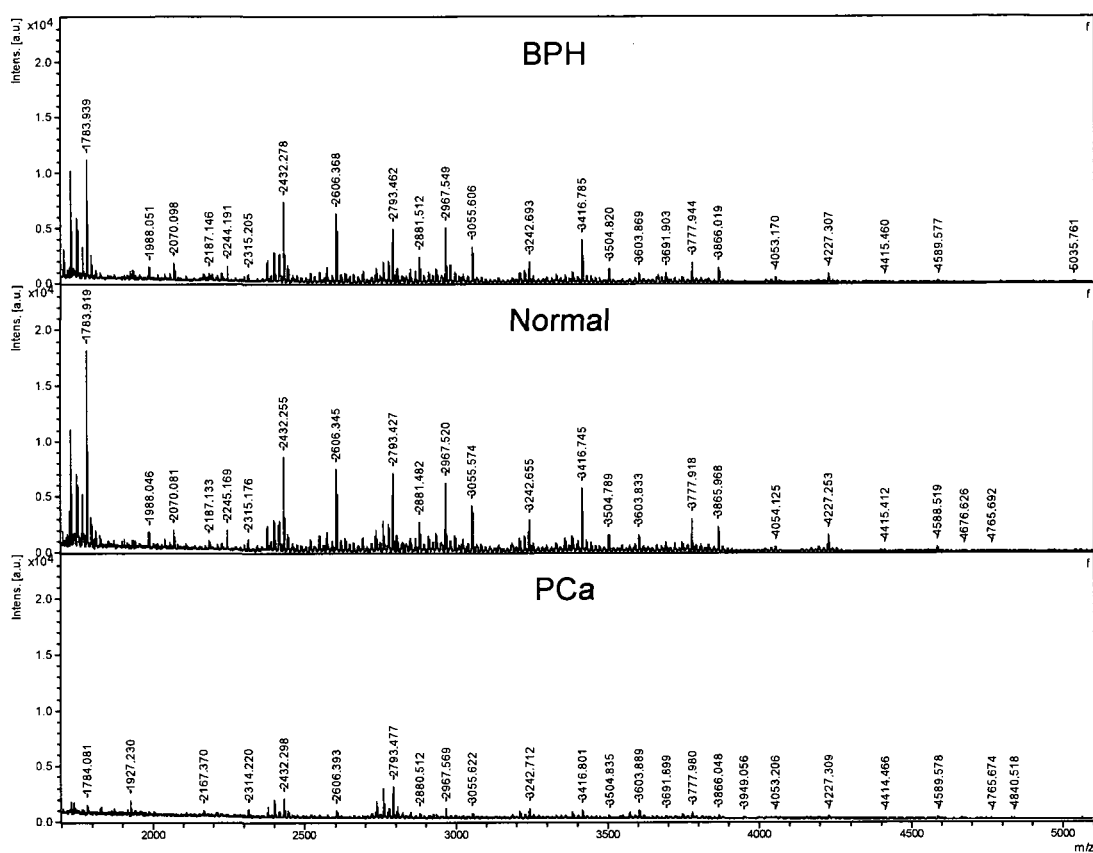



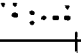


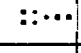
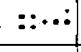


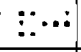
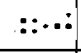



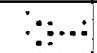
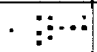
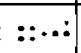
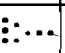
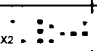
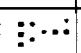
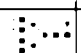
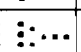


Figure 21. MALDI-TOF spectra of permethylated PAP glycans derived from EPS urine samples. Representative MALDI spectra for permethylated PAP glycans from BPH, normal, and PCa disease-defined pools are shown. Glycan structures corresponding to detected m/z peaks are listed in Table 8.

Table 9. Permethylated PSA glycans from normal, BPH, and PCa EPS urine pools analyzed by MALDI-TOF

Number	m/z	Proposed Glycan Structure	Sub-type
1	1579.872	Man5 	High Mannose
2	1783.983	Man6 	High Mannose
3	2112.12	Hex4HexNAc5 	Complex
4	2142.069	Hex4dHex3HexNAc3 	Hybrid
5	2243.344	Gal2N2M3N2F 	Complex
6	2316.137	Hex5HexNAc5 	Complex
7	2432.213	NeuAc1Gal2N2M3N2 	Complex
8	2444.26	Hex3dHex1HexNAc5NeuAc1 	Complex
9	2532.228	Hex4dHex1HexNAc6 	Complex
10	2551.332	Hex6dHex3HexNAc3 	Hybrid
11	2574.326	Hex4dHex2HexNAc4NeuAc1 	Complex
12	2606.261	NeuAc1Gal2N2M3N2F 	Complex
13	2677.434	NeuAc1Gal2N3M3N2 	Complex
14	2719.266	NeuAc1Gal1N4M3N2 	Complex
15	2793.228	NeuAc2Gal2N2M3N2 	Complex
16	2838.442	Hex5dHex3HexNAc5 	Complex
17	2893.333	Hex4dHex1HexNAc6NeuAc1 	Complex
18	2967.352	NeuAc2Gal2N2M3N2F 	Complex
19	3131.409	Gal6N3M3N2 	Complex
20	3198.373	Hex5dHex3HexNAc5NeuAc1 	N/A
21	3254.484	Hex3dHex1HexNAc6NeuAc2 	Complex
22	3549.569	Hex9dHex1HexNAc6 	Complex
23	3603.568	NeuAc3Gal3N3M3N2 	Complex

Identified m/z values were used for database searches, and corresponding masses that could be assigned to a biologically relevant N-glycan structure are listed. An asterisk denotes structures that are one representation of multiple possible glycoforms for a given mass. The shown structure in these cases was chosen based on its apparent prevalence in mammalian species. Cartoon representations are as follows: ■ =GlcNAc, ●

● =Mannose, ○ =Galactose, ▲ =Fucose, ◆ =NeuAc, □ =GalNAc

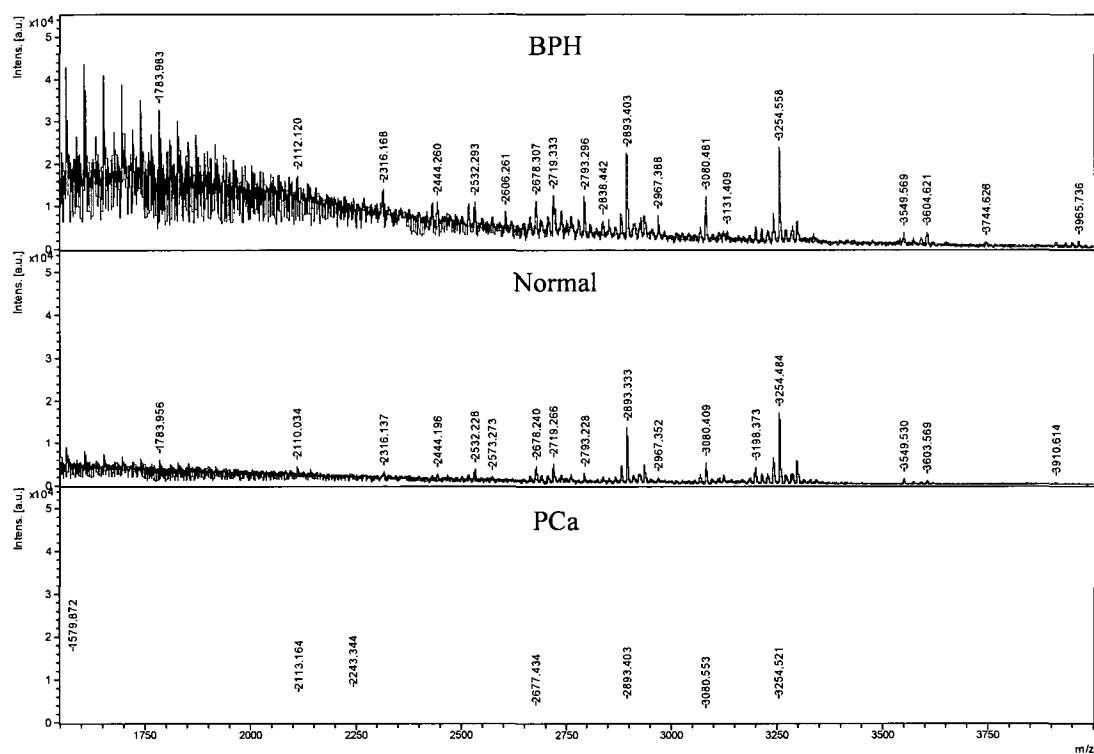


Figure 22. MALDI-TOF spectra of permethylated PSA glycans derived from EPS urine samples. Representative MALDI spectra for permethylated PSA glycans from BPH, normal, and PCa disease-defined pools are shown. Glycan structures corresponding to detected m/z peaks are listed in Table 9.

proteolytically digested with either trypsin or chymotrypsin prior to further sample separation by the in-line nanoLC system and mass spectrometry analysis. Precursor ion mode was utilized for the detection of oxonium ions 163, 292, and 366 as previously described in chapter III. Figure 23 illustrates an identified chymotrypsin digested glycopeptide with an attached high mannose glycan structure, while Figure 24 demonstrates a complex biantennary, singly sialylated N-glycan attached to a tryptic glycopeptide. Overall, we identified two complex structures attached to Asn-62, and one high mannose structure attached to Asn-301 (Table 10). These data correlate with our previous studies using seminal plasma-derived PAP peptides, however we did not successfully identify as many glycoforms attached to Asn-62 and Asn-301, nor did we positively identify any glycoforms at Asn-188.

Total glycan analysis of EPS urine and direct EPS pools by MALDI-TOF

In order to further characterize EPS fluids, glycan analysis on total pools was performed. A paired cohort of EPS urines deemed non-cancer and cancer were used as representatives of EPS urine fluids. The non-cancer pool consisted of normal and BPH classified individuals, while the cancer pool was generated from individuals with low, intermediate, or high-risk diagnosed prostate cancer. Each pool contained a total of 180 micrograms of protein (90 micrograms each of normal and BPH; 60 micrograms each of low, intermediate, and high risk PCa), and the pools were precipitated with 10% TCA prior to trypsin digestion. For direct EPS samples, a pool of low-risk prostate cancer individuals was compared to a pool containing intermediate-risk prostate cancer

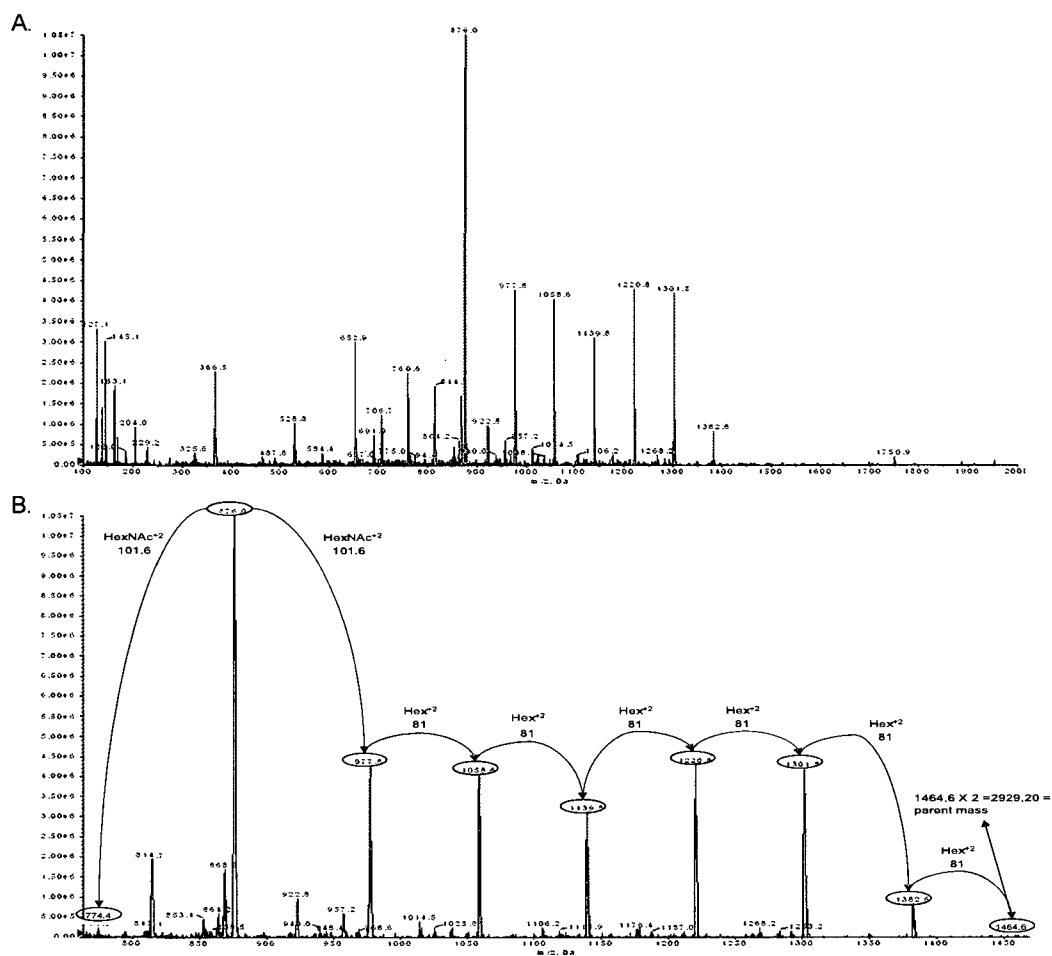


Figure 23. Precursor ion scan for 163 m/z hexose of chymotryptic EPS urine PAP peptides. A) Enhanced Product Ion (EPI) scan of a quadrupole-charged PAP glycopeptide with parent mass of 2929.35. B) Expanded window of above EPI scan showing fragmentation of the parent ion that corresponds to the chymotryptic peptide RNETQHEPYPLM containing the glycosylation site Asn-301 and a Man6 N-glycan.

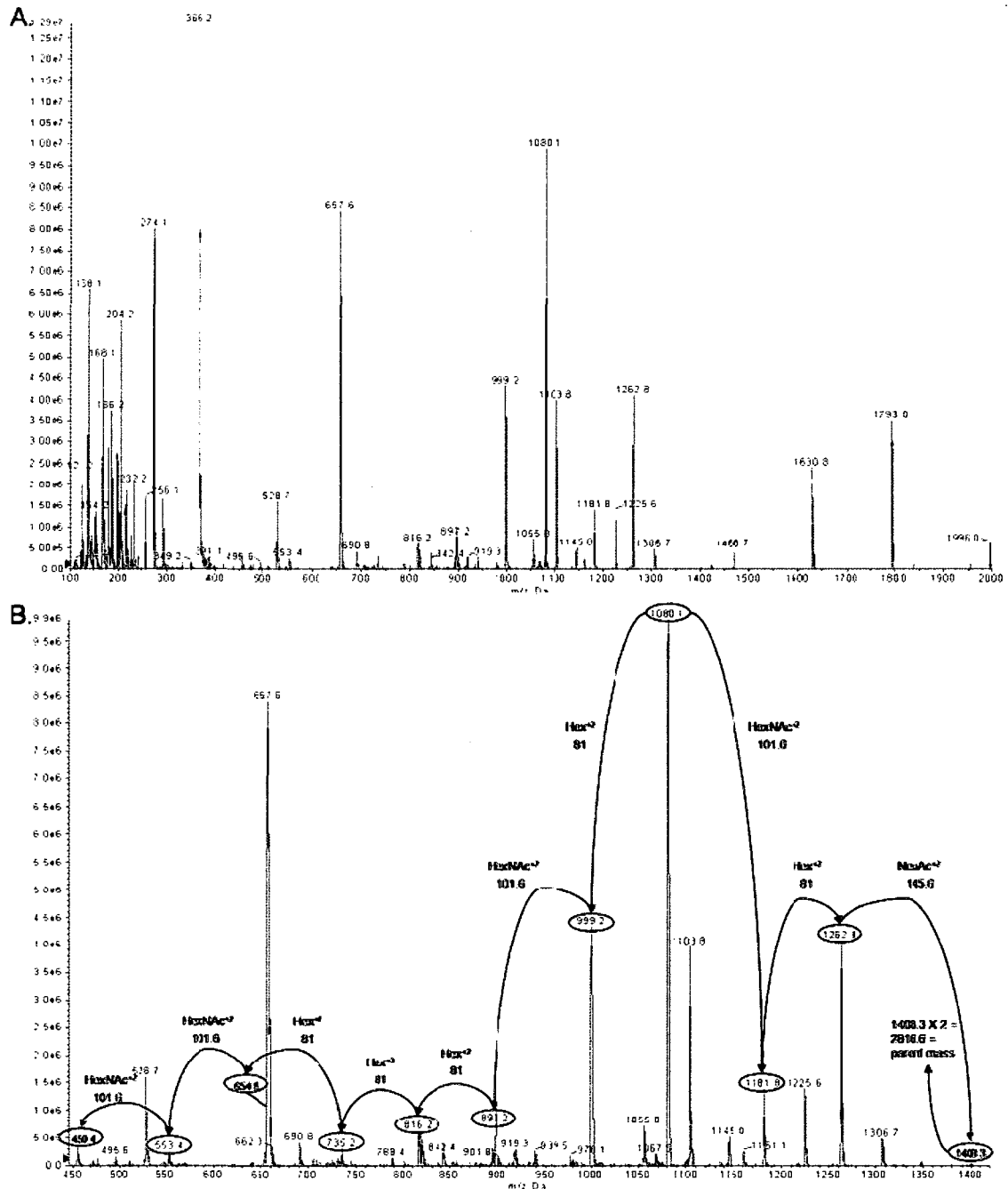
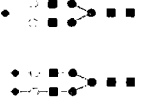
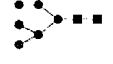


Figure 24. Precursor ion scan for 366 m/z hexose of tryptic EPS urine PAP peptides. A) Enhanced Product Ion (EPI) scan of a quadrupole-charged PAP glycopeptide with parent mass of 2816.31. B) Expanded window of above EPI scan showing fragmentation of the parent ion that corresponds to the tryptic peptide FLNESYK containing the glycosylation site Asn-62 and a complex biantennary, singly sialylated N-glycan.

Table 10. EPS urine PAP glycopeptides and their corresponding N-glycan structures identified by triple quadrupole MS/MS analysis

N-linked Glycosylation site	Peptides generated by enzymatic digestion	Structures Identified
Asn-62	Trypsin Digestion FLNESYK 900.45 FLNESYKHEQVYIR 1825.9 KFLNESYKHEQVYIR 1954.0	
	Chymotrypsin Digestion RKFLNESYKHEQVY 1840.9	
Asn-188	Trypsin Digestion N/A	N/A
	Chymotrypsin Digestion N/A	
Asn-301	Trypsin Digestion NETQHEPYPLMLPGCSPSCPLER 2712.2 GEYFVEMYRNETQHEPYPLMLPGCSPSCPLER 4049.9	
	Chymotrypsin Digestion RNETQHEPYPLM 1530.7	

Both tryptic and chymotryptic PAP digests were analyzed by the QTRAP as described in the experimental section. PI scans for oxonium ions 163, 366, and 292 are represented in the above table. Certain EPI scans revealed glycopeptide information that allowed for the assignment of both peptide and glycan.

individuals, with each pool containing 180 micrograms of total protein. These pools were also TCA precipitated and trypsin digested. The tryptic digestions were then treated with PNGase F and permethylated. The permethylated glycans were analyzed by MALDI-TOF/TOF (Figure 25 and Figure 26). Forty-three glycans were positively identified from the EPS urine fluids, while direct EPS fluids yielded 24 glycan structures (Table 11 and Table 12). For both EPS urine and direct EPS samples, mostly complex subtype glycans were observed, with some high-mannose and hybrid subtypes represented as well. There was extensive branching, sialylation, and fucosylation detected in all sample sets (Table 11 and Table 12), indicating the complexity of these fluids as well as the presence of many glycosylated proteins. Due to the high concentration of the EPS fluids, the mass spectra resulted in very intense peaks, thus allowing for MS/MS fragmentation analysis of several glycan structures. A representation of MALDI-TOF/TOF LIFT spectra is shown in Figure 27, demonstrating the fragmentation pattern of a permethylated complex, biantennary glycan containing one terminal sialic acid by the MALDI-TOF/TOF instrument.

Detection of fucosylation differences among disease states by ClinProt data analysis

Clinprot software (version 2.0) was used to analyze MALDI-TOF spectra for EPS urine PAP and EPS urine total glycan samples (Figure 21 and Figure 25). From these analyses, we found that glycan structures without a core fucosylation were represented in equivalent abundance among different disease states (i.e. normal, BPH, PCa), with an example shown in Figure 28. In comparison, we observed an overall decrease in intensity of fucosylated species in the cancer samples as compared to non-cancer samples, which is exemplified in Figure 29. The fucosylated glycans found to be

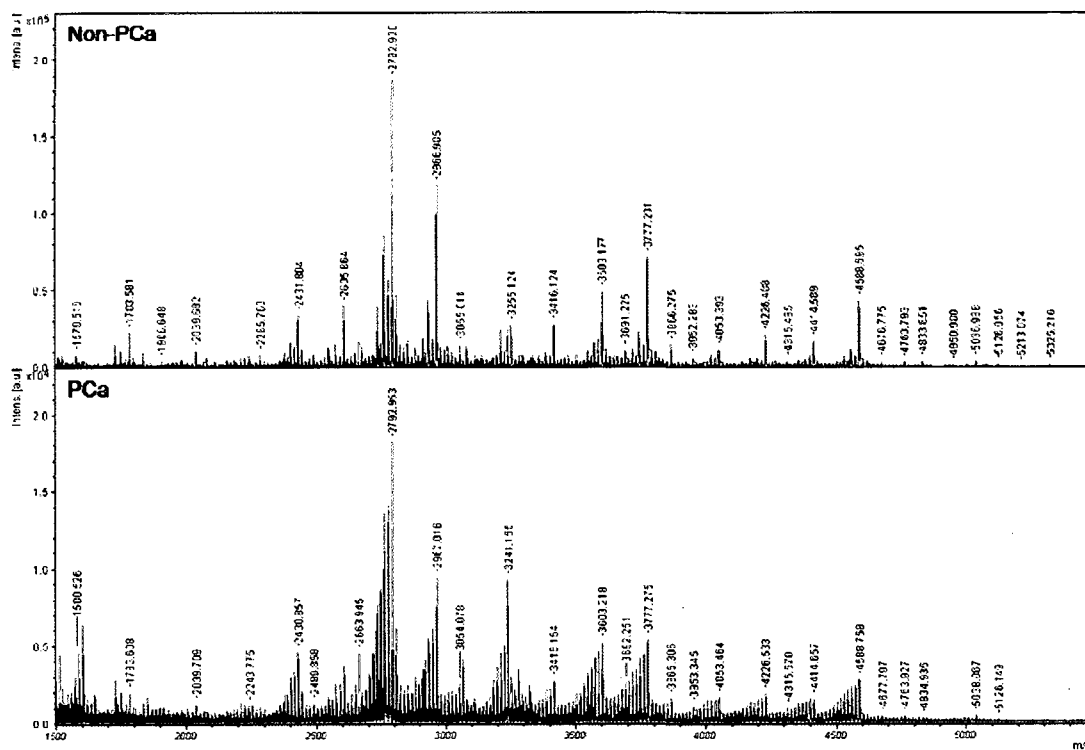


Figure 25. MALDI-TOF spectra of EPS urine N-glycans. Representative MALDI spectra for permethylated N-glycans from non-PCa and PCa disease-defined EPS urine pools are shown. Glycan structures corresponding to detected m/z peaks are listed in Table 11.

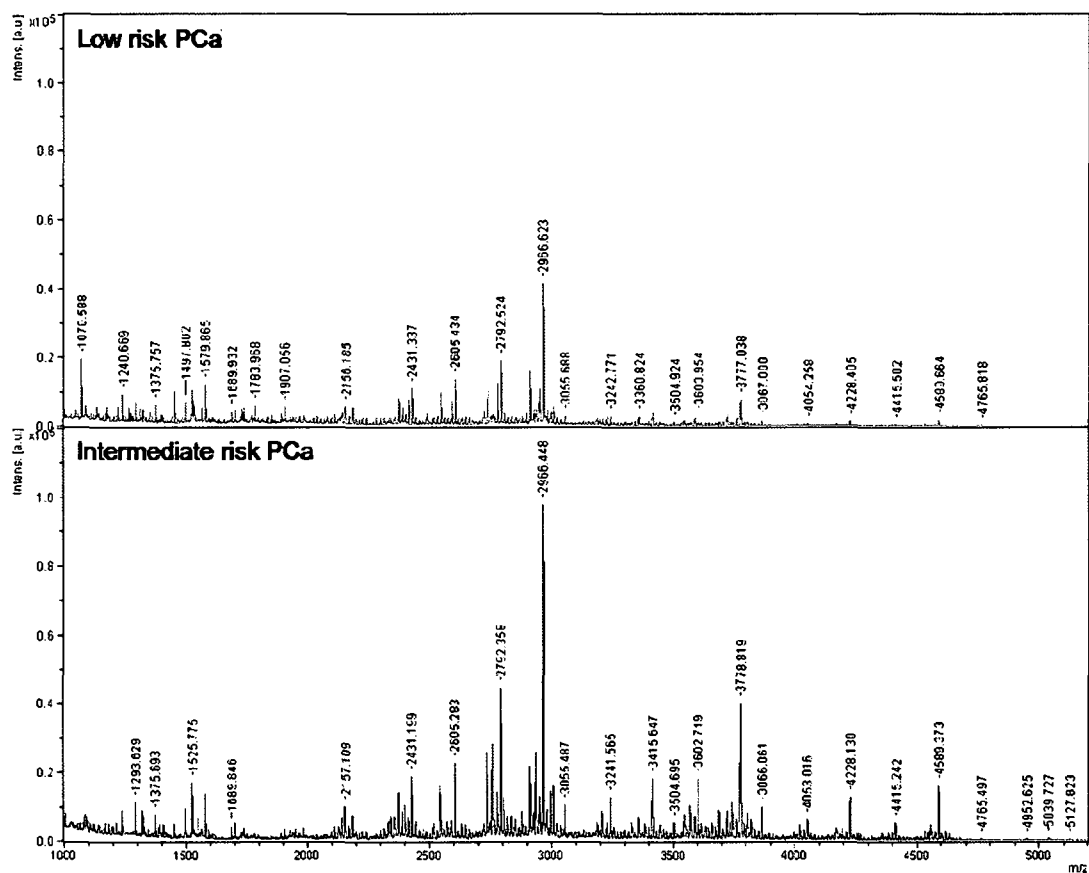


Figure 26. MALDI-TOF spectra for permethylated direct EPS N-glycans. Representative MALDI spectra for permethylated N-glycans from low risk PCa and intermediate risk PCa disease-defined direct EPS pools are shown. Glycan structures corresponding to detected m/z peaks are listed in Table 12.

Table 11. Permethylated glycans from EPS urine pools

Number	m/z	Proposed Glycan Structure	Sub-Type	Number	m/z	Proposed Glycan Structure	Sub-Type
1	1579.5	M5N2	High Mannose	23	3212.048	NeuAc2Gal2N3M3N2F	Complex
2	1783.557	M6N2	High Mannose	24	3242.063	NeuAc2Gal3N3M3N2	Complex
3	1835.595	N2M3N2F	N/A	25	3254.124	Hex3dHex1HexNAc6NeuAc2	Complex
4	1866.64	Gal1N2M3N2	Complex	26	3281.134	NeuAc2Gal2N4M3N2	Complex
5	1906.621	N3M3N2	Complex	27	3287.086	Hex6dHex3HexNAc6	Complex
6	1987.672	M7N2	High Mannose	28	3416.105	NeuAc2Gal3N3M3N2F	Complex
7	2039.664	GalN2M3N2F	Complex	29	3504.121	NeuAc1Gal4N4M3N2F	Complex
8	2069.675	Gal2N2M3N2	Complex	30	3603.148	NeuAc3Gal3N3M3N2	Complex
9	2080.682	N3M3N2F	Complex	31	3746.192	Hex6HexNAc10	Complex
10	2110.689	Hex4HexNAc5	Complex	32	3777.211	NeuAc3Gal3N3M3N2F	Complex
11	2185.703	Hex5HexNAc3NeuAc1	N/A	33	3866.241	NeuAc2Gal4N4M3N2F	Complex
12	2212.706	Hex4dHex2HexNAc4	Complex	34	3952.261	Hex8dHex1HexNAc7NeuAc1	Complex
13	2227.728	NeuAc1Gal1N2M3N2	Complex	35	4053.364	NeuAc3Gal4N4M3N2	Complex
14	2244.735	Gal2N2M3N2F	Complex	36	4227.458	NeuAc3Gal4N4M3N2F	Complex
15	2285.759	Gal1N3M3N2F	Complex	37	4314.459	Hex8dHex1HexNAc7NeuAc2	Complex
16	2431.795	NeuAc1Gal2N2M3N2	Complex	38	4414.553	NeuAc4Gal4N4M3N2	Complex
17	2489.82	Gal2N3M3N2F	Complex	39	4588.661	NeuAc4Gal4N4M3N2F	Complex
18	2605.853	NeuAc1Gal2N2M3N2F	Complex	40	4676.711	Hex8dHex1HexNAc7NeuAc3	Complex
19	2663.87	Gal2N3M3N2F2	Complex	41	4763.767	Hex11HexNAc10	Complex
20	2792.908	NeuAc2Gal2N2M3N2	Complex	42	4833.816	Hex7dHex1HexNAc7NeuAc4	Complex
21	2966.969	NeuAc2Gal2N2M3N2F	Complex	43	5038.946	Hex8dHex1HexNAc7NeuAc4	Complex
22	3054.996	NeuAc1Gal3N3M3N2F	Complex				

Identified m/z values were used for database searches, and corresponding masses that could be assigned to a biologically relevant N-glycan structure are listed. An asterisk denotes structures that are one representation of multiple possible glycoforms for a given mass. The shown structure in these cases was chosen based on its apparent prevalence in mammalian species. Cartoon representations are as follows: ■ =GlcNAc, ●

=Mannose, ○ =Galactose, ▲ =Fucose, ◆ =NeuAc, □ =GalNAc

Table 12. Permethylated glycans from low and intermediate direct EPS pools

Number	m/z	Proposed Glycan Structure	Sub-Type
1	1375.757	M4N2	High Mannose
2	1579.865	M5N2	High Mannose
3	1783.968	M6N2	High Mannose
4	1907.056	N3M3N2	Complex
5	2156.185	NeuAc1Gal1N1M3N2F	N/A
6	2186.199	Hex5HexNAc3NeuAc1	Hybrid
7	2431.337	NeuAc1Gal2N2M3N2	Complex
8	2605.434	NeuAc1Gal2N2M3N2F	Complex
9	2792.524	NeuAc2Gal2N2M3N2	Complex
10	2966.623	NeuAc2Gal2N2M3N2F	Complex
11	3055.688	NeuAc1Gal3N3M3N2F	Complex
12	3242.771	NeuAc2Gal3N3M3N2	Complex
13	3415.851	NeuAc2Gal3N3M3N2F	Complex
14	3504.924	NeuAc1Gal4N4M3N2F	Complex
15	3603.954	NeuAc3Gal3N3M3N2	Complex
16	3777.038	NeuAc3Gal3N3M3N2F	Complex
17	3867.088	NeuAc2Gal4N4M3N2F	Complex
18	4054.258	NeuAc3Gal4N4M3N2	Complex
19	4228.405	NeuAc3Gal4N4M3N2F	Complex
20	4359.486	Hex8dHex4HexNAc8	Complex
21	4415.502	NeuAc4Gal4N4M3N2	Complex
22	4589.664	Hex9HexNAc8NeuAc2	Complex
23	4765.818	Gal4N4Gal4N4M3N2	Complex
24	4952.625	Hex9dHex2HexNAc8NeuAc1	Complex

Identified m/z values were used for database searches, and corresponding masses that could be assigned to a biologically relevant N-glycan structure are listed. An asterisk denotes structures that are one representation of multiple possible glycoforms for a given mass. The shown structure in these cases was chosen based on its apparent prevalence in mammalian species. Cartoon representations are as follows: ■ =GlcNAc, ●

=Mannose, ○ =Galactose, ▲ =Fucose, ◆ =NeuAc, □ =GalNAc

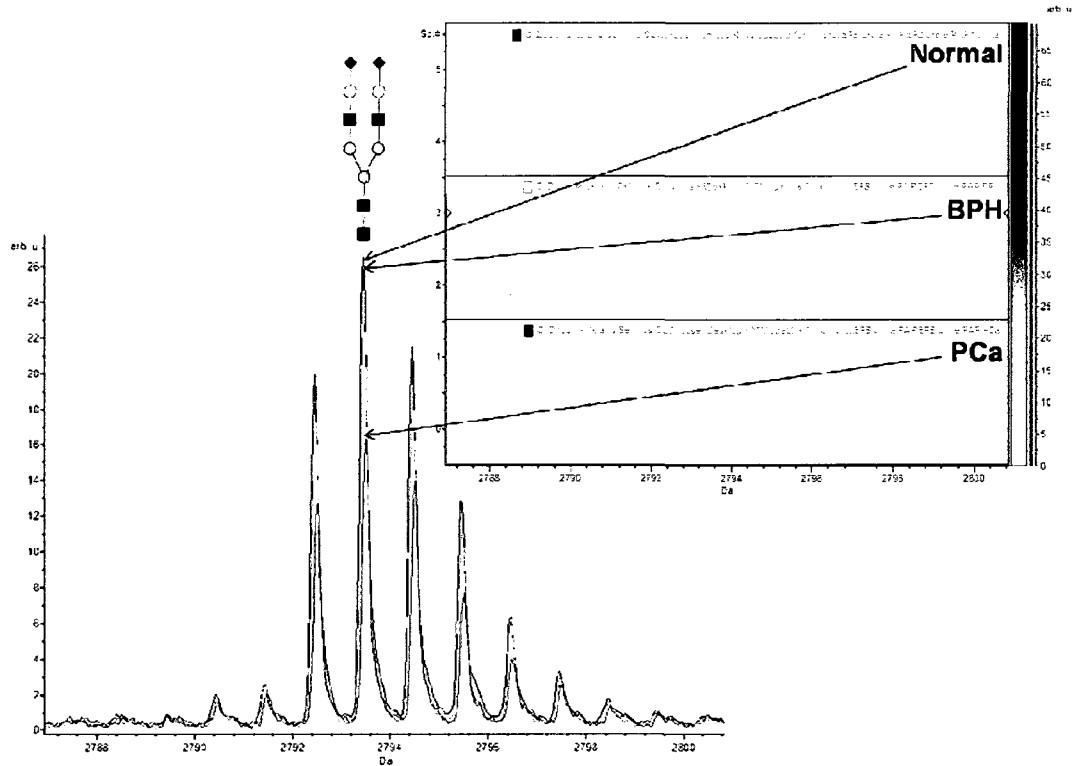


Figure 28. Heat map overview of MALDI-TOF spectra for peak 2793. MALDI-TOF spectra generated from EPS urine PAP samples were analyzed with Clinprot software, indicating the intensity of the spectra from each sample cohort as compared to the next. Each box represents spectra from one group, with normal being on top, BPH in the middle, and prostate cancer on the bottom. Arrows show the peak height for each corresponding heat map. Peak 2793 represents a complex, biantennary glycan with two terminal sialic acids. Cartoon representations are as follows: ■ =GlcNAc, ● =Mannose, ○ =Galactose, ▲ =Fucose, ◆ =NeuAc, □ =GalNAc

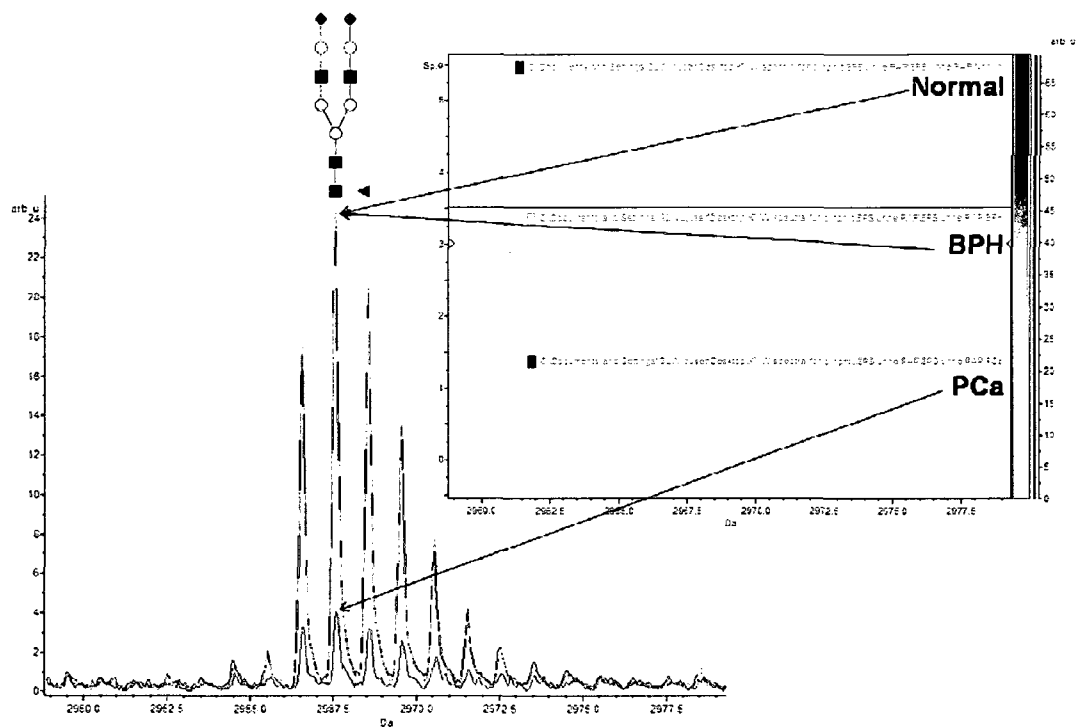


Figure 29. Heat map overview of MALDI-TOF spectra for peak 2967. MALDI-TOF spectra generated from EPS urine PAP samples were analyzed with Clinprot software, indicating the intensity of the spectra from each sample cohort as compared to the next. Each box represents spectra from one group, with normal being on top, BPH in the middle, and prostate cancer on the bottom. Arrows show the peak height for each corresponding heat map. Peak 2967 represents a complex, biantennary glycan with two terminal sialic acids and a core fucose residue. Cartoon representations are as follows:

■ =GlcNAc, ○ =Mannose, ○ =Galactose, ▲ =Fucose, ◆ =NeuAc, □ =GalNAc

differential between cancer and non-cancer samples were of the complex sub-type, with various branching and terminal sialic acids.

6.4 Discussion



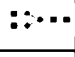
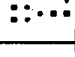
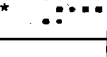
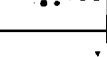
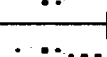
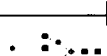
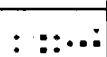
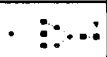




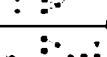
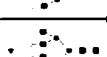

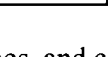
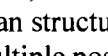
Using serum and plasma for biomarker discovery has proven to be difficult for many laboratories, therefore demanding the need for enriched sources of lower abundant proteins which are capable of differentiating between disease and non-disease states. While it is commonly known that both tissues and proximal fluids are enriched for potential biomarkers, the collection of such samples is not always within the parameters of a given study. For our studies, we have found that EPS urine fluids are readily obtained in the clinical setting, and are enriched for proteins directly related to the prostate, thus making these fluids ideal for biomarker discovery for the detection of early prostate cancer. In addition, EPS urines can be obtained at a routine physical exam, making it not only ideal for discovery, but also for clinical applications as a source of diagnostic markers for clinical assays. Direct EPS fluids are also enriched for prostate-derived proteins and are a great discovery tool, however due to their method of collection, they may not have utility for validation nor for future clinical assays.

Because glycosylation is known to be important to all aspects of cancer progression^{83, 93, 214}, the glycan profiles of clinically-relevant samples may provide the much needed diagnostic markers for early prostate carcinomas. While serum PSA is the current FDA-approved biomarker for prostate cancer, it is not without faults. Serum PSA has proven to be organ-specific, but is not cancer-specific, as elevated serum PSA levels are detected with BPH conditions as well³⁷⁻³⁹. Additionally, a more current problem

facing clinicians today is determining which patients have significant prostate cancer, indicating they indeed need radical surgery and treatment as compared to patients who in fact have indolent prostate cancer. In approximately 80% of radical prostatectomies it is found that the patient's prostate cancer was not expected to be an aggressive lethal form of tumor, despite their clinical risk factors indicating a different prognosis. This aspect alone reiterates why better biomarkers are needed for distinguishing clinically significant or aggressive forms of prostate cancers from more indolent tumors.

Being a glandular organ, the prostate is constantly secreting fluids full of proteins, most of which are glycosylated. PSA and PAP are two prominent prostate-specific proteins, and both are N-glycosylated, making them ideal targets for glycomic studies. Based on preliminary studies, we have identified 36 different PAP glycoforms in EPS urines, as compared to the 21 PAP glycoforms identified in our prior seminal plasma studies. Nineteen of these structures overlap between seminal plasma and EPS urines (Table 13). As seen with seminal plasma-derived PAP, the PAP glycoforms in EPS urines are mostly of the complex subtype, with multiple branching, sialylation, and fucosylation (Table 8). For EPS urine PSA, we observed 23 glycan structures, as compared to the 40 different glycoforms identified for seminal plasma PSA (Table 9). One explanation for this marked difference can be due to the dilution factor of EPS urines as compared to seminal plasma, as well as other experimental aspects. Further analysis of EPS urine PSA glycoforms will be necessary to appropriately compare these structures to those observed in seminal plasma samples.

Table 13. Shared PAP glycans between seminal plasma and EPS urine pools

Number	m/z	Glycan Structure	Sub-Type
1	1784.016	M6N2 	High Mannose
2	1987.958	M7N2 	High Mannose
3	2070.189	Gal2N2M3N2 	Complex
4	2244.268	Gal2N2M3N2F 	Complex
5	2314.091	Hex5HexNAc5 	Complex
6	2432.339	NeuAc1Gal2N2M3N2 	Complex
7	2606.425	NeuAc1Gal2N2M3N2F 	Complex
8	2793.503	NeuAc2Gal2N2M3N2 	Complex
9	2881.559	NeuAc1Gal3N3M3N2 	Complex
10	2967.587	NeuAc2Gal2N2M3N2F 	Complex
11	3055.647	NeuAc1Gal3N3M3N2F 	Complex
12	3242.719	NeuAc2Gal3N3M3N2 	Complex
13	3416.793	NeuAc2Gal3N3M3N2F 	Complex
14	3504.838	NeuAc1Gal4N4M3N2F 	Complex
15	3603.894	NeuAc3Gal3N3M3N2 	Complex
16	3777.971	NeuAc3Gal3N3M3N2F 	Complex
17	3867.027	NeuAc2Gal4N4M3N2F 	Complex
18	4053.873	NeuAc3Gal4N4M3N2 	Complex
19	4227.294	NeuAc3Gal4N4M3N2F 	Complex

Identified m/z values were used for database searches, and corresponding masses that could be assigned to a biologically relevant N-glycan structure are listed. An asterisk denotes structures that are one representation of multiple possible glycoforms for a given mass. The shown structure in these cases was chosen based on its apparent prevalence in mammalian species. Cartoon representations are as follows: ■ =GlcNAc, ●

● =Mannose, ○ =Galactose, ▲ =Fucose, ◆ =NeuAc, □ =GalNAc

We also wanted to identify individual glycans attached to each N-linked site on PAP using triple-quadrupole mass spectrometry, similar to those studies performed in Aim I with seminal plasma fluids. Table 10 shows the structures and their respective tryptic and chymotryptic peptides we observed using the precursor ion scan mode with nanoLC-triple quadrupole MS/MS for diagnostic oxonium ions 163, 292, and 366.

While we did not identify as many glycopeptides as seen with our seminal plasma studies, we were still successful in identifying three glycans, five tryptic glycopeptides, and two chymotryptic glycopeptides. One explanation for less coverage with EPS urine-derived PAP is the dilute nature of EPS urines as compared to seminal plasma. While EPS urines are enriched for PAP as compared to serum or plasma, it is not as concentrated as seminal fluid. Another possible explanation could be a decreased efficiency of chymotryptic digestion with the EPS urine studies, as the limited coverage observed arose from the chymotryptic digested experiments.

In addition to protein-targeted analyses, another useful glycomic approach involves the examination of the global glycosylation patterns for a given sample set. With this approach, one may observe an overall trend that differentiates between disease states. We used the total glycan approach with both EPS urine and direct EPS samples with the intention of examining the glycan structural isoforms (also termed glycoforms) present and monitoring for any significant changes between disease states and differing risk stratifications. Through our permethylation assays, we identified 43 glycoforms derived from EPS urines and 24 glycoforms from direct EPS fluids (Table 11 and Table 12). It is imperative to note that the glycoforms observed are structural representations of any number of anomeric isoforms. Therefore, while we are reporting a finite number of

structures, there are possibly many more glycoforms present, which will require additional analyses to define. When comparing non-PCa and PCa EPS urine PAP pools, we see an overall trend of a decrease in fucosylated species in the PCa pools as compared to the non-PCa pools, as represented by Figure 28 and Figure 29. Figure 28 depicts a non-fucosylated, biantennary complex glycan, and shows that the peak intensities are similar across the three groups, normal, BPH, and PCa. In contrast, Figure 29 shows the same complex glycan with a core fucose residue, with a marked decrease in peak intensity for the cancer group as compared to normal and BPH. These changes in fucosylation complement other studies indicating changes in fucosylation with cancerous states²¹⁵⁻²¹⁹. These data support the validity of EPS fluids as an excellent source for identifying potential carbohydrate-based biomarkers.

CHAPTER VI

CONCLUSIONS AND FUTURE DIRECTIONS

6.1 Aim I (Chapter III): Develop methodologies for the characterization of N-linked glycans of prostate-specific antigen and prostatic acid phosphatase in seminal fluids.

A. The results from this aim indicate that N-linked glycosylation of seminal plasma-derived PSA and PAP is very heterogeneous. In addition, we observed altered glycosylation trends across normal, BPH, and PCa disease states for PAP.

B. Thiophilic adsorption chromatography (TAC) of disease-defined seminal plasma pools successfully fractionated the protein mixture, providing further purified forms of PSA and PAP. PAP did not bind the TAC resin, and therefore was collected in the unbound fraction along with albumin and other non-binding proteins, as indicated by western blot analysis. We also observed by western blot analysis that PSA elutes in two separate fractions, those of 0.6M and 0.4M sodium sulfate concentration. We confirmed PSA and PAP identity by in-gel trypsin digestion and peptide mass fingerprint (PMF) analysis with MALDI-TOF mass spectrometry. This mass spectrometry analysis resulted in the statistically significant identification of both PSA and PAP, without the detection of any other proteins in the digested gel slice.

C. Normal phase HPLC separation of 2-AB derivatized N-linked glycans was completed on PSA and PAP isolated from normal, BPH, and PCa seminal plasma pools, with or without sialidase treatment. These results indicate clear differences among disease states for PAP glycans, in particular when comparing normal and BPH samples to cancer samples. A decrease in bi- and tetraantennary fucosylated structures as well as

high mannose structures is observed for PAP arising from cancer samples as compared to normal and BPH conditions. While no overall trend in disease-specific glycan changes detected for PSA were observed for PSA glycans, the N-glycans identified were consistent with previously reported structures observed for PSA, with high representation of bi-, tri-, and tetraantennary core fucosylated complex structures.

D. MALDI-TOF analysis of permethylated N-linked glycans yielded positive identification of 40 PSA glycan structures and 21 PAP glycan structures. While the majority of these structures are of the complex sub-type, we did observe a smaller representation of both high-mannose and hybrid sub-types. The PSA and PAP N-glycan structures identified by MALDI-TOF correlate well with the structures observed by our HPLC separation, and remain consistent with previously published data.

E. Triple quadrupole mass spectrometry analysis of PAP glycopeptides enabled us to determine which subtype of N-glycans are attached at each of the three N-linked glycosylation sites for PAP. We observed bi- and triantennary sialylated structures at Asn-62, bi- and tetraantennary sialylated structures at Asn-188, and high mannose structures at Asn-301. Tryptic digestion of PAP did not allow for the elucidation of any structures at Asn-188; however chymotryptic digestion of PAP created smaller glycopeptides, therefore bringing the glycopeptides into the range of detection for the triple quadrupole instrument. The observed high mannose structures present at Asn-301 and complex structures at Asn-188 correlate with previously published data on the crystal structure of PAP. It was previously thought that high mannose structures must be present at Asn-62; however we have confirmed the presence of complex structures at this N-

linked glycosylation site, with no evidence of a high-mannose structure present at this site.

6.2 Aim II (Chapter IV): Establish expressed prostatic secretions as a source of prostate specific antigen and prostatic acid phosphatase.

A. The results from this aim indicate that both EPS urine and direct EPS fluids are indeed an enriched source of PSA and PAP. Both prostate cancer biomarkers are readily detected in EPS fluids, and these fluids are compatible with our proteomic assays, allowing for future, more in-depth analyses using EPS fluids.

B. A pre-DRE urine and a post-DRE “EPS” urine sample were collected from an individual patient, on the same day, within one hour of each other. These samples were analyzed and compared for their protein content by both 2D-PAGE and LC-ESI-MS/MS. We observed relative protein differences between pre-DRE and post-DRE urines by visualizing the spot patterns of 2D-PAGE separation of the proteins in each sample with silver staining. Protein identification by mass spectrometry revealed an increase in the number of significantly scored proteins present in the post-DRE urine as compared to the pre-DRE urine. In addition, PSA and PAP were not identified in the pre-DRE urine; however they were in the top 10 significant protein hits in the post-DRE urine.

C. Direct EPS fluid from one individual was analyzed by LC-ESI-MS/MS in order to determine the proteins present in this prostatic fluid. We observed a large number of proteins significantly identified in the direct EPS fluid, with PSA and PAP both being in the top 10 significant hits. These results confirm that this fluid is indeed a great source of PSA and PAP, and thus could be used in future proteomic and glycomic

studies with the intention of discovering enhanced biomarkers for the early diagnosis and prognosis of prostate carcinomas.

D. Thiophilic adsorption chromatography (TAC) was utilized in order to fractionate EPS urine disease-define pools with the intent of obtaining purified forms of PSA and PAP for further analyses. PAP did not bind the TAC resin and therefore was collected in the unbound fraction, as was detected by 1D-PAGE and western blotting. PSA eluted in the 0.6M, 0.4M, and 0.2M sodium sulfate fractions, which was also determined by 1D-PAGE and western blotting. MALDI-TOF PMF analysis was used to confirm the identities of PSA and PAP which were run on 1D-PAGE, excised, and in-gel trypsin digested.

E. 2D-PAGE followed by western blotting was used in order to further examine PSA and PAP characteristics in EPS fluids. A large pool of EPS urines were separated by 2D-PAGE in duplicate, with one resulting gel being silver stained and the other gel being transferred to PVDF membrane for western blot analysis of PSA and PAP. The results from this analysis positively confirm the presence of multiple PSA and PAP isoforms in EPS urines, most of which are likely glycoforms that can be targeted in further studies.

F. ELISA analysis of PSA and PAP concentrations in individual EPS urine and direct EPS samples was performed in order to determine PSA and PAP levels in prostatic proximal fluids. We observed an overall decrease of both PSA and PAP levels in cancer samples as compared to non-cancer samples, with a detection range of 10-40 ug/ml for PSA and 3-10 ug/ml for PAP in EPS urines and a range of 80-120 ug/ml for PSA and 20-40 ug/ml for PAP in direct EPS fluids. These results indicate that PSA and PAP are less

prevalent in cancerous tissue as compared to normal and BPH tissues, however larger sample cohorts are necessary in order to truly understanding the status of these biomarkers in the diseased prostate.

6.3 Aim III (Chapter V): Application of new methodologies to expressed prostatic secretions for prostate cancer glycoprotein biomarker discovery.

A. The results from this aim indicate that protein-specific and total glycomic analyses can be performed using EPS urine and direct EPS fluids. We positively identified N-linked glycans for both PSA and PAP derived from EPS urines. In addition we observed a number of N-linked glycans in disease-defined pools of EPS urine and direct EPS fluids, indicating the feasibility of discovering new candidate carbohydrate-based biomarkers in EPS fluids for the early diagnosis and prognosis of prostate carcinomas.

B. Normal, BPH, and PCa disease-defined pools of EPS urines were generated and subsequently fractionated using thiophilic adsorption chromatography (TAC). As seen previously, PAP did not bind the TAC resin and was collected in the unbound fraction, while PSA eluted in the 0.6M, 0.4M, and 0.2M sodium sulfate fractions. PSA and PAP identities were positively confirmed in their respective fractions by silver staining and western blotting.

C. MALDI-TOF analysis of permethylated N-linked glycans was performed for PSA and PAP derived from EPS urine disease-defined pools (normal, BPH, PCa). We observed a total of 23 glycoforms for PSA and 36 glycoforms for PAP, with mostly complex subtypes being represented. High mannose and hybrid subtypes were also

present for PSA, with only the addition of high mannose structures positively identified for PAP. There were a number of glycoforms for PAP that the subtype could not be determined as either complex or hybrid. For both PSA and PAP, the complex glycans observed often contained terminal sialic acid residues and core fucose residues.

D. Triple quadrupole MS was used in the precursor ion scanning mode to examine the N-glycan subtypes present at each N-linked glycosylation site of PAP. After multiple experiments using the 163, 292, and 366 diagnostic ion masses, and using both trypsin and chymotrypsin digested PAP, we observed biantennary complex structures at Asn-62 and high mannose structures at Asn-301. We were unable to confirm the presence of any structures at Asn-188, which had proven to be difficult in our previous analyses using seminal plasma-derived PAP. These differences are likely due to either sample concentration, protease digestion efficiency, or both.

E. Total glycan analysis of permethylated N-linked glycans from EPS fluids was performed using MALDI-TOF. EPS urine pools defined as non-PCa and PCa resulted in a total of 43 glycoforms, while direct EPS pools (low risk PCa and intermediate risk PCa) resulted in 24 glycoforms. Again, complex N-linked glycan subtypes comprise the majority of glycoforms observed, with high mannose and hybrid structures also represented. Due to the high concentration of glycans present in the sample, fragmentation of a subset of individual glycoforms was accomplished using MALDI-TOF/TOF LIFT. This type of fragmentation is typically not performed, as ESI-MS/MS with an ion trap is the preferred instrumentation used for glycan fragmentation. We detected near complete fragmentation by manual annotation of the spectra, and likely

could confirm the presence of complete fragmentation with appropriate bioinformatic tools.

F. Clinprot software data analysis was performed on EPS urine PAP glycan and EPS urine total MALDI-TOF spectra. We observed an overall trend of decreased fucosylation in cancer samples as compared to normal and BPH samples. These results indicate that for PAP, and potentially other glycoproteins derived from the prostate, there is less fucosylation occurring in a cancerous prostate. These glycan targets will be useful for examining larger sample cohorts and determining the utility of a glycan-based biomarker for the detection or early prostate carcinomas, as well as distinguishing between significant and insignificant prostate carcinomas.

6.4 Concluding Remarks and Future Directions of Aims I, II, and III

Based on our present studies, we have gained knowledge about and catalogued the type of N-linked glycoforms attached to PSA and PAP in prostatic fluids. Additionally we have preliminary data confirming N-linked glycan differences among disease states (normal, benign, PCa) for PAP in seminal fluid and EPS. However, more in-depth studies are necessary to further elucidate novel candidate biomarkers for the early diagnosis and prognosis of prostate cancer. It has become common knowledge that while serum PSA is the best biomarker currently available for the detection of prostate carcinomas, especially when it is used in conjunction with a DRE exam, there is still a pressing need for better biomarkers. Many prostate cancers being detected today are in fact indolent diseases, and do not pose any lethal danger to the patient. Therefore, many patients are undergoing unnecessary biopsies, surgeries, and treatments, all of which can

cause physical and emotional hardships. Additionally, some patients suffer more from the resulting health complications that can develop post-treatment or post-surgery than they would have if their prostate cancer had remained untouched. A new classification scheme is being developed which differentiates between significant and insignificant prostate carcinomas. Under these new definitions, significant disease represent tumors which are most likely to progress to more aggressive cancers and therefore need to be treated, while insignificant disease represent tumors are least likely to progress and not affect the patient's life expectancy or livelihood. However, these classifications are currently only determined after the patient has undergone a radical prostatectomy, and examination of the removed prostate by a highly-specialized pathologist. In order to help future patients, a way to better determine these classifications prior to surgery or several biopsies is essential.

Because protein glycosylation has been shown to be involved in every aspect of cancer progression⁹³, it is plausible that the altered glycans can be detected reliably, further validated, and ultimately used in high-throughput clinical-based assays. PSA has one N-linked glycosylation site, while PAP contains three N-linked glycosylation sites, all of which have been confirmed to be occupied by glycans^{120, 124, 125}. PAP has been extensively reported in the literature to have wide-spread distribution throughout human tissue^{220, 221}, with past clinical assays relying solely on its enzymatic activity. Eventually it was found that the PAP activity being assayed in blood could not be correlated back to the prostate as the sole source of PAP. We have circumvented this issue by focusing on forms of PAP derived directly from prostatic fluids instead of from serum or plasma. Not only are we now analyzing prostate-specific PAP, these fluids are enriched for PAP as

compared to serum or plasma. For PSA, while it has been shown to be prostate-specific, and therefore still has high specificity when used in serum-based clinical assays, we are able to obtain enriched PSA by using our prostatic fluids.

Another advantage we have lies in our vast biorepository of seminal fluids and expressed prostatic secretions, with EPS collection an ongoing process with growing numbers of collections. In addition, we are collecting EPS fluids for different cohorts of patients, including but not limited to healthy, normal patients and patients with BPH or prostate cancer. We also have been able to classify the prostate cancer samples into different risk stratifications, giving us many different possible cohorts to examine for glycosylation changes to PSA and PAP.

Glycomic analyses do not always have to be performed on individual proteins in order to provide useful information, in fact, analysis of global glycomic changes have been reported^{175, 176}. These methods search for an overall alteration to glycosylation patterns in a given disease state which, in turn, is reflective of all proteins contributing to the glycosylation changes. Our studies have provided basic knowledge of the most abundant glycan structures present in EPS fluids, as well as those attached specifically to PSA and PAP. However, deeper analyses are necessary in order to identify less common structures, as well as to determine the changes that are occurring between disease states. We have observed trends indicating a decrease in overall levels of fucosylation when comparing prostate cancer samples to normal and BPH samples. Now that we have candidate glycoforms, additional analyses will be needed to confirm whether the differences seen are maintained in larger cohorts of individual samples. To do so,

optimization of current methodologies as well as the addition of enhanced glycomic strategies is required.

First, permethylated N-linked glycans can be readily detected by MALDI-TOF. This derivatization method stabilizes the glycans, more specifically the terminal sialic acid residues, as well as simplifies the resultant spectra by producing only sodium ion adducts. However, our current scheme utilizes a well-established liquid-phase permethylation technique¹⁹⁵ that does not allow for high-throughput analyses. While we are able to obtain robust results from this method, we can only analyze small numbers of samples at one time ($n \leq 5$), and it is a slow, tedious process. To overcome this time-consuming dilemma, a solid-phase permethylation approach may be implemented. This method calls for either the use of capillary columns or spin-columns, both of which allow for more rapid permethylation of each sample, and for higher amounts of samples to be processed at one time^{222, 223}. In addition to its high-throughput nature, the solid-phase protocol is highly quantitative and allows for the higher recovery of sample, therefore decreasing the amount of starting material needed for satisfactory results²²³. We would like to utilize the spin-column method, where the limiting factor is the number of sample holders in the centrifuge rotor (i.e. $n=18-30$). In this method, microcentrifuge spin-columns are used for the clean-up steps of the cleaved glycans prior to permethylation and the permethylation reaction itself. Sodium hydroxide beads bathed in acetonitrile are added to empty spin columns with an optimal bed volume, washed with DMSO, and the sample combined with iodomethane (source of methyl groups) is applied to the column up to 8 times repeatedly, and in a matter of minutes, the reaction is complete and ready for the final liquid-liquid (water-chloroform) extraction step. Not only does this method

require less time at the bench, it has also been shown to provide more complete permethylation as compared to the liquid-phase method²²³.

After employing the front-end sample preparative steps in a more rapid fashion, the mass spectrometry platforms need to be addressed. Our current MALDI-TOF analysis provides us with intact glycan information, giving us the mass of the parent structure which we can use to search a public database for potential structural matches. However, at this time, we are unable to determine the linkage information by MS/MS on the MALDI-TOF instrument for most samples. Fragmentation analysis with an ESI-LIT MS/MS instrument (i.e. ThermoFinnegan LTQ or Applied Biosystems QTRAP) will allow for input of small quantities of samples and subsequently resulting in the structural information necessary to determine monosaccharide linkage data.

Once the data has been collected, computer software programs are indispensable in the actual assignment of the structural linkages. One example of such commercially available software is SimGlycan (Applied Biosystems/PremierBiosoft), which takes MS/MS data directly from Applied Biosystems (ABI) and Bruker instruments, as well as accepts data from other mass spectrometers after a file conversion. The software needs user input of a number of factors such as the parent mass of the fragmented structure, the charge state of the parent mass, whether or not the structure has been derivatized. Also, if the experimental spectrum is derived from a glycopeptide instead of a cleaved glycan structure, then the user will need to also input peptide information such as the amino acid sequence and any peptide modifications that may be present. The software then takes all of the MS/MS masses and searches an internally developed glycan database, annotates

the data, and provides the user with a list of potential glycoforms that can fit the spectrum data provided.

Finally, after candidate glycoforms have been discovered by the above sample preparative steps and mass spectrometry analyses, validation of such structures is necessary, and subsequently clinical assays need to be developed that can accommodate the high-throughput detection of the given carbohydrate markers. One particular assay that will fit these criteria is the lectin fluorophore-linked immunosorbent (FLISA) assay^{199, 216}. This type of plate-based assay is similar to a sandwich ELISA assay in the sense that an antibody is used to capture the target protein, and then a lectin is used to detect and measure the specified monosaccharide on that protein, versus using a second antibody to detect and measure the protein of interest. For example, since the fucosylation state of various N-linked complex glycans is seen to be differential between disease states, this is a good candidate monosaccharide target to begin with. For the lectin FLISA, it is imperative to make sure that the capture antibody be modified if it is a glycosylated protein, therefore in the case of a fucose-targeted assay, the antibody will need to be defucosylated using a competing sugar such as alpha-galactose²¹⁶. After the plate wells are coated with the modified capture antibody, the experimental sample (i.e. serum, EPS urine fluid) is added to the wells and allowed to bind prior to the addition of a conjugated lectin (i.e. biotin-AAL). Finally the bound lectin is detected using an appropriate system (i.e. conjugated-streptavidin) and the signal intensity is measured with the preferred system²¹⁶. With this lectin FLISA assay, the amount of fucosylation in a given sample can be detected, and like a protein-based biomarker, a threshold can be set indicating at what level the fucosylation indicates disease versus non-disease. For some

cases, it may not simply be one monosaccharide contributing to the disease state, and therefore a panel of monosaccharides will be measured and used together to determine the disease state. In the case of prostate cancer, ideally these glycan changes will allow for differentiation between insignificant and significant disease, allowing for better patient prognosis profiles and therefore decreasing the number of unnecessary biopsies, treatments, and radical surgeries in men afflicted with prostate carcinomas.

REFERENCES

1. Jemal, A.; Siegel, R.; Ward, E.; Hao, Y.; Xu, J.; Thun, M. J., Cancer statistics, 2009. *CA Cancer J Clin* **2009**, 59 (4), 225-49.
2. Moul, J. W.; Anderson, J.; Penson, D. F.; Klotz, L. H.; Soloway, M. S.; Schulman, C. C., Early prostate cancer: prevention, treatment modalities, and quality of life issues. *Eur Urol* **2003**, 44 (3), 283-93.
3. Ward, A. M.; Catto, J. W.; Hamdy, F. C., Prostate specific antigen: biology, biochemistry and available commercial assays. *Ann Clin Biochem* **2001**, 38 (Pt 6), 633-51.
4. Kutikov, A.; Guzzo, T. J.; Malkowicz, S. B., Clinical approach to the prostate: an update. *Radiol Clin North Am* **2006**, 44 (5), 649-63, vii.
5. Wilt, T. J.; MacDonald, R.; Rutks, I.; Shamliyan, T. A.; Taylor, B. C.; Kane, R. L., Systematic review: comparative effectiveness and harms of treatments for clinically localized prostate cancer. *Ann Intern Med* **2008**, 148 (6), 435-48.
6. Humphrey, P. A., Gleason grading and prognostic factors in carcinoma of the prostate. *Mod Pathol* **2004**, 17 (3), 292-306.
7. Screening for prostate cancer: U.S. Preventive Services Task Force recommendation statement. *Ann Intern Med* **2008**, 149 (3), 185-91.
8. Herrala, A. M.; Porvari, K. S.; Kyllonen, A. P.; Vihko, P. T., Comparison of human prostate specific glandular kallikrein 2 and prostate specific antigen gene expression in prostate with gene amplification and overexpression of prostate specific glandular kallikrein 2 in tumor tissue. *Cancer* **2001**, 92 (12), 2975-84.
9. Lintula, S.; Stenman, J.; Bjartell, A.; Nordling, S.; Stenman, U. H., Relative concentrations of hK2/PSA mRNA in benign and malignant prostatic tissue. *Prostate* **2005**, 63 (4), 324-9.
10. Lundwall, A.; Clauss, A.; Olsson, A. Y., Evolution of kallikrein-related peptidases in mammals and identification of a genetic locus encoding potential regulatory inhibitors. *Biol Chem* **2006**, 387 (3), 243-9.
11. Flocks, R. H.; Bandhaur, K.; Patel, C.; Begley, B. J., Studies on spermagglutinating antibodies in antihuman prostate sera. *J Urol* **1962**, 87 475-8.
12. Lilja, H., A kallikrein-like serine protease in prostatic fluid cleaves the predominant seminal vesicle protein. *J Clin Invest* **1985**, 76 (5), 1899-903.

13. Lilja, H.; Oldbring, J.; Rannevik, G.; Laurell, C. B., Seminal vesicle-secreted proteins and their reactions during gelation and liquefaction of human semen. *J Clin Invest* **1987**, 80 (2), 281-5.
14. Hara, M.; Koyanagi, Y.; Inoue, T.; Fukuyama, T., [Some physico-chemical characteristics of " -seminoprotein", an antigenic component specific for human seminal plasma. Forensic immunological study of body fluids and secretion. VII]. *Nihon Hoigaku Zasshi* **1971**, 25 (4), 322-4.
15. Papsidero, L. D.; Wang, M. C.; Valenzuela, L. A.; Murphy, G. P.; Chu, T. M., A prostate antigen in sera of prostatic cancer patients. *Cancer Res* **1980**, 40 (7), 2428-32.
16. Ahlgren, G.; Rannevik, G.; Lilja, H., Impaired secretory function of the prostate in men with oligo-asthenozoospermia. *J Androl* **1995**, 16 (6), 491-8.
17. Savblom, C.; Malm, J.; Giwercman, A.; Nilsson, J. A.; Berglund, G.; Lilja, H., Blood levels of free-PSA but not complex-PSA significantly correlates to prostate release of PSA in semen in young men, while blood levels of complex-PSA, but not free-PSA increase with age. *Prostate* **2005**, 65 (1), 66-72.
18. Flocks, R. H.; Urich, V. C.; Patel, C. A.; Opitz, J. M., Studies on the antigenic properties of prostatic tissue. I. *J Urol* **1960**, 84, 134-43.
19. Yantorno, C.; Shulman, S.; Gonder, M. J.; Soanes, W. A.; Witebsky, E., Studies on organ specificity. 18. Immunologic and biophysical characterization of canine prostatic fluid. *J Immunol* **1966**, 96 (6), 1035-45.
20. Barnes, G. W.; Soanes, W. A.; Mamrod, L.; Gonder, M. J.; Shulman, S., Immunologic properties of human prostatic fluid. *J Lab Clin Med* **1963**, 61, 578-91.
21. Ablin, R. J.; Soanes, W. A.; Bronson, P.; Witebsky, E., Precipitating antigens of the normal human prostate. *J Reprod Fertil* **1970**, 22 (3), 573-4.
22. Ablin, R. J.; Bronson, P.; Soanes, W. A.; Witebsky, E., Tissue- and species-specific antigens of normal human prostatic tissue. *J Immunol* **1970**, 104 (6), 1329-39.
23. Ablin, R. J., Immunologic studies of normal, benign, and malignant human prostatic tissue. *Cancer* **1972**, 29 (6), 1570-4.
24. Li, T. S.; Beling, C. G., Isolation and characterization of two specific antigens of human seminal plasma. *Fertil Steril* **1973**, 24 (2), 134-44.
25. Wang, M. C.; Valenzuela, L. A.; Murphy, G. P.; Chu, T. M., Purification of a human prostate specific antigen. *Invest Urol* **1979**, 17 (2), 159-63.

26. Sensabaugh, G. F., Isolation and characterization of a semen-specific protein from human seminal plasma: a potential new marker for semen identification. *J Forensic Sci* **1978**, 23 (1), 106-15.
27. Sensabaugh, G. F.; Blake, E. T., Seminal plasma protein p30: simplified purification and evidence for identity with prostate specific antigen. *J Urol* **1990**, 144 (6), 1523-6.
28. Sokoll, L. J.; Chan, D. W., Prostate-specific antigen. Its discovery and biochemical characteristics. *Urol Clin North Am* **1997**, 24 (2), 253-9.
29. Rao, A. R.; Motiwala, H. G.; Karim, O. M., The discovery of prostate-specific antigen. *BJU Int* **2008**, 101 (1), 5-10.
30. Wang, M. C.; Papsidero, L. D.; Kuriyama, M.; Valenzuela, L. A.; Murphy, G. P.; Chu, T. M., Prostate antigen: a new potential marker for prostatic cancer. *Prostate* **1981**, 2 (1), 89-96.
31. Kuriyama, M.; Wang, M. C.; Papsidero, L. D.; Killian, C. S.; Shimano, T.; Valenzuela, L.; Nishiura, T.; Murphy, G. P.; Chu, T. M., Quantitation of prostate-specific antigen in serum by a sensitive enzyme immunoassay. *Cancer Res* **1980**, 40 (12), 4658-62.
32. Nadji, M.; Tabei, S. Z.; Castro, A.; Chu, T. M.; Murphy, G. P.; Wang, M. C.; Morales, A. R., Prostatic-specific antigen: an immunohistologic marker for prostatic neoplasms. *Cancer* **1981**, 48 (5), 1229-32.
33. Stamey, T. A.; Yang, N.; Hay, A. R.; McNeal, J. E.; Freiha, F. S.; Redwine, E., Prostate-specific antigen as a serum marker for adenocarcinoma of the prostate. *N Engl J Med* **1987**, 317 (15), 909-16.
34. Tricoli, J. V.; Schoenfeldt, M.; Conley, B. A., Detection of prostate cancer and predicting progression: current and future diagnostic markers. *Clin Cancer Res* **2004**, 10 (12 Pt 1), 3943-53.
35. Hudson, M. A.; Bahnson, R. R.; Catalona, W. J., Clinical use of prostate specific antigen in patients with prostate cancer. *J Urol* **1989**, 142 (4), 1011-7.
36. Catalona, W. J.; Smith, D. S.; Ratliff, T. L.; Dodds, K. M.; Coplen, D. E.; Yuan, J. J.; Petros, J. A.; Andriole, G. L., Measurement of prostate-specific antigen in serum as a screening test for prostate cancer. *N Engl J Med* **1991**, 324 (17), 1156-61.
37. Gann, P. H.; Hennekens, C. H.; Stampfer, M. J., A prospective evaluation of plasma prostate-specific antigen for detection of prostatic cancer. *JAMA* **1995**, 273 (4), 289-94.

38. Chan, D. W.; Sokoll, L. J., Prostate-specific antigen: update 1997. *J Int Fed Clin Chem* **1997**, 9 (3), 120-5.
39. Partin, A. W.; Oesterling, J. E., The clinical usefulness of percent free-PSA. *Urology* **1996**, 48 (6A Suppl), 1-3.
40. Lilja, H.; Ulmert, D.; Vickers, A. J., Prostate-specific antigen and prostate cancer: prediction, detection and monitoring. *Nat Rev Cancer* **2008**, 8 (4), 268-78.
41. Mikolajczyk, S. D.; Millar, L. S.; Wang, T. J.; Rittenhouse, H. G.; Marks, L. S.; Song, W.; Wheeler, T. M.; Slawin, K. M., A precursor form of prostate-specific antigen is more highly elevated in prostate cancer compared with benign transition zone prostate tissue. *Cancer Res* **2000**, 60 (3), 756-9.
42. Brawer, M. K., Complexed PSA: the newest advance in PSA testing. *Urology* **1999**, 54 (1), 2-3.
43. Djavan, B.; Waldert, M.; Ghawidel, C.; Marberger, M., Benign prostatic hyperplasia progression and its impact on treatment. *Curr Opin Urol* **2004**, 14 (1), 45-50.
44. Romas, N. A., Prostatic acid phosphatase: current concepts. *Semin Urol* **1983**, 1 (3), 177-85.
45. Foti, A. G.; Herschman, H.; Cooper, J. F., Comparison of human prostatic acid phosphatase by measurement of enzymatic activity and by radioimmunoassay. *Clin Chem* **1977**, 23 (1), 95-9.
46. Heller, J. E., Prostatic acid phosphatase: its current clinical status. *J Urol* **1987**, 137 (6), 1091-103.
47. Taira, A.; Merrick, G.; Wallner, K.; Dattoli, M., Reviving the acid phosphatase test for prostate cancer. *Oncology (Williston Park)* **2007**, 21 (8), 1003-10.
48. Han, M.; Piantadosi, S.; Zahurak, M. L.; Sokoll, L. J.; Chan, D. W.; Epstein, J. I.; Walsh, P. C.; Partin, A. W., Serum acid phosphatase level and biochemical recurrence following radical prostatectomy for men with clinically localized prostate cancer. *Urology* **2001**, 57 (4), 707-11.
49. Moul, J. W.; Connelly, R. R.; Perahia, B.; McLeod, D. G., The contemporary value of pretreatment prostatic acid phosphatase to predict pathological stage and recurrence in radical prostatectomy cases. *J Urol* **1998**, 159 (3), 935-40.
50. Gutman, A. B.; Gutman, E. B., An " Acid " Phosphatase Occurring in the Serum of Patients with Metastasizing Carcinoma of the Prostate Gland. *J Clin Invest* **1938**, 17 (4), 473-8.

51. Van Etten, R. L.; Saini, M. S., Selective purification of tartrate-inhibitable acid phosphatases: rapid and efficient purification (to homogeneity) of human and canine prostatic acid phosphatases. *Clin Chem* **1978**, 24 (9), 1525-30.
52. Roy, A. V.; Brower, M. E.; Hayden, J. E., Sodium thymolphthalein monophosphate: a new acid phosphatase substrate with greater specificity for the prostatic enzyme in serum. *Clin Chem* **1971**, 17 (11), 1093-102.
53. Stamey, T. A.; Kabalin, J. N.; McNeal, J. E.; Johnstone, I. M.; Freiha, F.; Redwine, E. A.; Yang, N., Prostate specific antigen in the diagnosis and treatment of adenocarcinoma of the prostate. II. Radical prostatectomy treated patients. *J Urol* **1989**, 141 (5), 1076-83.
54. O'Dowd, G. J.; Veltri, R. W.; Orozco, R.; Miller, M. C.; Oesterling, J. E., Update on the appropriate staging evaluation for newly diagnosed prostate cancer. *J Urol* **1997**, 158 (3 Pt 1), 687-98.
55. Reiter, R. E.; Gu, Z.; Watabe, T.; Thomas, G.; Szigeti, K.; Davis, E.; Wahl, M.; Nisitani, S.; Yamashiro, J.; Le Beau, M. M.; Loda, M.; Witte, O. N., Prostate stem cell antigen: a cell surface marker overexpressed in prostate cancer. *Proc Natl Acad Sci U S A* **1998**, 95 (4), 1735-40.
56. Gu, Z.; Thomas, G.; Yamashiro, J.; Shintaku, I. P.; Dorey, F.; Raitano, A.; Witte, O. N.; Said, J. W.; Loda, M.; Reiter, R. E., Prostate stem cell antigen (PSCA) expression increases with high gleason score, advanced stage and bone metastasis in prostate cancer. *Oncogene* **2000**, 19 (10), 1288-96.
57. Jalkut, M. W.; Reiter, R. E., Role of prostate stem cell antigen in prostate cancer research. *Curr Opin Urol* **2002**, 12 (5), 401-6.
58. Hara, N.; Kasahara, T.; Kawasaki, T.; Bilim, V.; Obara, K.; Takahashi, K.; Tomita, Y., Reverse transcription-polymerase chain reaction detection of prostate-specific antigen, prostate-specific membrane antigen, and prostate stem cell antigen in one milliliter of peripheral blood: value for the staging of prostate cancer. *Clin Cancer Res* **2002**, 8 (6), 1794-9.
59. Israeli, R. S.; Powell, C. T.; Corr, J. G.; Fair, W. R.; Heston, W. D., Expression of the prostate-specific membrane antigen. *Cancer Res* **1994**, 54 (7), 1807-11.
60. Pinto, J. T.; Suffoletto, B. P.; Berzin, T. M.; Qiao, C. H.; Lin, S.; Tong, W. P.; May, F.; Mukherjee, B.; Heston, W. D., Prostate-specific membrane antigen: a novel folate hydrolase in human prostatic carcinoma cells. *Clin Cancer Res* **1996**, 2 (9), 1445-51.

61. Silver, D. A.; Pellicer, I.; Fair, W. R.; Heston, W. D.; Cordon-Cardo, C., Prostate-specific membrane antigen expression in normal and malignant human tissues. *Clin Cancer Res* **1997**, 3 (1), 81-5.
62. Murphy, G. P.; Kenny, G. M.; Ragde, H.; Wolfert, R. L.; Boynton, A. L.; Holmes, E. H.; Misrock, S. L.; Bartsch, G.; Klocker, H.; Pointner, J.; Reissigl, A.; McLeod, D. G.; Douglas, T.; Morgan, T.; Gilbaugh, J., Jr., Measurement of serum prostate-specific membrane antigen, a new prognostic marker for prostate cancer. *Urology* **1998**, 51 (5A Suppl), 89-97.
63. Murphy, G. P.; Tino, W. T.; Holmes, E. H.; Boynton, A. L.; Erickson, S. J.; Bowes, V. A.; Barren, R. J.; Tjoa, B. A.; Misrock, S. L.; Ragde, H.; Kenny, G. M., Measurement of prostate-specific membrane antigen in the serum with a new antibody. *Prostate* **1996**, 28 (4), 266-71.
64. Murphy, G.; Ragde, H.; Kenny, G.; Barren, R., 3rd; Erickson, S.; Tjoa, B.; Boynton, A.; Holmes, E.; Gilbaugh, J.; Douglas, T., Comparison of prostate specific membrane antigen, and prostate specific antigen levels in prostatic cancer patients. *Anticancer Res* **1995**, 15 (4), 1473-9.
65. Sweat, S. D.; Pacelli, A.; Murphy, G. P.; Bostwick, D. G., Prostate-specific membrane antigen expression is greatest in prostate adenocarcinoma and lymph node metastases. *Urology* **1998**, 52 (4), 637-40.
66. Xiao, Z.; Adam, B. L.; Cazares, L. H.; Clements, M. A.; Davis, J. W.; Schellhammer, P. F.; Dalmasso, E. A.; Wright, G. L., Jr., Quantitation of serum prostate-specific membrane antigen by a novel protein biochip immunoassay discriminates benign from malignant prostate disease. *Cancer Res* **2001**, 61 (16), 6029-33.
67. Lin, B.; Ferguson, C.; White, J. T.; Wang, S.; Vessella, R.; True, L. D.; Hood, L.; Nelson, P. S., Prostate-localized and androgen-regulated expression of the membrane-bound serine protease TMPRSS2. *Cancer Res* **1999**, 59 (17), 4180-4.
68. Yu, J. X.; Chao, L.; Chao, J., Prostaticin is a novel human serine proteinase from seminal fluid. Purification, tissue distribution, and localization in prostate gland. *J Biol Chem* **1994**, 269 (29), 18843-8.
69. Verghese, G. M.; Gutknecht, M. F.; Caughey, G. H., Prostaticin regulates epithelial monolayer function: cell-specific Gpld1-mediated secretion and functional role for GPI anchor. *Am J Physiol Cell Physiol* **2006**, 291 (6), C1258-70.
70. Iftikhar, R.; Kladney, R. D.; Havlioglu, N.; Schmitt-Graff, A.; Gusmirovic, I.; Solomon, H.; Luxon, B. A.; Bacon, B. R.; Fimmel, C. J., Disease- and cell-specific expression of GP73 in human liver disease. *Am J Gastroenterol* **2004**, 99 (6), 1087-95.

71. Marrero, J. A.; Romano, P. R.; Nikolaeva, O.; Steel, L.; Mehta, A.; Fimmel, C. J.; Comunale, M. A.; D'Amelio, A.; Lok, A. S.; Block, T. M., GP73, a resident Golgi glycoprotein, is a novel serum marker for hepatocellular carcinoma. *J Hepatol* **2005**, 43 (6), 1007-12.
72. Bachert, C.; Fimmel, C.; Linstedt, A. D., Endosomal trafficking and proprotein convertase cleavage of cis Golgi protein GP73 produces marker for hepatocellular carcinoma. *Traffic* **2007**, 8 (10), 1415-23.
73. Schwegler, E. E.; Cazares, L.; Steel, L. F.; Adam, B. L.; Johnson, D. A.; Semmes, O. J.; Block, T. M.; Marrero, J. A.; Drake, R. R., SELDI-TOF MS profiling of serum for detection of the progression of chronic hepatitis C to hepatocellular carcinoma. *Hepatology* **2005**, 41 (3), 634-42.
74. Laxman, B.; Morris, D. S.; Yu, J.; Siddiqui, J.; Cao, J.; Mehra, R.; Lonigro, R. J.; Tsodikov, A.; Wei, J. T.; Tomlins, S. A.; Chinnaiyan, A. M., A first-generation multiplex biomarker analysis of urine for the early detection of prostate cancer. *Cancer Res* **2008**, 68 (3), 645-9.
75. Kristiansen, G.; Fritzsche, F. R.; Wassermann, K.; Jager, C.; Tolls, A.; Lein, M.; Stephan, C.; Jung, K.; Pilarsky, C.; Dietel, M.; Moch, H., GOLPH2 protein expression as a novel tissue biomarker for prostate cancer: implications for tissue-based diagnostics. *Br J Cancer* **2008**, 99 (6), 939-48.
76. Luo, J.; Zha, S.; Gage, W. R.; Dunn, T. A.; Hicks, J. L.; Bennett, C. J.; Ewing, C. M.; Platz, E. A.; Ferdinandusse, S.; Wanders, R. J.; Trent, J. M.; Isaacs, W. B.; De Marzo, A. M., Alpha-methylacyl-CoA racemase: a new molecular marker for prostate cancer. *Cancer Res* **2002**, 62 (8), 2220-6.
77. Rubin, M. A.; Zhou, M.; Dhanasekaran, S. M.; Varambally, S.; Barrette, T. R.; Sanda, M. G.; Pienta, K. J.; Ghosh, D.; Chinnaiyan, A. M., alpha-Methylacyl coenzyme A racemase as a tissue biomarker for prostate cancer. *Jama* **2002**, 287 (13), 1662-70.
78. Beach, R.; Gown, A. M.; De Peralta-Venturina, M. N.; Folpe, A. L.; Yaziji, H.; Salles, P. G.; Grignon, D. J.; Fanger, G. R.; Amin, M. B., P504S immunohistochemical detection in 405 prostatic specimens including 376 18-gauge needle biopsies. *Am J Surg Pathol* **2002**, 26 (12), 1588-96.
79. Jiang, Z.; Woda, B. A.; Wu, C. L.; Yang, X. J., Discovery and clinical application of a novel prostate cancer marker: alpha-methylacyl CoA racemase (P504S). *Am J Clin Pathol* **2004**, 122 (2), 275-89.
80. Slager, S. L.; Zarfes, K. E.; Brown, W. M.; Lange, E. M.; McDonnell, S. K.; Wojno, K. J.; Cooney, K. A., Genome-wide linkage scan for prostate cancer aggressiveness loci using families from the University of Michigan Prostate Cancer Genetics Project. *Prostate* **2006**, 66 (2), 173-9.

81. Zheng, S. L.; Chang, B. L.; Faith, D. A.; Johnson, J. R.; Isaacs, S. D.; Hawkins, G. A.; Turner, A.; Wiley, K. E.; Bleecker, E. R.; Walsh, P. C.; Meyers, D. A.; Isaacs, W. B.; Xu, J., Sequence variants of alpha-methylacyl-CoA racemase are associated with prostate cancer risk. *Cancer Res* **2002**, 62 (22), 6485-8.
82. Douglas, J. A.; Zuhlke, K. A.; Beebe-Dimmer, J.; Levin, A. M.; Gruber, S. B.; Wood, D. P.; Cooney, K. A., Identifying susceptibility genes for prostate cancer--a family-based association study of polymorphisms in CYP17, CYP19, CYP11A1, and LH-beta. *Cancer Epidemiol Biomarkers Prev* **2005**, 14 (8), 2035-9.
83. Couldrey, C.; Green, J. E., Metastases: the glycan connection. *Breast Cancer Res* **2000**, 2 (5), 321-3.
84. Dwek, M. V.; Ross, H. A.; Leatham, A. J., Proteome and glycosylation mapping identifies post-translational modifications associated with aggressive breast cancer. *Proteomics* **2001**, 1 (6), 756-62.
85. Fukuda, M., Cell surface glycoconjugates as onco-differentiation markers in hematopoietic cells. *Biochim Biophys Acta* **1985**, 780 (2), 119-50.
86. Dennis, J. W.; Laferte, S.; Waghorne, C.; Breitman, M. L.; Kerbel, R. S., Beta 1-6 branching of Asn-linked oligosaccharides is directly associated with metastasis. *Science* **1987**, 236 (4801), 582-5.
87. Polet, H.; Molnar, J., Demonstration that some of the nonhistone proteins, inducible to translocate into the nucleus, are glycosylated. *J Cell Physiol* **1988**, 135 (1), 47-54.
88. Davis, L. I.; Blobel, G., Nuclear pore complex contains a family of glycoproteins that includes p62: glycosylation through a previously unidentified cellular pathway. *Proc Natl Acad Sci U S A* **1987**, 84 (21), 7552-6.
89. Snow, C. M.; Senior, A.; Gerace, L., Monoclonal antibodies identify a group of nuclear pore complex glycoproteins. *J Cell Biol* **1987**, 104 (5), 1143-56.
90. Haltiwanger, R. S.; Blomberg, M. A.; Hart, G. W., Glycosylation of nuclear and cytoplasmic proteins. Purification and characterization of a uridine diphospho-N-acetylglucosamine:polypeptide beta-N-acetylglucosaminyltransferase. *J Biol Chem* **1992**, 267 (13), 9005-13.
91. Wells, L.; Vosseller, K.; Hart, G. W., Glycosylation of nucleocytoplasmic proteins: signal transduction and O-GlcNAc. *Science* **2001**, 291 (5512), 2376-8.
92. Varki, A., *Essentials of glycobiology*. 2nd ed.; Cold Spring Harbor Laboratory Press: Cold Spring Harbor, N.Y., 2009; p xxix, 784 p.

93. Fuster, M. M.; Esko, J. D., The sweet and sour of cancer: glycans as novel therapeutic targets. *Nat Rev Cancer* **2005**, 5 (7), 526-42.
94. Peracaula, R.; Barrabes, S.; Sarrats, A.; Rudd, P. M.; de Llorens, R., Altered glycosylation in tumours focused to cancer diagnosis. *Dis Markers* **2008**, 25 (4-5), 207-18.
95. Brooks, S. A.; Carter, T. M.; Royle, L.; Harvey, D. J.; Fry, S. A.; Kinch, C.; Dwek, R. A.; Rudd, P. M., Altered glycosylation of proteins in cancer: what is the potential for new anti-tumour strategies. *Anticancer Agents Med Chem* **2008**, 8 (1), 2-21.
96. Girnita, L.; Wang, M.; Xie, Y.; Nilsson, G.; Dricu, A.; Wejde, J.; Larsson, O., Inhibition of N-linked glycosylation down-regulates insulin-like growth factor-1 receptor at the cell surface and kills Ewing's sarcoma cells: therapeutic implications. *Anticancer Drug Des* **2000**, 15 (1), 67-72.
97. Komatsu, M.; Jepson, S.; Arango, M. E.; Carothers Carraway, C. A.; Carraway, K. L., Muc4/sialomucin complex, an intramembrane modulator of ErbB2/HER2/Neu, potentiates primary tumor growth and suppresses apoptosis in a xenotransplanted tumor. *Oncogene* **2001**, 20 (4), 461-70.
98. Chou, T. Y.; Hart, G. W., O-linked N-acetylglucosamine and cancer: messages from the glycosylation of c-Myc. *Adv Exp Med Biol* **2001**, 491, 413-8.
99. Takenaka, Y.; Fukumori, T.; Raz, A., Galectin-3 and metastasis. *Glycoconj J* **2004**, 19 (7-9), 543-9.
100. Bharathan, S.; Moriarty, J.; Moody, C. E.; Sherblom, A. P., Effect of tunicamycin on sialomucin and natural killer susceptibility of rat mammary tumor ascites cells. *Cancer Res* **1990**, 50 (17), 5250-6.
101. Seidenfaden, R.; Krauter, A.; Schertzinger, F.; Gerardy-Schahn, R.; Hildebrandt, H., Polysialic acid directs tumor cell growth by controlling heterophilic neural cell adhesion molecule interactions. *Mol Cell Biol* **2003**, 23 (16), 5908-18.
102. Jiang, X.; Couchman, J. R., Perlecan and tumor angiogenesis. *J Histochem Cytochem* **2003**, 51 (11), 1393-410.
103. Kim, Y. J.; Borsig, L.; Varki, N. M.; Varki, A., P-selectin deficiency attenuates tumor growth and metastasis. *Proc Natl Acad Sci U S A* **1998**, 95 (16), 9325-30.
104. Borsig, L.; Wong, R.; Hynes, R. O.; Varki, N. M.; Varki, A., Synergistic effects of L- and P-selectin in facilitating tumor metastasis can involve non-mucin ligands and implicate leukocytes as enhancers of metastasis. *Proc Natl Acad Sci U S A* **2002**, 99 (4), 2193-8.

105. Varki, A., Selectin ligands: will the real ones please stand up? *J Clin Invest* **1997**, 100 (11 Suppl), S31-5.
106. Kannagi, R., Carbohydrate antigen sialyl Lewis a--its pathophysiological significance and induction mechanism in cancer progression. *Chang Gung Med J* **2007**, 30 (3), 189-209.
107. Dimitroff, C. J.; Lechpammer, M.; Long-Woodward, D.; Kutok, J. L., Rolling of human bone-metastatic prostate tumor cells on human bone marrow endothelium under shear flow is mediated by E-selectin. *Cancer Res* **2004**, 64 (15), 5261-9.
108. Glithero, A.; Tormo, J.; Haurum, J. S.; Arsequell, G.; Valencia, G.; Edwards, J.; Springer, S.; Townsend, A.; Pao, Y. L.; Wormald, M.; Dwek, R. A.; Jones, E. Y.; Elliott, T., Crystal structures of two H-2Db/glycopeptide complexes suggest a molecular basis for CTL cross-reactivity. *Immunity* **1999**, 10 (1), 63-74.
109. Cozzi, P. J.; Wang, J.; Delprado, W.; Perkins, A. C.; Allen, B. J.; Russell, P. J.; Li, Y., MUC1, MUC2, MUC4, MUC5AC and MUC6 expression in the progression of prostate cancer. *Clin Exp Metastasis* **2005**, 22 (7), 565-73.
110. Garbar, C.; Mascaux, C.; Wespes, E., Expression of MUC1 and sialyl-Tn in benign prostatic glands, high-grade prostate intraepithelial neoplasia and malignant prostatic glands: a preliminary study. *Anal Quant Cytol Histol* **2008**, 30 (2), 71-7.
111. Arai, T.; Fujita, K.; Fujime, M.; Irimura, T., Expression of sialylated MUC1 in prostate cancer: relationship to clinical stage and prognosis. *Int J Urol* **2005**, 12 (7), 654-61.
112. de Leoz, M. L.; An, H. J.; Kronewitter, S.; Kim, J.; Beecroft, S.; Vinall, R.; Miyamoto, S.; de Vere White, R.; Lam, K. S.; Lebrilla, C., Glycomic approach for potential biomarkers on prostate cancer: profiling of N-linked glycans in human sera and pRNS cell lines. *Dis Markers* **2008**, 25 (4-5), 243-58.
113. Holmes, E. H.; Greene, T. G.; Tino, W. T.; Boynton, A. L.; Aldape, H. C.; Misrock, S. L.; Murphy, G. P., Analysis of glycosylation of prostate-specific membrane antigen derived from LNCaP cells, prostatic carcinoma tumors, and serum from prostate cancer patients. *Prostate Suppl* **1996**, 7, 25-9.
114. Fujimura, T.; Shinohara, Y.; Tissot, B.; Pang, P. C.; Kuroguchi, M.; Saito, S.; Arai, Y.; Sadilek, M.; Murayama, K.; Dell, A.; Nishimura, S.; Hakomori, S. I., Glycosylation status of haptoglobin in sera of patients with prostate cancer vs. benign prostate disease or normal subjects. *Int J Cancer* **2008**, 122 (1), 39-49.
115. Peracaula, R.; Tabares, G.; Royle, L.; Harvey, D. J.; Dwek, R. A.; Rudd, P. M.; de Llorens, R., Altered glycosylation pattern allows the distinction between prostate-specific antigen (PSA) from normal and tumor origins. *Glycobiology* **2003**, 13 (6), 457-70.

116. Prakash, S.; Robbins, P. W., Glycotyping of prostate specific antigen. *Glycobiology* **2000**, 10 (2), 173-6.
117. Okada, T.; Sato, Y.; Kobayashi, N.; Sumida, K.; Satomura, S.; Matsuura, S.; Takasaki, M.; Endo, T., Structural characteristics of the N-glycans of two isoforms of prostate-specific antigens purified from human seminal fluid. *Biochim Biophys Acta* **2001**, 1525 (1-2), 149-60.
118. Tabares, G.; Radcliffe, C. M.; Barrabes, S.; Ramirez, M.; Aleixandre, R. N.; Hoesel, W.; Dwek, R. A.; Rudd, P. M.; Peracaula, R.; de Llorens, R., Different glycan structures in prostate-specific antigen from prostate cancer sera in relation to seminal plasma PSA. *Glycobiology* **2006**, 16 (2), 132-45.
119. Belanger, A.; van Halbeek, H.; Graves, H. C.; Grandbois, K.; Stamey, T. A.; Huang, L.; Poppe, I.; Labrie, F., Molecular mass and carbohydrate structure of prostate specific antigen: studies for establishment of an international PSA standard. *Prostate* **1995**, 27 (4), 187-97.
120. Armbruster, D. A., Prostate-specific antigen: biochemistry, analytical methods, and clinical application. *Clin Chem* **1993**, 39 (2), 181-95.
121. Mattsson, J. M.; Valmu, L.; Laakkonen, P.; Stenman, U. H.; Koistinen, H., Structural characterization and anti-angiogenic properties of prostate-specific antigen isoforms in seminal fluid. *Prostate* **2008**, 68 (9), 945-54.
122. Tabares, G.; Jung, K.; Reiche, J.; Stephan, C.; Lein, M.; Peracaula, R.; de Llorens, R.; Hoesel, W., Free PSA forms in prostatic tissue and sera of prostate cancer patients: analysis by 2-DE and western blotting of immunopurified samples. *Clin Biochem* **2007**, 40 (5-6), 343-50.
123. Tajiri, M.; Ohyama, C.; Wada, Y., Oligosaccharide profiles of the prostate specific antigen in free and complexed forms from the prostate cancer patient serum and in seminal plasma: a glycopeptide approach. *Glycobiology* **2008**, 18 (1), 2-8.
124. Jakob, C. G.; Lewinski, K.; Kuciel, R.; Ostrowski, W.; Lebioda, L., Crystal structure of human prostatic acid phosphatase. *Prostate* **2000**, 42 (3), 211-8.
125. Yoshida, K. I.; Honda, M.; Arai, K.; Hosoya, Y.; Moriguchi, H.; Sumi, S.; Ueda, Y.; Kitahara, S., Serial lectin affinity chromatography with concavalin A and wheat germ agglutinin demonstrates altered asparagine-linked sugar-chain structures of prostatic acid phosphatase in human prostate carcinoma. *J Chromatogr B Biomed Sci Appl* **1997**, 695 (2), 439-43.
126. Rifai, N.; Gillette, M. A.; Carr, S. A., Protein biomarker discovery and validation: the long and uncertain path to clinical utility. *Nat Biotechnol* **2006**, 24 (8), 971-83.

127. Schmidt, A.; Aebersold, R., High-accuracy proteome maps of human body fluids. *Genome Biol* **2006**, 7 (11), 242.
128. Pilch, B.; Mann, M., Large-scale and high-confidence proteomic analysis of human seminal plasma. *Genome Biol* **2006**, 7 (5), R40.
129. Zhang, W. M.; Leinonen, J.; Kalkkinen, N.; Dowell, B.; Stenman, U. H., Purification and characterization of different molecular forms of prostate-specific antigen in human seminal fluid. *Clin Chem* **1995**, 41 (11), 1567-73.
130. Hassan, M. I.; Kumar, V.; Kashav, T.; Alam, N.; Singh, T. P.; Yadav, S., Proteomic approach for purification of seminal plasma proteins involved in tumor proliferation. *J Sep Sci* **2007**, 30 (12), 1979-88.
131. Meares, E. M.; Stamey, T. A., Bacteriologic localization patterns in bacterial prostatitis and urethritis. *Invest Urol* **1968**, 5 (5), 492-518.
132. Tinzl, M.; Marberger, M.; Horvath, S.; Chypre, C., DD3PCA3 RNA analysis in urine--a new perspective for detecting prostate cancer. *Eur Urol* **2004**, 46 (2), 182-6; discussion 187.
133. Sokoll, L. J.; Ellis, W.; Lange, P.; Noteboom, J.; Elliott, D. J.; Deras, I. L.; Blase, A.; Koo, S.; Sarno, M.; Rittenhouse, H.; Groskopf, J.; Vessella, R. L., A multicenter evaluation of the PCA3 molecular urine test: Pre-analytical effects, analytical performance, and diagnostic accuracy. *Clin Chim Acta* **2008**, 389 (1-2), 1-6.
134. Hessels, D.; Smit, F. P.; Verhaegh, G. W.; Witjes, J. A.; Cornel, E. B.; Schalken, J. A., Detection of TMPRSS2-ERG fusion transcripts and prostate cancer antigen 3 in urinary sediments may improve diagnosis of prostate cancer. *Clin Cancer Res* **2007**, 13 (17), 5103-8.
135. Venter, J. C.; Adams, M. D.; Myers, E. W.; Li, P. W.; Mural, R. J.; Sutton, G. G.; Smith, H. O.; Yandell, M.; Evans, C. A.; Holt, R. A.; Gocayne, J. D.; Amanatides, P.; Ballew, R. M.; Huson, D. H.; Wortman, J. R.; Zhang, Q.; Kodira, C. D.; Zheng, X. H.; Chen, L.; Skupski, M.; Subramanian, G.; Thomas, P. D.; Zhang, J.; Gabor Miklos, G. L.; Nelson, C.; Broder, S.; Clark, A. G.; Nadeau, J.; McKusick, V. A.; Zinder, N.; Levine, A. J.; Roberts, R. J.; Simon, M.; Slayman, C.; Hunkapiller, M.; Bolanos, R.; Delcher, A.; Dew, I.; Fasulo, D.; Flanigan, M.; Florea, L.; Halpern, A.; Hannenhalli, S.; Kravitz, S.; Levy, S.; Mobarry, C.; Reinert, K.; Remington, K.; Abu-Threideh, J.; Beasley, E.; Biddick, K.; Bonazzi, V.; Brandon, R.; Cargill, M.; Chandramouliswaran, I.; Charlab, R.; Chaturvedi, K.; Deng, Z.; Di Francesco, V.; Dunn, P.; Eilbeck, K.; Evangelista, C.; Gabrielian, A. E.; Gan, W.; Ge, W.; Gong, F.; Gu, Z.; Guan, P.; Heiman, T. J.; Higgins, M. E.; Ji, R. R.; Ke, Z.; Ketchum, K. A.; Lai, Z.; Lei, Y.; Li, Z.; Li, J.; Liang, Y.; Lin, X.; Lu, F.; Merkulov, G. V.; Milshina, N.; Moore, H. M.; Naik, A. K.; Narayan, V. A.; Neelam, B.; Nuskern, D.; Rusch, D. B.; Salzberg, S.; Shao, W.; Shue, B.; Sun, J.; Wang, Z.; Wang, A.; Wang, X.; Wang, J.; Wei, M.; Wides, R.; Xiao, C.; Yan, C.; Yao, A.; Ye,

J.; Zhan, M.; Zhang, W.; Zhang, H.; Zhao, Q.; Zheng, L.; Zhong, F.; Zhong, W.; Zhu, S.; Zhao, S.; Gilbert, D.; Baumhueter, S.; Spier, G.; Carter, C.; Cravchik, A.; Woodage, T.; Ali, F.; An, H.; Awe, A.; Baldwin, D.; Baden, H.; Barnstead, M.; Barrow, I.; Beeson, K.; Busam, D.; Carver, A.; Center, A.; Cheng, M. L.; Curry, L.; Danaher, S.; Davenport, L.; Desilets, R.; Dietz, S.; Dodson, K.; Doup, L.; Ferriera, S.; Garg, N.; Gluecksmann, A.; Hart, B.; Haynes, J.; Haynes, C.; Heiner, C.; Hladun, S.; Hostin, D.; Houck, J.; Howland, T.; Ibegwam, C.; Johnson, J.; Kalush, F.; Kline, L.; Koduru, S.; Love, A.; Mann, F.; May, D.; McCawley, S.; McIntosh, T.; McMullen, I.; Moy, M.; Moy, L.; Murphy, B.; Nelson, K.; Pfannkoch, C.; Pratts, E.; Puri, V.; Qureshi, H.; Reardon, M.; Rodriguez, R.; Rogers, Y. H.; Romblad, D.; Ruhfel, B.; Scott, R.; Sitter, C.; Smallwood, M.; Stewart, E.; Strong, R.; Suh, E.; Thomas, R.; Tint, N. N.; Tse, S.; Vech, C.; Wang, G.; Wetter, J.; Williams, S.; Williams, M.; Windsor, S.; Winn-Deen, E.; Wolfe, K.; Zaveri, J.; Zaveri, K.; Abril, J. F.; Guigo, R.; Campbell, M. J.; Sjolander, K. V.; Karlak, B.; Kejariwal, A.; Mi, H.; Lazareva, B.; Hatton, T.; Narechania, A.; Diemer, K.; Muruganujan, A.; Guo, N.; Sato, S.; Bafna, V.; Istrail, S.; Lippert, R.; Schwartz, R.; Walenz, B.; Yooseph, S.; Allen, D.; Basu, A.; Baxendale, J.; Blick, L.; Caminha, M.; Carnes-Stine, J.; Caulk, P.; Chiang, Y. H.; Coyne, M.; Dahlke, C.; Mays, A.; Dombroski, M.; Donnelly, M.; Ely, D.; Esparham, S.; Fosler, C.; Gire, H.; Glanowski, S.; Glasser, K.; Glodek, A.; Gorokhov, M.; Graham, K.; Gropman, B.; Harris, M.; Heil, J.; Henderson, S.; Hoover, J.; Jennings, D.; Jordan, C.; Jordan, J.; Kasha, J.; Kagan, L.; Kraft, C.; Levitsky, A.; Lewis, M.; Liu, X.; Lopez, J.; Ma, D.; Majoros, W.; McDaniel, J.; Murphy, S.; Newman, M.; Nguyen, T.; Nguyen, N.; Nodell, M.; Pan, S.; Peck, J.; Peterson, M.; Rowe, W.; Sanders, R.; Scott, J.; Simpson, M.; Smith, T.; Sprague, A.; Stockwell, T.; Turner, R.; Venter, E.; Wang, M.; Wen, M.; Wu, D.; Wu, M.; Xia, A.; Zandieh, A.; Zhu, X., The sequence of the human genome. *Science* **2001**, 291 (5507), 1304-51.

136. Aebersold, R., A mass spectrometric journey into protein and proteome research. *J Am Soc Mass Spectrom* **2003**, 14 (7), 685-95.

137. Ornstein, D. K.; Petricoin, E. F., 3rd, Proteomics to diagnose human tumors and provide prognostic information. *Oncology (Williston Park)* **2004**, 18 (4), 521-9; discussion 529-32.

138. Klose, J., Protein mapping by combined isoelectric focusing and electrophoresis of mouse tissues. A novel approach to testing for induced point mutations in mammals. *Humangenetik* **1975**, 26 (3), 231-43.

139. O'Farrell, P. H., High resolution two-dimensional electrophoresis of proteins. *J Biol Chem* **1975**, 250 (10), 4007-21.

140. Bjellqvist, B.; Ek, K.; Righetti, P. G.; Gianazza, E.; Gorg, A.; Westermeier, R.; Postel, W., Isoelectric focusing in immobilized pH gradients: principle, methodology and some applications. *J Biochem Biophys Methods* **1982**, 6 (4), 317-39.

141. Sanger, F., The free amino groups of insulin. *Biochem J* **1945**, 39 (5), 507-15.

142. Simpson, R. J., *Proteins and proteomics : a laboratory manual*. Cold Spring Harbor Laboratory Press: Cold Spring Harbor, NY, 2003; p xiii, 926 pp.
143. Abderhalden, E.; Brockmann, H., The contribution determining the composition of proteins especially polypeptides (German). *Biochemische Zeitschrift* **1930**, 225, 386-408.
144. Edman, P., A method for the determination of amino acid sequence in peptides. *Arch Biochem* **1949**, 22 (3), 475.
145. Edman, P.; Begg, G., A protein sequenator. *Eur J Biochem* **1967**, 1 (1), 80-91.
146. Laursen, R. A., Solid-phase Edman degradation. An automatic peptide sequencer. *Eur J Biochem* **1971**, 20 (1), 89-102.
147. Grayson, M. A., *Measuring mass : from positive rays to proteins*. Chemical Heritage Press: Philadelphia, PA, 2002; p ix, 149 p.
148. Barber, M.; Bordoli, R. S.; Sedgwick, R. D.; Tyler, A. N., Fast atom bombardment of solids as an ion source in mass spectrometry. *Nature* **1981**, 293, 270-275.
149. Hunt, D. F.; Buko, A. M.; Ballard, J. M.; Shabanowitz, J.; Giordani, A. B., Sequence analysis of polypeptides by collision activated dissociation on a triple quadrupole mass spectrometer. *Biomed Mass Spectrom* **1981**, 8 (9), 397-408.
150. Karas, M.; Hillenkamp, F., Laser desorption ionization of proteins with molecular masses exceeding 10,000 daltons. *Anal Chem* **1988**, 60 (20), 2299-301.
151. Fenn, J. B.; Mann, M.; Meng, C. K.; Wong, S. F.; Whitehouse, C. M., Electrospray ionization for mass spectrometry of large biomolecules. *Science* **1989**, 246 (4926), 64-71.
152. Hunt, D. F.; Henderson, R. A.; Shabanowitz, J.; Sakaguchi, K.; Michel, H.; Sevilir, N.; Cox, A. L.; Appella, E.; Engelhard, V. H., Characterization of peptides bound to the class I MHC molecule HLA-A2.1 by mass spectrometry. *Science* **1992**, 255 (5049), 1261-3.
153. Anderson, N. G.; Anderson, L., The Human Protein Index. *Clin Chem* **1982**, 28 (4 Pt 2), 739-48.
154. Garrels, J. I., The QUEST system for quantitative analysis of two-dimensional gels. *J Biol Chem* **1989**, 264 (9), 5269-82.
155. Garrels, J. I.; Franza, B. R., Jr., Transformation-sensitive and growth-related changes of protein synthesis in REF52 cells. A two-dimensional gel analysis of SV40-

- adenovirus-, and Kirsten murine sarcoma virus-transformed rat cells using the REF52 protein database. *J Biol Chem* **1989**, 264 (9), 5299-312.
156. Garrels, J. I.; Franza, B. R., Jr., The REF52 protein database. Methods of database construction and analysis using the QUEST system and characterizations of protein patterns from proliferating and quiescent REF52 cells. *J Biol Chem* **1989**, 264 (9), 5283-98.
157. Anderson, N. L.; Hofmann, J. P.; Gemmell, A.; Taylor, J., Global approaches to quantitative analysis of gene-expression patterns observed by use of two-dimensional gel electrophoresis. *Clin Chem* **1984**, 30 (12 Pt 1), 2031-6.
158. Aebersold, R.; Goodlett, D. R., Mass spectrometry in proteomics. *Chem Rev* **2001**, 101 (2), 269-95.
159. Henzel, W. J.; Billeci, T. M.; Stults, J. T.; Wong, S. C.; Grimley, C.; Watanabe, C., Identifying proteins from two-dimensional gels by molecular mass searching of peptide fragments in protein sequence databases. *Proc Natl Acad Sci U S A* **1993**, 90 (11), 5011-5.
160. Yates, J. R., 3rd; Speicher, S.; Griffin, P. R.; Hunkapiller, T., Peptide mass maps: a highly informative approach to protein identification. *Anal Biochem* **1993**, 214 (2), 397-408.
161. James, P.; Quadroni, M.; Carafoli, E.; Gonnet, G., Protein identification in DNA databases by peptide mass fingerprinting. *Protein Sci* **1994**, 3 (8), 1347-50.
162. Pappin, D. J.; Hojrup, P.; Bleasby, A. J., Rapid identification of proteins by peptide-mass fingerprinting. *Curr Biol* **1993**, 3 (6), 327-32.
163. Mann, M.; Hojrup, P.; Roepstorff, P., Use of mass spectrometric molecular weight information to identify proteins in sequence databases. *Biol Mass Spectrom* **1993**, 22 (6), 338-45.
164. Yates, J. R., 3rd; Eng, J. K.; McCormack, A. L.; Schieltz, D., Method to correlate tandem mass spectra of modified peptides to amino acid sequences in the protein database. *Anal Chem* **1995**, 67 (8), 1426-36.
165. Perkins, D. N.; Pappin, D. J.; Creasy, D. M.; Cottrell, J. S., Probability-based protein identification by searching sequence databases using mass spectrometry data. *Electrophoresis* **1999**, 20 (18), 3551-67.
166. Mann, M.; Wilm, M., Error-tolerant identification of peptides in sequence databases by peptide sequence tags. *Anal Chem* **1994**, 66 (24), 4390-9.

167. Lander, E. S.; Linton, L. M.; Birren, B.; Nusbaum, C.; Zody, M. C.; Baldwin, J.; Devon, K.; Dewar, K.; Doyle, M.; FitzHugh, W.; Funke, R.; Gage, D.; Harris, K.; Heaford, A.; Howland, J.; Kann, L.; Lehoczky, J.; LeVine, R.; McEwan, P.; McKernan, K.; Meldrim, J.; Mesirov, J. P.; Miranda, C.; Morris, W.; Naylor, J.; Raymond, C.; Rosetti, M.; Santos, R.; Sheridan, A.; Sougnez, C.; Stange-Thomann, N.; Stojanovic, N.; Subramanian, A.; Wyman, D.; Rogers, J.; Sulston, J.; Ainscough, R.; Beck, S.; Bentley, D.; Burton, J.; Clee, C.; Carter, N.; Coulson, A.; Deadman, R.; Deloukas, P.; Dunham, A.; Dunham, I.; Durbin, R.; French, L.; Grafham, D.; Gregory, S.; Hubbard, T.; Humphray, S.; Hunt, A.; Jones, M.; Lloyd, C.; McMurray, A.; Matthews, L.; Mercer, S.; Milne, S.; Mullikin, J. C.; Mungall, A.; Plumb, R.; Ross, M.; Shownkeen, R.; Sims, S.; Waterston, R. H.; Wilson, R. K.; Hillier, L. W.; McPherson, J. D.; Marra, M. A.; Mardis, E. R.; Fulton, L. A.; Chinwalla, A. T.; Pepin, K. H.; Gish, W. R.; Chissole, S. L.; Wendl, M. C.; Delehaunty, K. D.; Miner, T. L.; Delehaunty, A.; Kramer, J. B.; Cook, L. L.; Fulton, R. S.; Johnson, D. L.; Minx, P. J.; Clifton, S. W.; Hawkins, T.; Branscomb, E.; Predki, P.; Richardson, P.; Wenning, S.; Slezak, T.; Doggett, N.; Cheng, J. F.; Olsen, A.; Lucas, S.; Elkin, C.; Uberbacher, E.; Frazier, M.; Gibbs, R. A.; Muzny, D. M.; Scherer, S. E.; Bouck, J. B.; Sodergren, E. J.; Worley, K. C.; Rives, C. M.; Gorrell, J. H.; Metzker, M. L.; Naylor, S. L.; Kucherlapati, R. S.; Nelson, D. L.; Weinstock, G. M.; Sakaki, Y.; Fujiyama, A.; Hattori, M.; Yada, T.; Toyoda, A.; Itoh, T.; Kawagoe, C.; Watanabe, H.; Totoki, Y.; Taylor, T.; Weissenbach, J.; Heilig, R.; Saurin, W.; Artiguenave, F.; Brottier, P.; Bruls, T.; Pelletier, E.; Robert, C.; Wincker, P.; Smith, D. R.; Doucette-Stamm, L.; Rubenfield, M.; Weinstock, K.; Lee, H. M.; Dubois, J.; Rosenthal, A.; Platzer, M.; Nyakatura, G.; Taudien, S.; Rump, A.; Yang, H.; Yu, J.; Wang, J.; Huang, G.; Gu, J.; Hood, L.; Rowen, L.; Madan, A.; Qin, S.; Davis, R. W.; Federspiel, N. A.; Abola, A. P.; Proctor, M. J.; Myers, R. M.; Schmutz, J.; Dickson, M.; Grimwood, J.; Cox, D. R.; Olson, M. V.; Kaul, R.; Raymond, C.; Shimizu, N.; Kawasaki, K.; Minoshima, S.; Evans, G. A.; Athanasiou, M.; Schultz, R.; Roe, B. A.; Chen, F.; Pan, H.; Ramser, J.; Lehrach, H.; Reinhardt, R.; McCombie, W. R.; de la Bastide, M.; Dedhia, N.; Blocker, H.; Hornischer, K.; Nordsiek, G.; Agarwala, R.; Aravind, L.; Bailey, J. A.; Bateman, A.; Batzoglu, S.; Birney, E.; Bork, P.; Brown, D. G.; Burge, C. B.; Cerutti, L.; Chen, H. C.; Church, D.; Clamp, M.; Copley, R. R.; Doerks, T.; Eddy, S. R.; Eichler, E. E.; Furey, T. S.; Galagan, J.; Gilbert, J. G.; Harmon, C.; Hayashizaki, Y.; Haussler, D.; Hermjakob, H.; Hokamp, K.; Jang, W.; Johnson, L. S.; Jones, T. A.; Kasif, S.; Kasprzyk, A.; Kennedy, S.; Kent, W. J.; Kitts, P.; Koonin, E. V.; Korf, I.; Kulp, D.; Lancet, D.; Lowe, T. M.; McLysaght, A.; Mikkelsen, T.; Moran, J. V.; Mulder, N.; Pollara, V. J.; Ponting, C. P.; Schuler, G.; Schultz, J.; Slater, G.; Smit, A. F.; Stupka, E.; Szustakowski, J.; Thierry-Mieg, D.; Thierry-Mieg, J.; Wagner, L.; Wallis, J.; Wheeler, R.; Williams, A.; Wolf, Y. I.; Wolfe, K. H.; Yang, S. P.; Yeh, R. F.; Collins, F.; Guyer, M. S.; Peterson, J.; Felsenfeld, A.; Wetterstrand, K. A.; Patrinos, A.; Morgan, M. J.; de Jong, P.; Catanese, J. J.; Osoegawa, K.; Shizuya, H.; Choi, S.; Chen, Y. J., Initial sequencing and analysis of the human genome. *Nature* **2001**, 409 (6822), 860-921.

168. Harvey, D. J., Structural determination of N-linked glycans by matrix-assisted laser desorption/ionization and electrospray ionization mass spectrometry. *Proteomics* **2005**, 5 (7), 1774-86.

169. Kuster, B.; Krogh, T. N.; Mortz, E.; Harvey, D. J., Glycosylation analysis of gel-separated proteins. *Proteomics* **2001**, 1 (2), 350-61.
170. Royle, L.; Mattu, T. S.; Hart, E.; Langridge, J. I.; Merry, A. H.; Murphy, N.; Harvey, D. J.; Dwek, R. A.; Rudd, P. M., An analytical and structural database provides a strategy for sequencing O-glycans from microgram quantities of glycoproteins. *Anal Biochem* **2002**, 304 (1), 70-90.
171. Elder, J. H.; Alexander, S., endo-beta-N-acetylglucosaminidase F: endoglycosidase from *Flavobacterium meningosepticum* that cleaves both high-mannose and complex glycoproteins. *Proc Natl Acad Sci U S A* **1982**, 79 (15), 4540-4.
172. Taga, E. M.; Waheed, A.; Van Etten, R. L., Structural and chemical characterization of a homogeneous peptide N-glycosidase from almond. *Biochemistry* **1984**, 23 (5), 815-22.
173. Tarentino, A. L.; Gomez, C. M.; Plummer, T. H., Jr., Deglycosylation of asparagine-linked glycans by peptide:N-glycosidase F. *Biochemistry* **1985**, 24 (17), 4665-71.
174. Geyer, H.; Geyer, R., Strategies for analysis of glycoprotein glycosylation. *Biochim Biophys Acta* **2006**, 1764 (12), 1853-69.
175. Morelle, W.; Michalski, J. C., Glycomics and mass spectrometry. *Curr Pharm Des* **2005**, 11 (20), 2615-45.
176. Budnik, B. A.; Lee, R. S.; Steen, J. A., Global methods for protein glycosylation analysis by mass spectrometry. *Biochim Biophys Acta* **2006**, 1764 (12), 1870-80.
177. Emmett, M. R., Determination of post-translational modifications of proteins by high-sensitivity, high-resolution Fourier transform ion cyclotron resonance mass spectrometry. *J Chromatogr A* **2003**, 1013 (1-2), 203-13.
178. Mirgorodskaya, E.; Roepstorff, P.; Zubarev, R. A., Localization of O-glycosylation sites in peptides by electron capture dissociation in a Fourier transform mass spectrometer. *Anal Chem* **1999**, 71 (20), 4431-6.
179. Hakansson, K.; Cooper, H. J.; Emmett, M. R.; Costello, C. E.; Marshall, A. G.; Nilsson, C. L., Electron capture dissociation and infrared multiphoton dissociation MS/MS of an N-glycosylated tryptic peptic to yield complementary sequence information. *Anal Chem* **2001**, 73 (18), 4530-6.
180. Nagy, K.; Vekey, K.; Imre, T.; Ludanyi, K.; Barrow, M. P.; Derrick, P. J., Electrospray ionization fourier transform ion cyclotron resonance mass spectrometry of human alpha-1-acid glycoprotein. *Anal Chem* **2004**, 76 (17), 4998-5005.

181. Syka, J. E.; Coon, J. J.; Schroeder, M. J.; Shabanowitz, J.; Hunt, D. F., Peptide and protein sequence analysis by electron transfer dissociation mass spectrometry. *Proc Natl Acad Sci U S A* **2004**, 101 (26), 9528-33.
182. Hogan, J. M.; Pitteri, S. J.; Chrisman, P. A.; McLuckey, S. A., Complementary structural information from a tryptic N-linked glycopeptide via electron transfer ion/ion reactions and collision-induced dissociation. *J Proteome Res* **2005**, 4 (2), 628-32.
183. Kuster, B.; Wheeler, S. F.; Hunter, A. P.; Dwek, R. A.; Harvey, D. J., Sequencing of N-linked oligosaccharides directly from protein gels: in-gel deglycosylation followed by matrix-assisted laser desorption/ionization mass spectrometry and normal-phase high-performance liquid chromatography. *Anal Biochem* **1997**, 250 (1), 82-101.
184. Packer, N. H.; Lawson, M. A.; Jardine, D. R.; Redmond, J. W., A general approach to desalting oligosaccharides released from glycoproteins. *Glycoconj J* **1998**, 15 (8), 737-47.
185. Wilkinson, B. A.; Hamdy, F. C., State-of-the-art staging in prostate cancer. *BJU Int* **2001**, 87 (5), 423-30.
186. Makarov, D. V.; Carter, H. B., The discovery of prostate specific antigen as a biomarker for the early detection of adenocarcinoma of the prostate. *J Urol* **2006**, 176 (6 Pt 1), 2383-5.
187. Menez, R.; Michel, S.; Muller, B. H.; Bossus, M.; Ducancel, F.; Jolivet-Reynaud, C.; Stura, E. A., Crystal structure of a ternary complex between human prostate-specific antigen, its substrate acyl intermediate and an activating antibody. *J Mol Biol* **2008**, 376 (4), 1021-33.
188. Ronquist, G.; Brody, I., The prostasome: its secretion and function in man. *Biochim Biophys Acta* **1985**, 822 (2), 203-18.
189. Kawinski, E.; Levine, E.; Chadha, K., Thiophilic interaction chromatography facilitates detection of various molecular complexes of prostate-specific antigen in biological fluids. *Prostate* **2002**, 50 (3), 145-53.
190. Porath, J.; Maisano, F.; Belew, M., Thiophilic adsorption--a new method for protein fractionation. *FEBS Lett* **1985**, 185 (2), 306-10.
191. Gupta, S.; Suresh, M., Affinity chromatography and co-chromatography of bispecific monoclonal antibody immunoconjugates. *J Biochem Biophys Methods* **2002**, 51 (3), 203-16.
192. Block, T. M.; Comunale, M. A.; Lowman, M.; Steel, L. F.; Romano, P. R.; Fimmel, C.; Tennant, B. C.; London, W. T.; Evans, A. A.; Blumberg, B. S.; Dwek, R. A.; Mattu, T. S.; Mehta, A. S., Use of targeted glycoproteomics to identify serum

glycoproteins that correlate with liver cancer in woodchucks and humans. *Proc Natl Acad Sci USA* **2005**, 102 (3), 779-84.

193. Mehta, A.; Carrouee, S.; Conyers, B.; Jordan, R.; Butters, T.; Dwek, R. A.; Block, T. M., Inhibition of hepatitis B virus DNA replication by imino sugars without the inhibition of the DNA polymerase: therapeutic implications. *Hepatology* **2001**, 33 (6), 1488-95.

194. Guile, G. R.; Rudd, P. M.; Wing, D. R.; Prime, S. B.; Dwek, R. A., A rapid high-resolution high-performance liquid chromatographic method for separating glycan mixtures and analyzing oligosaccharide profiles. *Anal Biochem* **1996**, 240 (2), 210-26.

195. Ciucanu, I.; Kerek, F., A simple and rapid method for the permethylation of carbohydrates. *Carbohydrate Research* **1984**, 131, 209-217.

196. Ceroni, A.; Dell, A.; Haslam, S. M., The GlycanBuilder: a fast, intuitive and flexible software tool for building and displaying glycan structures. *Source Code Biol Med* **2007**, 2, 3.

197. Sandra, K.; Devreese, B.; Van Beeumen, J.; Stals, I.; Claeysens, M., The Q-Trap mass spectrometer, a novel tool in the study of protein glycosylation. *J Am Soc Mass Spectrom* **2004**, 15 (3), 413-23.

198. Carr, S. A.; Huddleston, M. J.; Bean, M. F., Selective identification and differentiation of N- and O-linked oligosaccharides in glycoproteins by liquid chromatography-mass spectrometry. *Protein Sci* **1993**, 2 (2), 183-96.

199. Mehta, A. S.; Long, R. E.; Comunale, M. A.; Wang, M.; Rodemich, L.; Krakover, J.; Philip, R.; Marrero, J. A.; Dwek, R. A.; Block, T. M., Increased levels of galactose-deficient anti-Gal immunoglobulin G in the sera of hepatitis C virus-infected individuals with fibrosis and cirrhosis. *J Virol* **2008**, 82 (3), 1259-70.

200. Atwood, J. A., 3rd; Cheng, L.; Alvarez-Manilla, G.; Warren, N. L.; York, W. S.; Orlando, R., Quantitation by isobaric labeling: applications to glycomics. *J Proteome Res* **2008**, 7 (1), 367-74.

201. Prien, J. M.; Huysentruyt, L. C.; Ashline, D. J.; Lapadula, A. J.; Seyfried, T. N.; Reinhold, V. N., Differentiating N-linked glycan structural isomers in metastatic and nonmetastatic tumor cells using sequential mass spectrometry. *Glycobiology* **2008**, 18 (5), 353-66.

202. Wuhrer, M.; Catalina, M. I.; Deelder, A. M.; Hokke, C. H., Glycoproteomics based on tandem mass spectrometry of glycopeptides. *J Chromatogr B Analyt Technol Biomed Life Sci* **2007**, 849 (1-2), 115-28.

203. Nickel, J. C.; Alexander, R. B.; Schaeffer, A. J.; Landis, J. R.; Knauss, J. S.; Prokert, K. J., Leukocytes and bacteria in men with chronic prostatitis/chronic pelvic pain syndrome compared to asymptomatic controls. *J Urol* **2003**, 170 (3), 818-22.
204. Ludwig, M.; Schroeder-Printzen, I.; Ludecke, G.; Weidner, W., Comparison of expressed prostatic secretions with urine after prostatic massage--a means to diagnose chronic prostatitis/inflammatory chronic pelvic pain syndrome. *Urology* **2000**, 55 (2), 175-7.
205. Fujita, K.; Ewing, C. M.; Sokoll, L. J.; Elliott, D. J.; Cunningham, M.; De Marzo, A. M.; Isaacs, W. B.; Pavlovich, C. P., Cytokine profiling of prostatic fluid from cancerous prostate glands identifies cytokines associated with extent of tumor and inflammation. *Prostate* **2008**, 68 (8), 872-82.
206. Marks, L. S.; Fradet, Y.; Deras, I. L.; Blase, A.; Mathis, J.; Aubin, S. M.; Cancio, A. T.; Desaulniers, M.; Ellis, W. J.; Rittenhouse, H.; Groskopf, J., PCA3 molecular urine assay for prostate cancer in men undergoing repeat biopsy. *Urology* **2007**, 69 (3), 532-5.
207. van Gils, M. P.; Cornel, E. B.; Hessels, D.; Peelen, W. P.; Witjes, J. A.; Mulders, P. F.; Rittenhouse, H. G.; Schalken, J. A., Molecular PCA3 diagnostics on prostatic fluid. *Prostate* **2007**, 67 (8), 881-7.
208. van Gils, M. P.; Hessels, D.; van Hooij, O.; Jannink, S. A.; Peelen, W. P.; Hanssen, S. L.; Witjes, J. A.; Cornel, E. B.; Karthaus, H. F.; Smits, G. A.; Dijkman, G. A.; Mulders, P. F.; Schalken, J. A., The time-resolved fluorescence-based PCA3 test on urinary sediments after digital rectal examination; a Dutch multicenter validation of the diagnostic performance. *Clin Cancer Res* **2007**, 13 (3), 939-43.
209. Groskopf, J.; Aubin, S. M.; Deras, I. L.; Blase, A.; Bodrug, S.; Clark, C.; Brentano, S.; Mathis, J.; Pham, J.; Meyer, T.; Cass, M.; Hodge, P.; Macairan, M. L.; Marks, L. S.; Rittenhouse, H., APTIMA PCA3 molecular urine test: development of a method to aid in the diagnosis of prostate cancer. *Clin Chem* **2006**, 52 (6), 1089-95.
210. Deras, I. L.; Aubin, S. M.; Blase, A.; Day, J. R.; Koo, S.; Partin, A. W.; Ellis, W. J.; Marks, L. S.; Fradet, Y.; Rittenhouse, H.; Groskopf, J., PCA3: a molecular urine assay for predicting prostate biopsy outcome. *J Urol* **2008**, 179 (4), 1587-92.
211. Mehra, R.; Tomlins, S. A.; Shen, R.; Nadeem, O.; Wang, L.; Wei, J. T.; Pienta, K. J.; Ghosh, D.; Rubin, M. A.; Chinnaiyan, A. M.; Shah, R. B., Comprehensive assessment of TMPRSS2 and ETS family gene aberrations in clinically localized prostate cancer. *Mod Pathol* **2007**, 20 (5), 538-44.
212. Alexander, H.; Stegner, A. L.; Wagner-Mann, C.; Du Bois, G. C.; Alexander, S.; Sauter, E. R., Proteomic analysis to identify breast cancer biomarkers in nipple aspirate fluid. *Clin Cancer Res* **2004**, 10 (22), 7500-10.

213. Drake, R. R.; White, K. Y.; Fuller, T. W.; Igwe, E.; Clements, M. A.; Nyalwidhe, J. O.; Given, R. W.; Lance, R. S.; Semmes, O. J., Clinical collection and protein properties of expressed prostatic secretions as a source for biomarkers of prostatic disease. *Journal of Proteomics* **2009**, 72 (6), 907-917.
214. Lau, K. S.; Dennis, J. W., N-Glycans in cancer progression. *Glycobiology* **2008**, 18 (10), 750-60.
215. Mehta, A.; Block, T. M., Fucosylated glycoproteins as markers of liver disease. *Dis Markers* **2008**, 25 (4-5), 259-65.
216. Comunale, M. A.; Wang, M.; Hafner, J.; Krakover, J.; Rodemich, L.; Kopenhaver, B.; Long, R. E.; Junaidi, O.; Bisceglie, A. M.; Block, T. M.; Mehta, A. S., Identification and development of fucosylated glycoproteins as biomarkers of primary hepatocellular carcinoma. *J Proteome Res* **2009**, 8 (2), 595-602.
217. Miyoshi, E.; Nakano, M., Fucosylated haptoglobin is a novel marker for pancreatic cancer: detailed analyses of oligosaccharide structures. *Proteomics* **2008**, 8 (16), 3257-62.
218. Kyselova, Z.; Mechref, Y.; Kang, P.; Goetz, J. A.; Dobrolecki, L. E.; Sledge, G. W.; Schnaper, L.; Hickey, R. J.; Malkas, L. H.; Novotny, M. V., Breast cancer diagnosis and prognosis through quantitative measurements of serum glycan profiles. *Clin Chem* **2008**, 54 (7), 1166-75.
219. Qiu, Y.; Patwa, T. H.; Xu, L.; Shedden, K.; Misek, D. E.; Tuck, M.; Jin, G.; Ruffin, M. T.; Turgeon, D. K.; Synal, S.; Bresalier, R.; Marcon, N.; Brenner, D. E.; Lubman, D. M., Plasma glycoprotein profiling for colorectal cancer biomarker identification by lectin glycoarray and lectin blot. *J Proteome Res* **2008**, 7 (4), 1693-703.
220. Quintero, I. B.; Araujo, C. L.; Pulkka, A. E.; Wirkkala, R. S.; Herrala, A. M.; Eskelinen, E. L.; Jokitalo, E.; Hellstrom, P. A.; Tuominen, H. J.; Hirvikoski, P. P.; Vihko, P. T., Prostatic acid phosphatase is not a prostate specific target. *Cancer Res* **2007**, 67 (14), 6549-54.
221. Cunha, A. C.; Weigle, B.; Kiessling, A.; Bachmann, M.; Rieber, E. P., Tissue-specificity of prostate specific antigens: comparative analysis of transcript levels in prostate and non-prostatic tissues. *Cancer Lett* **2006**, 236 (2), 229-38.
222. Kang, P.; Mechref, Y.; Klouckova, I.; Novotny, M. V., Solid-phase permethylation of glycans for mass spectrometric analysis. *Rapid Commun Mass Spectrom* **2005**, 19 (23), 3421-8.
223. Kang, P.; Mechref, Y.; Novotny, M. V., High-throughput solid-phase permethylation of glycans prior to mass spectrometry. *Rapid Commun Mass Spectrom* **2008**, 22, (5), 721-34.

**APPENDIX A
COPYRIGHT INFORMATION FOR REPRINT OF PUBLICATION IN
DISSERTATION**

License Number	2287371103597
License Date	Oct 13, 2009
Licensed content publisher	American Chemical Society
Licensed content publication	Journal of Proteome Research
Licensed content title	Glycomic Characterization of Prostate-Specific Antigen and Prostatic Acid Phosphatase in Prostate Cancer and Benign Disease Seminal Plasma Fluids
Licensed content author	Krista Y. White et al.
Licensed content date	Feb 1, 2009
Volume number	8
Issue number	2
Type of Use	Thesis/Dissertation
Requestor type	Not specified
Format	Print
Portion	Full article

**ACS / RIGHTSLINK TERMS & CONDITIONS
THESIS/DISSERTATION**

INTRODUCTION

The publisher for this copyrighted material is the American Chemical Society. By clicking "accept" in connection with completing this licensing transaction, you agree that the following terms and conditions apply to this transaction (along with the Billing and Payment terms and conditions established by Copyright Clearance Center, Inc. ("CCC"), at the time that you opened your Rightslink account and that are available at any time at <<http://myaccount.copyright.com>>).

LIMITED LICENSE

Publisher hereby grants to you a non-exclusive license to use this material. Licenses are for one-time use only with a maximum distribution equal to the number that you identified in the licensing process; any form of republication must be completed within 60 days from the date hereof (although copies prepared before then may be distributed thereafter).

GEOGRAPHIC RIGHTS: SCOPE

Licenses may be exercised anywhere in the world.

RESERVATION OF RIGHTS

Publisher reserves all rights not specifically granted in the combination of (i) the license details provided by you and accepted in the course of this licensing transaction, (ii) these terms and conditions and (iii) CCC's Billing and Payment terms and conditions.

PORTION RIGHTS STATEMENT: DISCLAIMER

If you seek to reuse a portion from an ACS publication, it is your responsibility to examine each portion as published to determine whether a credit to, or copyright notice of, a third party owner was published adjacent to the item. You may only obtain permission via Rightslink to use material owned by ACS. Permission to use any material published in an ACS publication, journal, or article which is reprinted with permission of a third party must be obtained from the third party owner. ACS disclaims any responsibility for any use you make of items owned by third parties without their permission.

REVOCACTION

The American Chemical Society reserves the right to revoke a license for any reason, including but not limited to advertising and promotional uses of ACS content, third party usage, and incorrect figure source attribution.

LICENSE CONTINGENT ON PAYMENT

While you may exercise the rights licensed immediately upon issuance of the license at the end of the licensing process for the transaction, provided that you have disclosed complete and accurate details of your proposed use, no license is finally effective unless and until full payment is received from you (by CCC) as provided in CCC's Billing and Payment terms and conditions. If full payment is not received on a timely basis, then any license preliminarily granted shall be deemed automatically revoked and shall be void as if never granted. Further, in the event that you breach any of these terms and conditions or any of CCC's Billing and Payment terms and conditions, the license is automatically revoked and shall be void as if never granted. Use of materials as described in a revoked license, as well as any use of the materials beyond the scope of an unrevoked license, may constitute copyright infringement and publisher reserves the right to take any and all action to protect its copyright in the materials.

COPYRIGHT NOTICE: DISCLAIMER

You must include the following copyright and permission notice in connection with any reproduction of the licensed material: "Reprinted ("Adapted" or "in part") with permission from REFERENCE CITATION. Copyright YEAR American Chemical Society."

WARRANTIES: NONE

Publisher makes no representations or warranties with respect to the licensed material.

INDEMNITY

You hereby indemnify and agree to hold harmless publisher and CCC, and their respective officers, directors, employees and agents, from and against any and all claims arising out of your use of the licensed material other than as specifically authorized pursuant to this license.

NO TRANSFER OF LICENSE

This license is personal to you or your publisher and may not be sublicensed, assigned, or transferred by you to any other person without publisher's written permission.

NO AMENDMENT EXCEPT IN WRITING

This license may not be amended except in a writing signed by both parties (or, in the case of publisher, by CCC on publisher's behalf).

OBJECTION TO CONTRARY TERMS

Publisher hereby objects to any terms contained in any purchase order, acknowledgment, check endorsement or other writing prepared by you, which terms are inconsistent with these terms and conditions or CCC's Billing and Payment terms and conditions. These terms and conditions, together with CCC's Billing and Payment terms and conditions (which are incorporated herein), comprise the entire agreement between you and publisher (and CCC) concerning this licensing transaction. In the event of any conflict between your obligations established by these terms and conditions and those established by CCC's Billing and Payment terms and conditions, these terms and conditions shall control.

JURISDICTION

This license transaction shall be governed by and construed in accordance with the laws of the District of Columbia. You hereby agree to submit to the jurisdiction of the courts located in the District of Columbia for purposes of resolving any disputes that may arise in connection with this licensing transaction.

THESES/DISSERTATION TERMS

Publishing implications of electronic publication of theses and dissertation material

Students and their mentors should be aware that posting of theses and dissertation material on the Web prior to submission of material from that thesis or dissertation to an ACS journal may affect publication in that journal. Whether Web posting is considered prior publication may be evaluated on a case-by-case basis by the journal's editor. If an ACS journal editor considers Web posting to be "prior publication", the paper will not be accepted for publication in that journal. If you intend to submit your unpublished paper to ACS for publication, check with the appropriate editor prior to posting your manuscript electronically.

If your paper has already been published by ACS and you want to include the text or portions of the text in your thesis/dissertation in **print or microfilm formats**, please print the ACS copyright credit line on the first page of your article: "Reproduced (or

'Reproduced in part') with permission from [FULL REFERENCE CITATION.]
Copyright [YEAR] American Chemical Society." Include appropriate information.

Submission to a Dissertation Distributor: If you plan to submit your thesis to UMI or to another dissertation distributor, you should not include the unpublished ACS paper in your thesis if the thesis will be disseminated electronically, until ACS has published your paper. After publication of the paper by ACS, you may release the entire thesis (**not the individual ACS article by itself**) for electronic dissemination through the distributor; ACS's copyright credit line should be printed on the first page of the ACS paper.

Use on an Intranet: The inclusion of your ACS unpublished or published manuscript is permitted in your thesis in print and microfilm formats. If ACS has published your paper you may include the manuscript in your thesis on an intranet that is not publicly available. Your ACS article cannot be posted electronically on a publicly available medium (i.e. one that is not password protected), such as but not limited to, electronic archives, Internet, library server, etc. The only material from your paper that can be posted on a public electronic medium is the article abstract, figures, and tables, and you may link to the article's DOI or post the article's author-directed URL link provided by ACS. This paragraph does not pertain to the dissertation distributor paragraph above.

Other conditions:

vi.1

VITA

KRISTA YAUDES WHITE

Education:

- 2009 Doctor of Philosophy, Biomedical Sciences
Eastern Virginia Medical School (EVMS) and Old Dominion University
Department of Microbiology and Molecular Cell Biology, EVMS,
Norfolk, VA
- 2001 Bachelor of Science, Marine Biology
University of North Carolina at Wilmington, Wilmington, NC

Publications:

Drake, RR, **White, KY**, Fuller, TW, Igwe, E, Clements, MA, Nyalwidhe, JO, Given, RW, Lance, RS, and Semmes, OJ. (2009) Clinical collection and protein properties of expressed prostatic secretions as a source for biomarkers of prostatic disease. *Journal of Proteomics* 72 (6): 907-917.

White, KY, Rodemich, L, Nyalwidhe, JO, Comunale, MA, Clements, MA, Lance, RS, Schellhammer, P, Mehta, A, Semmes, OJ, and Drake, RR. (2009) Glycomic characterization of prostate specific antigen and prostatic acid phosphatase in prostate cancer and benign disease seminal plasma fluids. *Journal of Proteome Research* 8 (2): 620-630.

Olson KN, Melton RS, **Yaudes KM**, Norwood KG and Freshwater DW. (2004) Characteristics and utility of plastid-encoded 16S rRNA gene sequence data in phylogenetic studies of red algae. *Journal of the North Carolina Academy of Science* 120: 143-151.

Awards:

- 2007 Scholar-in-Training Travel Award for Poster Presentation, American Association for Cancer Research: Advances in Proteomics in Cancer Research, Amelia Island, FL.